TELMA SARAIVA DOS SANTOS

ATIVIDADE TERAPÊUTICA E MECANISMOS DE AÇÃO DO MEDIADOR LIPÍDICO PRÓ-RESOLUÇÃO LIPOXINA A4 E DO POLIFENOL CURCUMINA NA DOR E INFLAMAÇÃO EM MODELO ANIMAL DE ARTRITE POR COMPONENTE DE PRÓTESE

Londrina

2022

TELMA SARAIVA DOS SANTOS

ATIVIDADE TERAPÊUTICA E MECANISMOS DE AÇÃO DO MEDIADOR LIPÍDICO PRÓ-RESOLUÇÃO LIPOXINA A4 E DO POLIFENOL CURCUMINA NA DOR E INFLAMAÇÃO EM MODELO ANIMAL DE ARTRITE POR COMPONENTE DE PRÓTESE

Tese de doutorado apresentada ao Programa de Pós Graduação em Patologia Experimental da Universidade Estadual de Londrina, como requisito parcial à obtenção do título de Doutor em Patologia Experimental.

Orientação: Prof. Dr. Waldiceu Aparecido Verri Júnior

Londrina

2022

Ficha catalográfica

Ficha de identificação da obra elaborada pelo autor, através do Programa de GeraçãoAutomática do Sistema de Bibliotecas da UEL

S243a Saraiva-Santos, Telma.
Atividade terapêutica e mecanismos de ação do mediador lipídico pró-resolução lipoxina A4 e do polifenol curcumina na dor e inflamação em modelo animal de artrite por componente de prótese / Telma Saraiva-Santos. -Londrina, 2022.
127 f. : il.

Orientador: Waldiceu Aparecido Verri Junior.
Tese (Doutorado em Patologia Experimental) - Universidade Estadual de Londrina, Centro de Ciências Biológicas, Programa de Pós-Graduação em Patologia Experimental, 2022.
Inclui bibliografia.

1. Dor - Tese. 2. Inflamação - Tese. 3. Artrite - Tese. 4. Artroplastia - Tese. I. Aparecido Verri Junior, Waldiceu . II. Universidade Estadual de Londrina. Centro de Ciências Biológicas. Programa de Pós-Graduação em Patologia Experimental. III. Título.

CDU 574

TELMA SARAIVA DOS SANTOS

ATIVIDADE TERAPÊUTICA E MECANISMOS DE AÇÃO DO MEDIADOR LIPÍDICO PRÓ-RESOLUÇÃO LIPOXINA A4 E DO POLIFENOL CURCUMINA NA DOR E INFLAMAÇÃO EM MODELO ANIMAL DE ARTRITE POR COMPONENTE DE PRÓTESE

Tese de doutorado apresentada ao Programa de Pós Graduação em Patologia Experimental da Universidade Estadual de Londrina, como requisito parcial para obtenção do título de Doutor em Patologia Experimental.

BANCA EXAMINADORA

Prof. Dr. Waldiceu Aparecido Verri Junior

Universidade Estadual de Londrina- UEL

Profa. Dra. Graziela Scalianti Ceravolo

Universidade Estadual de Londrina- UEL

Prof. Dr. Sérgio Marques Borghi

Universidade do Norte do Paraná- Unopar

Profa. Dra. Cássia Calixto de Campos
Faculdade de Apucarana

Profa. Dra. Camila Rodrigues Ferraz
University of Maryland School of Medicine

Londrina, 20 de Dezembro de 2022

AGRADECIMENTOS

Á minha família, meus pais Selma Saraiva e Valdir Santos e minha irmã Valdinéia Saraiva que são meus exemplos, por todo apoio durante toda a minha formação. A eles sou grata por todos os ensinamentos e sacrifícios.

Ao meu marido, André Lucas, por estar caminhando ao meu lado durante todos os momentos e compartilhando dos meus objetivos e realizações. Por sempre dispor de tempo e paciência, me apoiando e suportando todas as adversidades. A ele agradeço por todo amor, carinho e por ter levado todos os problemas de maneira tão leve, tornando todas as dificuldades insignificantes. Sem você nada disso seria possível. À minha sogra, sogro e meus cunhados, família que sempre esteve me apoiando.

Ao meu orientador Prof. Dr. Waldiceu Aparecido Verri Jr., pelo acolhimento, confiança, paciência e ensinamentos. Me sinto honrada pela oportunidade e agradeço imensamente por tê-lo como orientador.

Agradeço grandemente as agências de fomento CNPq e CAPES que financiaram as bolsas de estudo que possibilitaram o desenvolvimento desse trabalho durante esses anos.

Á banca examinadora, escolhida com carinho, Profa. Dra. Graziela Scalianti Ceravolo, Prof. Dr. Sergio Borghi, Profa. Dra. Cássia Calixto e Profa. Dra. Camila Rodrigues Ferraz pela disponibilidade, dedicação e contribuição essencial para meu trabalho.

Aos meus amigos e companheiros de todos os dias do LADINC, que auxiliaram no desenvolvimento dessa tese e estiveram ao meu lado, contribuindo com minha formação e aprimoramento. Agradeço a essa família que me recebeu de braços abertos: Victor Fattori, Fernanda Rasquel, Thacyana Carvalho, Marília Manchope, Nayara Artero, Ane Franciosi, Rosângela de Paula, Stephanie Garcia, Ketlem Andrade, Amanda Dionisio, Soraia Pierotti, Ana Carolina Rossaneis e Larissa Staurengo-Ferrari que de contribuíram para meu trabalho. Em especial aos amigos que fiz durante esse período, Tiago Zaninelli, Mariana Bertozzi e Camila Rodrigues Ferraz, pessoas e profissionais incríveis que estiveram comigo dia e noite e não pouparam esforços para sempre me ajudar.

Agradeço o apoio durante essa caminhada e pelo privilégio de aprender com vocês.

Todo voo é feito de tempo, aproveite a paisagem.

Natália Sousa

Santos, Telma Saraiva. **ATIVIDADE TERAPÊUTICA E MECANISMOS DE AÇÃO DO MEDIADOR LIPÍDICO PRÓ-RESOLUÇÃO LIPOXINA A4 E DO POLIFENOL CURCUMINA NA DOR E INFLAMAÇÃO EM MODELO ANIMAL DE ARTRITE POR COMPONENTE DE PRÓTESE**. 2022. 127 páginas. Tese de doutorado (Patologia Experimental) – Universidade Estadual de Londrina, Londrina, 2022.

RESUMO

Lipoxina A4 (LXA_4) é um mediador lipídico pró-resolução (MLPR) e a curcumina é um polifenol com importante efeito anti-inflamatório e a com funções anti-inflamatórias e resolutivas na inflamação. Nós avaliamos os efeitos de ambos os tratamentos na artrite induzida por dióxido de titânio (TiO_2). Camundongos foram estimulados com TiO_2 (3mg) na articulação do joelho e vinte e quatro horas após, os animais foram tratados diariamente com curcumina (100µl de 10 ou 100 mg/kg, via oral) ou com veículo (20% tween 80 em salina), e com administração de LXA_4 (0,1, 1 ou 10 ng/animal) ou veículo (etanol 3,2% em salina) a cada dois dias, por 30 dias. A hiperalgesia mecânica e térmica, inflamação e dosagens foram realizadas para avaliar os efeitos dos tratamentos. O tratamento com LXA_4 também reduziu a hiperalgesia mecânica e térmica, dano histopatológico, edema e recrutamento de leucócitos sem induzir toxicidade. LXA_4 reduziu a migração de leucócitos e modulou a produção de TNF-α, IL-1β, IL-6 e IL-10. Esses efeitos foram explicados pela ativação reduzida do fator nuclear kappa B (NF-κB) nos leucócitos do líquido sinovial. A LXA_4 melhorou os parâmetros antioxidantes (níveis reduzidos de glutationa [GSH] e 2,2-azino-bis 3-etilbenzotiazolina-6 sulfonato [ABTS], expressão do fator nuclear eritróide 2 relacionado ao fator 2 [Nrf2]) reduzindo a detecção de espécies reativas de oxigênio [ROS] induzida por TiO_2. Demonstramos o aumento da marcação do receptor ALX/FPR2 em neurônios TRPV1 positivos induzidos por TiO_2. O tratamento com LXA_4 modulou negativamente a ativação neuronal e a resposta à capsaicina (agonista TRPV1) e AITC (agonista TRPA1) de neurônios do GRD, além de reduzir expressão de TRPV1 e TRPA1 induzida por TiO_2, bem como TRPV1 colocalizado com p-NFκB, indicando ativação neuronal. A curcumina reduziu a hiperalgesia mecânica e térmica, edema e alterações histopatológicas (pela coloração de hematoxilina-eosina [HE]) na articulação do joelho induzida por TiO_2. A curcumina também reduziu o recrutamento de leucócitos (atividade de MPO e NAG, contagem total e diferencial), nível de IL-1β e estresse oxidativo (peroxidação lipídica [TBARS], ânion superóxido [redução de nitroazul tetrazólio], bem como detecção de ROS e NO) induzido por TiO_2 na articulação do joelho e líquido sinovial. A curcumina inibiu a ativação neuronal induzida por TiO_2 e responsividade à capsaicina e AITC em neurônios DRG, diminuindo a marcação de TRPV1 em neurônios GRD, bem como TRPV1 colocalizado com p-NFκB. Concluindo, a curcumina e o LXA_4 podem ter como alvo leucócitos recrutados e neurônios nociceptivos aferentes primários para exercer atividades analgésicas e anti-inflamatórias em um modelo de inflamação semelhante ao observado em pacientes com inflamação induzida por prótese.

Palavras-chave: mediador lipídico; artrite; artroplastia; polifenol; dor, inflamação.

Santos, Telma Saraiva. **THERAPEUTIC ACTIVITY AND MECHANISMS OF ACTION OF THE PRO-RESOLUTION LIPID MEDIATOR LIPOXIN A4 AND POLYPHENOL CURCUMIN IN PAIN AND INFLAMMATION IN AN ANIMAL MODEL OF ARTHRITIS BY PROSTHESIS COMPONENT.** 2022. 127 pages. PhD thesis (Experimental Pathology) – Universidade Estadual de Londrina, Londrina, 2022.

Lipoxin A4 (LXA_4) is a specialized pro-resolving mediator (SPM) and curcumin is a polyphenol with important anti-inflammatory effect and with anti-inflammatory and resolutive roles in inflammation. We evaluated the effects of both treatments in titanium dioxide (TiO_2)-induced arthritis. Mice were stimulated with TiO_2 (3mg) in the knee joint and twenty-four after, the animals were treated daily with curcumin (100µl of 10 or 100 mg/kg, orally) or with vehicle (20% tween 80 in saline), and with LXA_4 (0.1, 1, or 10ng/animal) or vehicle (ethanol 3.2% in saline) administration every other, for 30 days. Mechanical and thermal hyperalgesia, inflammation, and dosages were performed to assess the effects of treatments. LXA_4 treatment also reduced mechanical and thermal hyperalgesia, histopathological damage, edema, and recruitment of leukocytes without toxicity. LXA_4 reduced leukocyte migration and modulated the production of TNF-α, IL-1β, IL-6, and IL-10. These effects were explained by reduced nuclear factor kappa B (NF-κB) activation in synovial fluid leukocytes. LXA_4 improved antioxidant parameters (reduced glutathione [GSH] and 2,2-azino-bis 3-ethylbenzothiazoline-6 sulfonate [ABTS] levels, nuclear factor erythroid 2-related factor 2 [Nrf2] expression) reducing reactive oxygen species [ROS] detection induced by TiO_2. We show the increase of ALX/FPR2 receptor staining in TRPV1 positive neurons induced by TiO_2. The treatment with LXA_4 down-modulated neuronal activation and response to capsaicin (TRPV1 agonist) and AITC (TRPA1 agonist) of DRG neurons. LXA_4 reduced TiO_2-induced TRPV1 and TRPA1 expression, as well TRPV1 co-stained with p-NFκB, indicating neuronal activation. Curcumin also reduced mechanical and thermal hyperalgesia, edema, and histopathological alterations (using hematoxylin-eosin stain [HE]) in the knee joint induced by TiO_2. Curcumin also reduced leukocyte recruitment (MPO and NAG activity, total and deferential count), IL-1β level, and oxidative stress (lipid peroxidation [TBARS], superoxide anion [nitroblue tetrazolium reduction], ROS and NO detection) induced by TiO_2 in knee joint sample and synovial fluid. Curcumin inhibited TiO_2-induced neuronal activation and responsiveness to capsaicin and AITC activation on DRG neurons, decreasing TRPV1 staining in DRG neurons, as well TRPV1 co-stained with p-NFκB. Concluding, curcumin and LXA_4 might target recruited leukocytes and primary afferent nociceptive neurons to exert analgesic and anti-inflammatory activities in an inflammation model resembling that observed in patients with prosthesis inflammation.

Keywords: lipid mediator; arthritis; arthroplasty; polyphenol; pain, inflammation.

LISTA DE ILUSTRAÇÕES

LISTA DE ABREVIATURAS E SIGLAS

AA	Ácido araquidônico
AhR	Receptor nuclear hidrocarboneto de arila
$AINE_S$	Anti-inflamatórios não esteroidais
ALX/FPR2	Receptor de peptídeo formilado tipo 2 ou receptor de LXA_4
ATP	Trifosfato de adenosina
COX-2	Ciclo-oxigenase-2
DAMPs	Padrões moleculares associados a danos
DHA	Àcido docosaexaenoico
DNA	Ácido desoxirribonucleico
EPA	Ácido eicosapentaenoico
EROs	Espécies reativas de oxigênio
fMLP	Peptídeos formilados
GPCRs	Receptores acoplado a proteína G
GRD	Gânglios da raiz dorsal
HO	Heme-oxigenase
IL-1β	Interleucina-1β
IL-33	Interleucina-33
IL-6	Interleucina-6
IL-8	Interleucina-8
LOX	Lipoxigenase
LTB_4	Leucotrieno B_4
LXA_4	Lipoxina A_4
LXB_4	Lipoxina B_4
LXs	Lipoxinas
MAPK	MAP quinase
MaR	Maresinas
MLPI	Mediadores lipídicos pró-inflamatórios
MLPR	Mediadores lipídicos pró-resolução

NF-κB	Fator nuclear κappa B
NO	Oxido nítrico
Nrf2	Fator nuclear eritróide relacionado ao fator 2
PAMPs	Padrões moleculares associados a patógenos
PGE_2	Prostaglandinas E2
PGI_2	Prostaglandinas I2
PMN	Polimorfonucleares
PRRs	Receptores de reconhecimento padrão
RANKL	Receptor ativador do fator nuclear κB ligante
Rvs	Resolvinas
Th1	T helper 1
Th2	T helper 2
TiO_2	Dióxido de titânio
TNF-α	Fator de necrose tumoral-alpha
TRPA1	Receptor de potencial transitório anquirina 1
TRPV1	Receptor de potencial transitório vanilóide tipo 1

SUMÁRIO

1. INTRODUÇÃO

1.1. INFLAMAÇÃO

A inflamação é uma resposta de células imunes e seus produtos frente a estímulos e/ou circunstâncias nocivas, como infecção causada por patógenos, corpos estranhos ou injúria tecidual (MEDZHITOV, 2008). A resposta inflamatória visa à neutralização e remoção de estímulos lesivos, remodelamento e reparação tecidual (FLOWER, 2006; MEDZHITOV, 2008; SAMUELSSON, 2012a). O processo inflamatório é altamente regulado, autolimitado e indispensável para a manutenção da saúde, uma vez que visa o reestabelecimento da homeostase (SERHAN, 2007).

A resposta inflamatória aguda é caracterizada por uma série de eventos vasculares e celulares que culminam na geração de cinco sinais cardinais clássicos: eritema (rubor), edema, calor e dor (algia) decorrentes do aumento da permeabilidade do endotélio vascular com extravasamento de células imunes e componentes séricos. Quando exacerbados, esses sinais podem culminar na destruição de tecidos, fibrose e perda da função tecidual (TAKEUCHI; AKIRA, 2010).

A resposta imune inata e adaptativa começou a ser desvendada em 1908 a partir de achados dos pesquisadores Ilya Metchnikoff e Paul Ehrlich, que descreveram os tipos e funções das células imune, rendendo um prémio Nobel em Fisiologia no mesmo ano (SCHMALSTIEG; GOLDMAN, 2008). Na resposta imune inata leucócitos como macrófagos, células dendríticas, neutrófilos, células NK, dentre outros, iniciam o processo inflamatório a partir do reconhecimento de antígenos por meio de receptores denominados receptores de reconhecimento de padrões (PRRs) específicos para epítopos conservados de micro-organismos, que não estão presentes nos hospedeiros, denominados padrões moleculares associados a patógenos (PAMPs), e moléculas endógenas liberadas por células danificadas, denominadas padrões moleculares associados a danos (DAMPs), (JANEWAY, 1989). Receptores do tipo Toll (TLR) estão presentes em insetos e vertebrados e participam do reconhecimento principalmente de bactérias e seus produtos, assim como ácidos nucleicos virais (BERNARD; TEDGUI, 1992). Também existem sensores intracelulares denominados receptores do tipo NOD que reconhecem fragmentos de

peptideoglicano e proteína (FRITZ et al., 2006; INOHARA et al., 2005). Além disso, os receptores do tipo NOD também são importantes para formação do inflamassoma, um complexo multiproteico intracelular que atua na ativação da protease caspase-1, responsável por processar a pró-interleucina 1 (IL-1) em uma forma madura ativa e liberada (IL-1) (MARIATHASAN; MONACK, 2007).

A partir do reconhecimento de PAMPs ou DAMPs, ocorre ativação das células imunes inatas que culminam no aumento da transcrição de genes de citocinas pró-inflamatórias como fator de necrose tumoral-α (TNF-α), IL-1β e interleucina-6 (IL-6), quimiocinas (AKIRA, 2011; SHELDON; OWENS; TURNER, 2017), e aminas vasoativas como histamina e serotonina, que promovem alteração do fluxo sanguíneo com aumento do extravasamento de líquidos e permeabilidade endotelial, conduzindo neutrófilos para o foco inflamatório, caracterizando os eventos vasculares inflamatórios (MCDONALD et al., 2010). A partir desses eventos ocorre a fase celular da inflamação, caracterizada pela marginalização de leucócitos que entram em contato com células endoteliais ativadas por meio de moléculas de adesão, promovendo rolamento, adesão e transmigração de leucócitos do vaso sanguíneo em direção ao foco inflamatório (SPECTOR; WILLOUGHBY, 1964). A atração e direcionamento dos neutrófilos ao foco inflamatório infeccioso ou não infeccioso é dependente de moléculas quimioatraentes locais como C5a e peptídeos formilados (fMLP), bem como moléculas adjacentes (provenientes do endotélio vascular, por exemplo), como interleucina-8 (IL-8) e leucotrieno B4 (LTB_4) (FOXMAN; CAMPBELL; BUTCHER, 1997). Após a chegada dessas células para o sítio da lesão/infecção ocorre a destruição de antígenos e precede as respostas adaptativas (MEDZHITOV, 2007).

Inicialmente os estudos cerca da resposta inflamatória se concentravam nas fases iniciais da resposta, esclarecendo os mecanismos e moléculas que participam dessa etapa, como citocinas, quimiocinas e mediadores lipídicos pró-inflamatórios (MLPI). Os MLPI produzidos a partir do ácido araquidônico (AA), como prostaglandinas E2 e I2 (PGE2 e PGI2) (FLOWER, 2006) e LTB4 (MALAWISTA et al., 2008), em conjunto com mediadores locais como histamina, produtos do complemento (C5a, C3b) e as quimiocinas atuam como quimiotáticos para neutrófilos que respondem através da diapedese das vênulas

para combater lesões e agentes invasores (FLOWER, 2006; MALAWISTA et al., 2008).

Apesar da identificação de MLPI terem aberto um novo caminho para o desenvolvimento de ferramentas terapêuticas usadas no tratamento de doenças inflamatórias, essas moléculas também demonstraram diversos efeitos colaterais, como por exemplo: os anti-inflamatórios não esteroidais (AINEs) que aumentam a incidência de sangramentos gastrointestinais (GOLDSTEIN; CRYER, 2015) e anti-TNFs que aumentam a incidência de infecções (MINOZZI et al., 2016). Diante disso, posteriormente foi demonstrado que o AA era substrato na biossíntese de moléculas protetoras e anti-inflamatórias como as lipoxinas (LXs), e não apenas na síntese de prostaglandinas e leucotrienos, trazendo à tona um novo conceito de que a etapa seguinte do processo inflamatório, denominada resolução é um processo ativo (LEVY et al., 2001; SERHAN; HAMBERG; SAMUELSSON, 1984b).

Dentre os possíveis desfechos da inflamação, a resolução ocorre quando a lesão é limitada e de curta duração, ou quando há pouca destruição tecidual, restaurando o local da inflamação aguda e retornando à normalidade. A presença de células apoptóticas, como neutrófilos, associados à produção de PGE2 induz uma troca de classe, de MLPI para mediadores lipídicos pró-resolução (MLPR) (LEVY et al., 2001). O processo resolutivo se caracteriza pelo decaimento espontâneo dos mediadores inflamatórios locais com retorno da permeabilidade vascular normal, encerramento da infiltração leucocitária, morte celular (apoptose de neutrófilos, por exemplo), remoção de edema e de agentes estranhos e debris celulares no sítio inflamatório, promovendo retorno da homeostasia (SERHAN, 2007).

Quando a inflamação não é controlada pode culminar em diversas doenças de ampla ocorrência, como doenças cardiovasculares, metabólicas e doenças inflamatórias clássicas, como artrite e doença periodontal, bem como câncer (NATHAN; DING, 2010; SERHAN, 2010).

1.2. DOR INFLAMATÓRIA

Como citado anteriormente, a dor é um dos sinais cardinais da inflamação caracterizada pela percepção desagradável de uma sensação nociceptiva e

segundo a Associação internacional para o Estudo da Dor (IASP) ela pode ser definida como uma experiência sensitiva e emocional desagradável associada, ou semelhante àquela associada, a uma lesão tecidual real ou potencial (DESANTANA et al., 2020).

A nocicepção confere ao indivíduo a capacidade de autopreservação, onde a percepção dolorosa permite a identificação de situações que possam causar danos ou controlar aquelas já existentes em uma lesão. As sensações nociceptivas agudas, e principalmente as crônicas causam diminuição na qualidade de vida e sua persistência é fator de risco consistente na saúde pública (CALATI et al., 2015)

A dor pode ser classificada como: fisiológica, inflamatória ou neuropática. A dor fisiológica é gerada por um estímulo nocivo, enquanto a dor inflamatória é resultante de injúria tecidual e/ou ativação das células imunes, já a dor neuropática está associada a uma lesão e má adaptação do sistema nervoso. As dores com origem inflamatória compõem transtornos clínicos que afetam pacientes, podendo cronificar-se e permanecem sem terapia realmente eficazes na grande maioria dos casos. Esses processos são caracterizados por estados de hipersensibilidade no foco ou gatilho da lesão e na área adjacente (WOOLF; SALTER, 2000).

A sensação dolorosa está ligada a interações moleculares e celulares entre sistema nervoso e imunológico. Nessa interação, células imunes liberam mediadores que modulam a atividade dos neurônios nociceptores e a sensibilidade à dor, enquanto os nociceptores liberam neuropeptídeos e neurotransmissores que atuam nas células imunes inatas e adaptativas para modular suas funções. Diante disso, a sinalização neuronal pode definir o padrão das respostas imunes e contribuir para o desenvolvimento de doenças inflamatórias locais e sistêmicas (PINHO-RIBEIRO; VERRI; CHIU, 2017).

Os neurônios aferentes primários especializados que detectam estímulos químicos, térmicos e mecânicos nocivos são denominados nociceptores (LEVINE; FIELDS; BASBAUM, 1993). Os nociceptores inervam os tecidos periféricos, como pele, articulações, trato respiratório e gastrointestinal, sendo os primeiros a responder a patógenos e lesões teciduais (PINHO-RIBEIRO; VERRI; CHIU, 2017). A sensibilização dos nociceptores sensoriais é denominada hiperalgesia, onde há uma resposta aumentada a um estímulo que

normalmente é doloroso, ou alodinia, que é a dor gerada por um estímulo que normalmente não provoca dor (VERRI et al., 2006b). Diversos mediadores podem sensibilizar diretamente os neurônios nociceptivos, como por exemplo, endotelina, substância P e prostaglandinas (FERREIRA; NAKAMURA, 1979; FERREIRA; ROMITELLI; DE NUCCI, 1989; HENRY, 1976).

Os corpos celulares desses neurônios são encontrados no gânglio da raiz trigeminal e dorsal (GRD), que fornecem inervação sensorial para vários tecidos. Por meio de receptores especializados, canais e vias sintéticas ajudam a definir a especificidade de subtipos de nociceptores específicos, que permitem a detecção e sinalização de estímulos nocivos agudos e crônicos (SCHUMACHER; GUAN; HELLMAN, 2016).

Os três principais neurônios/ fibras axonais sensoriais do sistema nervoso periférico são as fibras Aβ, Aδ (delta) e C que respondem e transmitem informações sensoriais (D'MELLO; DICKENSON, 2008; MILLIGAN; WATKINS, 2009). Os neurônios nociceptivos fibra C são neurônios não mielinizados que apresenta condução lenta e são sensíveis principalmente à capsaicina e frequentemente medeiam a sensibilidade à dor térmica. Já os neurônios Aβ e Aδ são neurônios que apresentam uma condução mais rápida e são mielinizados, frequentemente mediando a sensibilidade mecânica (PINHO-RIBEIRO; VERRI; CHIU, 2017). As fibras Aδ e C estão associadas à inflamação e após sensibilização podem transduzir em impulsos elétricos, estímulos mecânicos, térmicos ou químicos que são transmitidos ao sistema nervoso central (RANG; BEVAN; DRAY, 1991). Deste modo, estímulos dolorosos agudos são detectados inicialmente pelos nociceptores e retransmitidos para os níveis espinais, supraespinais e para múltiplas áreas do córtex que estão associadas com a percepção consciente da dor (MILLIGAN; WATKINS, 2009).

Após o início da percepção sensorial que acontece na periferia, posteriormente ocorre a transdução destas informações para o corno dorsal da medula espinal, onde terminam as extremidades dessas fibras. Os corpos celulares desses neurônios encontram-se nos gânglios trigeminais e nos GRD, dependendo da localização da interação estímulo/sistema.

A dor é um sintoma presente na maioria das doenças inflamatórias, podendo até mesmo levar à perda da função de tecidos e/ou órgãos afetados. Durante a inflamação ocorre a ativação de mecanismos responsáveis pela

indução de edema, migração de leucócitos e hiperalgesia. A produção de espécies reativas de oxigênio (EROs) e citocinas pró-inflamatórias possuem participação na resposta inflamatória e no desenvolvimento da dor (SERHAN, 2014).

A dor inflamatória tem como origem a interação do tecido comprometido com os neurônios sensoriais nociceptivos periféricos (HARDY; WOLFF; GOODELL, 1950) que são sensibilizados por mediadores pró-inflamatórios, como IL-1β, TNF- α, LTB4, PGE2, ATP e C5a, que por sua vez são liberados pelas células lesionadas após reconhecimento de agentes estranhos por células de defesa residentes como macrófagos (FERREIRA, 1993; RIBEIRO et al., 2000). A associação desses eventos, coopera com o aumento da sensibilidade neuronal a estímulos que em condições naturais produzem dor moderada ou dor alguma. Essa sensibilização neuronal é uma característica importante da dor inflamatória, e o bloqueio deste fenômeno representa o principal mecanismo de ação dos analgésicos e anti-inflamatórios comercializados (CUNHA et al., 1992; FERREIRA, 1993; SACHS et al., 2002; WATKINS et al., 1995).

Os neutrófilos desempenham um papel essencial na manutenção da dor inflamatória (CUNHA et al., 2008), produzindo citocinas pró-inflamatórias como IL-1β, TNF-α, interleucina-33 (IL-33), dentre outras (VERRI et al., 2006a). Após o estímulo nocivo, uma cascata de citocinas pró-inflamatórias antecedem a liberação de aminas simpáticas e PGE2 que levam a sensibilização dos nociceptores (BRAZ et al., 2014; SCHOLZ; WOOLF, 2002).

A dor decorrente de processos inflamatórios pode ser associada a diversas doenças, onde a exacerbação ou persistência desse sinal é a principal causa de procura por atendimento médico (Mogil et al., 2000; Woolf e Salter, 2000; Scholz e Woolf, 2002; Verri et al., 2006; Guerrero et al., 2008; Braz et al., 2014).

1.3. CANAIS ENVOLVIDOS NA NOCICEPÇÃO

Terminais nervosos nociceptores expressam canais iônicos controlados por ligante e voltagem, incluindo receptor de potencial transitório vanilóide tipo 1 (TRPV1), receptor de potencial transitório anquirina 1 (TRPA1), Nav1.7, Nav1.8 e Nav1.9 (PINHO-RIBEIRO; VERRI; CHIU, 2017). Nav1.7, Nav1.8 e Nav1.9 são

canais de sódio controlados por voltagem presentes em neurônios nociceptivos, modulam a geração de potencial de ação e são críticos para a despolarização dos neurônios nociceptivos, mediando o início da sinalização da dor (DIB-HAJJ; WAXMAN, 2014).

Dentre os principais receptores/canais que foram identificados e caracterizados em nociceptores que detectam estímulos inflamatórios nocivos, podemos citar os canais TRPV1 e TRPA1 (SCHUMACHER; GUAN; HELLMAN, 2016). Ambos os canais são membros da família TRP de canais catiônicos não seletivos, e são tetrâmeros formados por subunidades com seis domínios transmembranas e poros catiônicos seletivos que frequentemente apresentam alta permeabilidade ao cálcio (LATORRE; ZAELZER; BRAUCHI, 2009). Esses canais desempenham papel integral na dor e inflamação neurogênica por meio da ativação do nervo sensorial. Os nervos sensoriais de pequeno diâmetro, fibras Aδ e C foram o local de descoberta para TRPV1 e TRPA1 (FERNANDES; FERNANDES; KEEBLE, 2012).

O TRPV1 foi inicialmente relatado como um integrador de múltiplos estímulos nocivos por meio da demonstração de que diversos produtos da inflamação podem ativar esse canal, como por exemplo, prótons, bradicinina (SCHUMACHER, 2010; TOMINAGA et al., 1998), derivados de dopamina (DE PETROCELLIS et al., 2004; HUANG et al., 2002), fator de crescimento do nervo (WINTER et al., 1988) entre outros (SCHUMACHER, 2010) . Esse canal tem sido associado a estados hiperalgésicos térmicos e mecânicos (GHILARDI et al., 2005).

Os canais TRP vanilóides são divididos em seis membros, no entanto, apenas o TRPV1 da subfamília TRPV é de fato ativado por vanilóides, incluindo a capsaicina, componente pungente das pimentas (FERNANDES; FERNANDES; KEEBLE, 2012). Historicamente, a capacidade da capsaicina de ativar neurônios sensoriais foi determinada na década de 1960 (JANCSÓ; JANCSÓ-GÁBOR; SZOLCSÁNYI, 1967) sendo só posteriormente descrita a presença de receptor de capsaicina na membrana de nervos sensoriais (SZOLCSANYI; JANCSO GABOR, 1976). Posteriormente, veio a confirmação de que o calor acima de 43°C e pH acima de 5,9 também ativam TRPV1 (TOMINAGA et al., 1998). No entanto, a administração repetida ou exposição prolongada a capsaicina pode dessensibilizar o receptor de TRPV1

(SZOLCSÁNYI; JANCSÓ-GÁBOR; JOÓ, 1975) e em altas doses destroem seletivamente os nervos sensoriais C e Aδ, impedindo completamente a ativação nervosa (SZALLASI et al., 1995).

O TRPA1 desempenha um papel importante complementar ao TRPV1 no desenvolvimento e manutenção de estados de dor inflamatória, corroborando com relatos de que o TRPA1 é ativado por mediadores inflamatórios endógenos e exógenos (KOIVISTO et al., 2014). Esse canal tem sido associado a modelos de dor inflamatória, hipersensibilidade mecânica e ao frio (GARRISON; STUCKY, 2014). O óleo de mostarda foi identificado como clássico agonista de TRPA1, e induz inflamação de maneira semelhante à capsaicina (FERNANDES; FERNANDES; KEEBLE, 2012).

Com relação a população neural que expressa esses canais, 97% dos neurônios sensoriais que expressam TRPA1 também expressam TRPV1, enquanto apenas 30% dos neurônios TRPV1 positivos expressam TRPA1 (STORY et al., 2003). Diante disso, ambos os canais possuem interações, e agonistas de TRPV1 e TRPA1 são capazes de pelo menos em partes dessensibilizar as vias de TRPV1 e TRPA1 de maneira heteróloga (RUPAREL et al., 2008).

Diante do papel do TRPV1 e TRPA1 na sinalização da dor inflamatória, tem sido explorado o desenvolvimento de antagonistas de alta afinidade para ambos. Inibidores endógenos desses canais incluem mediadores lipídicos envolvidos na resolução, como resolvinas (Rv) (XU et al., 2010) e maresinas (MaR) (FATTORI et al., 2019; SERHAN et al., 2012b) . A inibição completa de ambos os canais, no entanto, pode resultar em efeitos colaterais indesejados, como hipotermia ou inibição da dor aguda protetiva (NASH et al., 2012), devido a expressão desses canais em tipos celulares neuronais e não neuronais (FERNANDES; FERNANDES; KEEBLE, 2012).

1.4. DIÓXIDO DE TITÂNIO

Diversos produtos desenvolvidos atualmente são à base de nanopartículas (NP) e são amplamente aplicados na indústria. O titânio é considerado um dos elementos mais abundantes e biodisponíveis, sendo considerado o segundo metal mais abundante (DAR; SAEED; WU, 2020). Aproximadamente quatro milhões de toneladas de dióxido de titânio (TiO_2) são

consumidas anualmente no mundo (ORTLIEB, 2010). O TiO_2 é um pó branco e inodoro que vem sendo explorado por suas amplas aplicações biomédicas devido a suas características, como biocompatibilidade, foto estabilidade, propriedades antioxidantes e disponibilidade (FEI YIN et al., 2013).

Essa nanopartícula é amplamente usada na indústria na fabricação de tintas, revestimentos, plásticos, papéis, medicamentos, produtos farmacêuticos, produtos alimentícios, cosméticos, protetor solar e cremes dentais (KAIDA et al., 2004; WANG; SANDERSON; WANG, 2007; WOLF et al., 2003). Além disso também são comumente usados como componente de próteses articulares, especialmente próteses de quadril e joelho (JACOBS et al., 1991; SUL, 2010).

Nanopartículas como o TiO_2 pode ser absorvido pelo corpo por via respiratória, digestiva, injeção intravenosa ou dérmica (DAR; SAEED; WU, 2020). Uma vez absorvidas na circulação sistêmica, elas podem ser distribuídas para todos os órgãos e tecidos do corpo (SHI et al., 2013a).

Apesar disso, esses compostos são capazes de interagir e prejudicar funções biológicas. Grande parte dos efeitos biológicos negativos do TiO_2 através da indução do estresse oxidativo tem sido associado a produção de espécies reativas de oxigênio que são associadas em grande parte a danos celulares (DAR; SAEED; WU, 2020).

Diversos estudos vêm sendo realizados acerca da segurança do uso de TiO_2, empregando diferentes vias de administração para avaliação desse efeito tóxico, como, inalação, exposição dérmica, via oral, intragástrica, intraperitoneal ou intravenosa (SHI et al., 2013a). Em um estudo de toxicidade, doses altas de TiO_2 (entre a faixa de 0,3 a 2.000 mg/kg) via intraperitoneal demonstraram migração e acúmulo de nanopartículas no baço, fígado, rins e pulmões (CHEN et al., 2009). Diante dos estudos acerca da toxicidade do TiO_2 pela sua atividade oxidante, foi possível observar que altas concentrações de TiO_2 estão relacionadas ao alto nível de estresse oxidativo que conduz dano celular, enquanto concentrações menores se relacionam mais com a indução de resposta inflamatória por vias sensíveis a EROs (WANG et al., 2009).

A toxicidade e capacidade inflamatória do TiO_2 na articulação foi demonstrada por Wang e colaboradores (WANG et al., 2009), onde a administração de 20mg/kg de TiO_2 intra-articular demonstrando alterações

histopatológicas no coração, pulmão e fígado. Além disso, foi observado a indução do estresse oxidativo e produção de citocinas na articulação exposta.

A estimulação intratecal (i.t.) com TiO_2 demonstrou promover aumento da capacidade quimiotáxica, expressão de complexo principal de histocompatibilidade classe 2 em células superficiais e aumento da secreção de oxido nítrico (NO) e TNF-α em macrófagos pulmonares (LIU et al., 2010). Os feitos lesivos do TiO_2 são estudados principalmente por meio de duas vias de sinalização, via fator nuclear kappa B (NF-κB) e MAP quinase (MAPK) (WU; TANG, 2018). As nanopartículas de TiO_2 também causam lesão após atravessar a membrana celular, produzindo estresse oxidativo e inflamação, danificando o ácido desoxirribonucleico (DNA) e levando a apoptose (MAKUMIRE et al., 2014; SHI et al., 2013b).

1.5. ARTRITE INDUZIDA POR DIÓXIDO DE TITÂNIO

O processo inflamatório articular crônico pode acarretar alterações morfológicas caracterizadas pela destruição da superfície de suporte articular, evoluindo de maneira a necessitar de artroplastia, uma cirurgia de substituição parcial ou total da articulação que tem como objetivo melhorar a qualidade de vida do paciente e do estado funcional articular (ARDEN; NEVITT, 2006; BRUYÈRE et al., 2012; LAWRENCE et al., 2008).

A artroplastia total articular do quadril e joelho é um procedimento ortopédico comum (KANE et al., 2005) e eficaz para o tratamento de pacientes com osteoartrite, artrite reumatoide, fraturas e necrose avascular que apresentam níveis altos de dor (NÚÑEZ et al., 2007) , aliviando o desconforto e melhorando o estado funcional (CALLAHAN et al., 1995). O crescimento da demanda por cirurgias de substituição articular nos últimos anos deve-se à alta prevalência de artrite e maior necessidade de mobilidade e qualidade de vida (KREMERS et al., 2015). Em 2010, cerca de 7 milhões de estadunidenses já haviam realizado a substituição total do joelho ou quadril e acredita-se que até 2030 mais de 3 milhões irão realizar tais procedimentos (KREMERS et al., 2015; KURTZ et al., 2007). Entre os anos de 2008 e 2015 foram feitas 189.457 cirurgias de artroplastia parcial e total de quadril e joelho pelo Sistema Único de Saúde (SUS-Brasil), gerando grandes gastos econômicos anuais (MACIEJ SERDA et al., 2018). Apesar da artroplastia ser um procedimento de sucesso na medicina

moderna, cerca de 10-15% desses procedimentos tendem a falhar (Harris, 2001).

As próteses metálicas podem apresentar efeito nocivo a longo prazo devido à liberação de nanopartículas, que ativam macrófagos residentes no espaço periprotético, estimulam a produção de mediadores por essas células, como o ligante do receptor ativador do fator nuclear κB ligante (RANKL), citocinas pró-inflamatórias (TNF-α, IL-1β e IL-6), bem como produção de EROs (DÖRNER et al., 2006). Estes mediadores promovem a ativação do NF-κB, o qual é responsável pela manutenção do processo inflamatório asséptico no tecido (COBELLI et al., 2011; WANG et al., 2010; WOOLEY et al., 2002). O microambiente pró-inflamatório induz osteoclastogênese e ativação de osteoclastos, promovendo reabsorção óssea e osteólise em 5-20% dos pacientes com artroplastia (HARRIS, 2001). A ativação do sistema imune pelas nanopartículas metálicas resulta na rejeição da prótese e necessidade de revisão cirúrgica. Atualmente, as terapias mais utilizadas para tratamento desses casos são os AINEs, corticosteroides e opióides; medicamentos que apresentam eficácia limitada e oferecem efeitos adversos intensos (ZOBDEH et al., 2022).

Como mencionado, umas dessas nanopartículas amplamente usadas na fabricação de próteses metálicas é o TiO_2, e o modelo animal de artrite crônica relacionada ao uso de prótese induzida por TiO_2 foi recentemente padronizada, demonstrando que a administração intra-articular de 3 mg de TiO_2 induz dor crônica durante 30 dias e intenso recrutamento de leucócitos com degradação de proteoglicanos, estresse oxidativo e produção de citocinas inflamatórias (BORGHI et al., 2018). Com isso em vista, o modelo animal de artrite induzida por TiO_2 proporciona melhor compreensão dos mecanismos celulares e moleculares relacionado ao processo inflamatório asséptico mediado por partículas liberadas no espaço periprotético, bem como serve como ferramenta de estudo para alvos terapêuticos.

1.6. MEDIADORES LIPÍDICOS PRÓ-RESOLUÇÃO

A resposta inflamatória em excesso é vista atualmente como componente frequente de doenças crônicas a qual preocupa a saúde pública, como síndromes metabólicas, doenças vasculares e outras. Os pontos endógenos de

controle da inflamação trazem uma nova perspectiva a respeito de novas abordagens terapêuticas (SERHAN, 2014).

Por muitos anos a resolução da inflamação era tida apenas como uma simples diluição dos mediadores inflamatórios, levando consequentemente ao restabelecimento da função tecidual (SERHAN, 1994). No entanto, hoje está claro que a inflamação excessiva ou descontroladas é decorrente do desequilíbrio entre mediadores lipídicos pró-inflamatórios e especializados (BUCKLEY; GILROY; SERHAN, 2014a). Charles Serhan identificou as moléculas com a capacidade de resolver a inflamação ativamente, denominadas MLPR (BANNENBERG et al., 2005; SERHAN et al., 2000, 2002, 2009)

Esses MLPR são biosintetizados a partir de ácidos graxos ômega-6, como AA, ou ômega-3, como ácido eicosapentaenoico (EPA), ácido docosapentaenoico (DPA) e ácido docosahexaenoico (DHA). Diante das diferenças estruturais, os MLPR foram divididos em famílias; as LXs, derivadas do AA), as Rvs, derivadas do EPA [série E] ou derivadas de DHA/DPA [série D]), as protectinas (PDs, derivadas de DHA/DPA) ou as MaRs, derivadas de DHA/DPA) (CHIANG; SERHAN, 2017; SERHAN, 2017a; SERHAN et al., 2015) (Figura 1).

Figura 1- Perfil dos mediadores lipídicos pró-resolução.

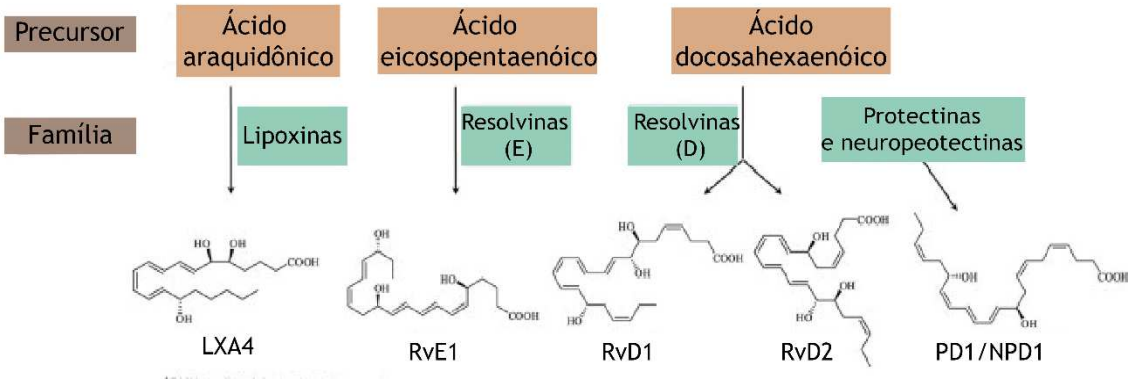

Fonte: adaptado (SERHAN, 2010).

A descoberta dos MLPR possibilitou o interesse nas vias de resolução e nos mecanismos imunes envolvidos na homeostase, uma vez que essas moléculas atuam como agonistas que estimulam os eventos celulares da resolução, como a interrupção no influxo de polimorfonucleares (PMN) e

remoção de restos apoptóticos por macrófagos (MADERNA; GODSON, 2009), além de reduzir os eicosanoides pró-inflamatórios (SERHAN; CHIANG, 2013).

Os MLPR atuam nos receptores acoplados a proteína G (GPCRs) para que tenham seus efeitos. A dose necessária de MLPR para cessar a inflamação está na faixa de pico a nanomolar (SERHAN, 2017b; SERHAN; CHIANG; DALLI, 2015). Esses mediadores podem ser agonistas, inibidores ou agonistas alostéricos de receptores específicos expressos por células imunes ou neurônios para modular a resposta do hospedeiro (PAMPLONA et al., 2012; PARK, 2015; SERHAN et al., 2009; XU et al., 2010). Além disso, alguns MLPR estimulam a biossíntese de outras famílias de MLPR. Por exemplo, RvE1 estimula a produção de LXA_4 no pulmão de camundongos (LEVY; SERHAN, 2014).

Além das características analgésicas, anti-inflamatórias, resolutivas e imunomoduladora, esses MLPR não possuem atividade imunossupressora e apesar da meia-vida curta em meio aquoso (AURSNES et al., 2015), apresentam efeito biológico duradouro, na faixa de dias (SERHAN et al., 2012a), fazendo destas moléculas fortes candidatas a testes clínicos. De fato, a RvE1 derivada do EPA alcançou a clínica como RX-10045® para testes no tratamento da síndrome do olho seco, contribuindo para melhora significativa dos pacientes de maneira dose-dependente (Clinicaltrials.gov identificação NCT00799552) (LEE, 2012; NORLING; PERRETTI, 2013).

Huang e colaboradores (HUANG et al., 2011) demonstraram que o tratamento i.t. com RvD1 produz efeito analgésico durante 30 dias em modelo de dor pós-operatória. Um único pré-tratamento com MaR1 demonstrou efeito analgésico durante 5 dias (FATTORI et al., 2019). Corroborando com esses achados Allen e colaboradores demonstraram que o tratamento com MaR1 apresentou efeito analgésico de 14 dias após tratamentos repetidos (ALLEN et al., 2020). Com relação ao efeito desses mediadores em células imunes, a produção inicial de MLPR é seguida pelo recrutamento de uma subpopulação distinta de macrófago pró-resolução que se correlaciona com a resolução da inflamação (BANNENBERG et al., 2005).

Dentre os mecanismos de ação dos MLPR estão; inibição de NF-κB (BUCKLEY; GILROY; SERHAN, 2014b), com consequente diminuição de marcadores inflamatórios, como proteína C reativa, fibrinogênio, IL-1β, IL-6 e TNF-α (BUFFON et al., 1999; LIUZZO et al., 1999) e quimiocinas como CXCL1

e CXCL3 (BUCKLEY; GILROY; SERHAN, 2014b), indução de mudança de classe de macrófagos do fenótipo M1 para M2, resposta que promove mudança do padrão T helper 1 (Th1) para T helper 2 (Th2), gerando um ambiente pró-resolução (BUCKLEY; GILROY; SERHAN, 2014b; DALLI; SERHAN, 2016).

Na artrite, já foi demonstrado que a deficiência de 12/15-lipoxigenases, enzimas chave na síntese de SPMs e está relacionada a resultados piores em modelo de artrite de transferência de soro em camundongos K/BxN (KRÖNKE et al., 2009). Evidências demonstraram a diferença entre o estado da doença na artrite e os níveis de mediadores lipídicos (ARNARDOTTIR et al., 2016; HASHIMOTO et al., 2007; JIN et al., 2018), onde o desequilíbrio nos níveis desses mediadores se correlaciona com a agressividade ou patogênese da doença, indicando a importância na produção desses mediadores para controlar o estado da doença (ARNARDOTTIR et al., 2016). Tendo em vista as propriedades, mecanismos de ação, efeitos e estudos em animais de experimentação, os MLPR são fortes candidatos terapêuticos para diversas doenças inflamatórias e uso em testes clínicos (FATTORI; AMARAL; VERRI, 2016).

1.7. LIPOXINA A4

A Lipoxina A4 (LXA_4) (Figura 2) e a Lipoxina B4 (LXB_4) foram os primeiros mediadores lipídicos a serem descritos por Serhan em 1984 (SERHAN; HAMBERG; SAMUELSSON, 1984a). As LXs são eicosanoides derivados de lipoxigenases a partir do AA; um ácido graxo ômega-6 liberado e mobilizado no processo inflamatório (SAMUELSSON, 2012b; SHIMIZU, 2009). Sua biossíntese se dá via eventos metabólicos transcelulares durante a interação de leucócitos com células da mucosa e dentro dos vasos durante interações plaqueta-leucócitos (SERHAN, 2007; SERHAN; SAVILL, 2005).

Figura 2- Estrutura química da LXA_4 ($C_{20}H_{32}O_5$).

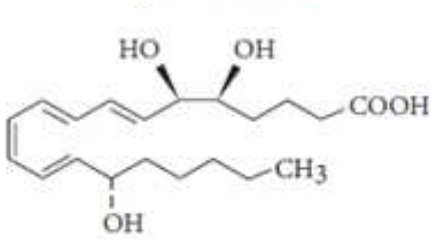

Fonte: (HAN et al., 2016).

A formação da LXA_4 pode acontecer através de duas vias de biossíntese diferentes, de forma independente ou simultânea na circulação sanguínea (FIORE; SERHAN, 1990). A primeira via acontece em eosinófilos, monócitos ou células epiteliais, e nessa via ocorre a inserção de O_2 ao grupo hidroxila do carbono 15 do AA, reação catalisada pela 15-Lipoxigenase. O produto intermediário 15S-H-(p)-ETE é liberado destas células, entrando em PMN ou monócitos, onde 5-Lipoxigenase gera 5S,6S, 15S-epoxitetraeno que então é hidrolisado dentro destas células por LXA_4 hidrolase, dando origem a LXA_4 bioativa (SERHAN; HAMBERG; SAMUELSSON, 1984a). Outra via de biossíntese da LXA_4 resulta da geração de LTA_4 a partir do AA por meio de 5-LOX nos leucócitos ou células epiteliais que posteriormente é liberada, captada pelas plaquetas e sofre metabolismo pela 12-LOX para produção de LXA_4 (EDENIUS; HAEGGSTRÖM; LINDGREN, 1988; FIORE; SERHAN, 1990) (Figura 3).

Figura 3- Vias de biossíntese da LXA_4. PMN (neutrófilos polimorfonucleares); PLT (plaquetas); LO (lipoxigenase).

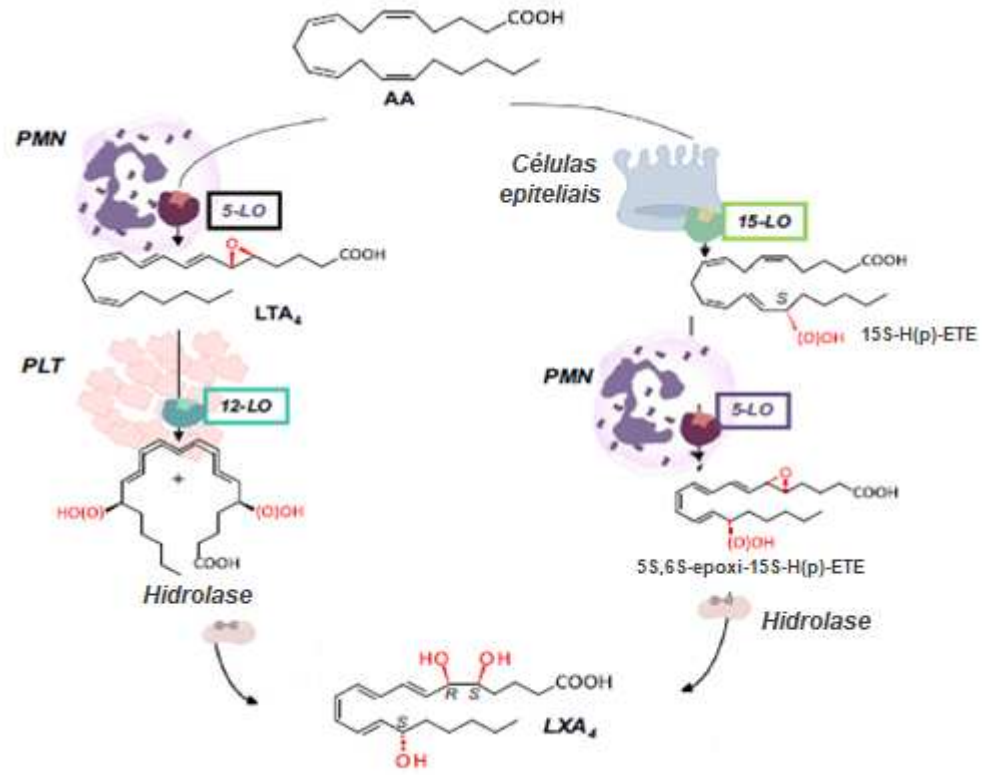

Fonte: Adaptado de (ROMANO et al., 2015). Polimorfonucleares (PMN), plaquetas (PLT), lipoxigenase (LO).

A LX atua na faixa de pico e nanogramas, possui ações como limitação do recrutamento, da quimiotaxia e da adesão de PMN, encerrando a lesão tecidual causada por essas células (MORRIS et al., 2009; SERHAN; SAVILL, 2005). Os membros da família das LXs atuam mediante interação ligante-receptor, sinalizando através de dois receptores, um receptor nuclear hidrocarboneto de arila (AhR) ou o GPCR conhecido como receptor de peptídeo formilado tipo 2 ou receptor de LXA_4 (ALX/FPR2), que foi o primeiro receptor eicosanoide derivado da lipoxigenase (LOX), isolado e clonado em tecidos humanos e animais (SERHAN, 1997). Em humanos o receptor ALX está presente em PMN, monócitos, células T e células residentes como macrófagos, sinoviais, fibroblastos e células epiteliais intestinais (CHIANG et al., 2006). De fato, em modelo de artrite induzida por soro K/BxN, camundongos que não expressam o receptor ALX/ FPR2 exibem maior gravidade da doença (DUFTON et al., 2010).

O papel da LXA_4 na resolução dos sinais de dor induzida pela inflamação já foi demonstrado em modelos murinos, onde houve diminuição da hiperalgesia térmica com baixas doses de 10 µg/kg administrados por via intravenosa (i.v.) ou 0,3 nmol i.t. (SVENSSON; ZATTONI; SERHAN, 2007). Posteriormente foi observado que a LXA_4 atenua liberação de citocinas pelos astrócitos espinhais e suprime a hiperalgesia mecânica no mesmo modelo, com administração de 0,1-1 µl i.t. de LXA_4 (SERHAN et al., 2003).

Trabalhos confirmam que a LXA_4 pode suprimir funções como a apresentação de antígeno e promover mudança do padrão de citocinas Th1 para Th2 (LIAO et al., 2013; PARKINSON, 2006), bem como inibir a translocação nuclear de NF-κB (SHI et al., 2017). Além do mais, possui forte papel antioxidante com inibição do estresse oxidativo (CUI et al., 2018), pela indução da expressão de fator nuclear eritróide relacionado ao fator 2 (Nrf2) e heme-oxigenase (HO), corroborando com trabalhos que apontam uma neuroproteção com redução de escore neurológico (WU et al., 2013). Outro achado indica uma proteção da LXA_4 na perda de memória induzida pelo peptídeo β-amiloide (PAMPLONA et al., 2012; PRÜSS et al., 2013).

Existem evidencias de que a LX pode ter impacto nas doenças articulares inflamatórias, pois foi observado que a LXA_4 inibe a liberação de metaloproteinases da matriz e citocinas por fibroblastos sinoviais humanos (SODIN-SEMRL et al., 2000). Também já foi observado aumento da expressão de ALX/FPR2 em pacientes acometidos por artrite reumatoide (HASHIMOTO et al., 2007). O tratamento com LXA_4 também demonstrou efeito protetor em modelo de artrite induzida por zimosan (CONTE et al., 2010). Tratamento local com LXA4 reduz o edema e o recrutamento de leucócitos de maneira dependente do receptor, pois o tratamento com BOC-1, um antagonista do receptor ALX/FPR2, anula os efeitos do LXA_4. Além disso, o tratamento com BML-111, um potente agonista de ALX/FPR2, também diminui o recrutamento de células imunes para a articulação do joelho (CONTE et al., 2010; ZHANG et al., 2008). Portanto, os diversos estudos a respeito da LXA_4 e seu efeito em modelos inflamatórios levaram a avaliação da eficácia da LXA_4 no modelo animal de artrite induzida de prótese.

1.8. PRODUTOS NATURAIS POLIFENÓLICOS

Produtos naturais fazem parte do cotidiano e necessidades básicas, como comidas, roupas, remédios e outros fins industriais durante muitas décadas. O uso de plantas ou parte delas para fins médicos são datados a mais de 2mil anos a.C (ALVES; ROSA, 2007; HUANG; CAI; ZHANG, 2010). Os polifenóis são considerados os principais agentes responsáveis pelas funções biológicas desses produtos naturais (KUMAR; PRUTHI; GOEL, 2015).

Existem diversos compostos fenólicos presentes em plantas medicinais e comestíveis, como flavonoides, curcuminoides, bioflavonoides, chalconoides, ácidos fenólicos, dentre outros (PERVEEN et al., 2017). Os biofenois naturais são um grupo amplo que compreende mais de 8 mil moléculas encontradas no reino vegetal. Suas moléculas apresentam um ou mais anéis aromáticos com um ou mais grupos hidroxilas. Os polifenóis vegetais incluem não flavonoides ou flavonoides. Dentre os mais estudados devido às suas propriedades saudáveis, como a curcumina que é encontrado no rizoma da *Curcuma longa*, assim como quercetina e miricetina, flavonoides presentes no chá, cebola, cacau e vinho (BRAVO, 1998). Especula-se que a ingestão dietética média de polifenóis seja de cerca de 1 g/dia (LERI et al., 2020).

A atividade antioxidante de polifenóis depende da estrutura de seus grupos funcionais e o número de grupos hidroxila influencia em vários mecanismos antioxidantes como por exemplo, eliminação de radicais livres, e capacidade de quelação de íons metálicos (HEIM; TAGLIAFERRO; BOBILYA, 2002). Essa atividade antioxidante se relaciona com a supressão da formação de EROs por inibição de envolvidas em sua produção, eliminação de EROs e regulação ou proteção das defesas antioxidantes (MISHRA et al., 2013). Também já foi descrito a atividade de polifenóis na inibição da atividade de xantina oxidase (NIJVELDT et al., 2001). Além disso, alguns estudos demonstraram o efeito do resveratrol em distúrbios neurodegenerativos por sua ação antioxidante, protegendo contra o declínio de memória (ZHAO et al., 2013).

Grande parte do efeito biológico estudo dos polifenóis é atribuído as propriedades antioxidantes, porém esses compostos apresentam outros efeitos importantes (LERI et al., 2020), como por exemplo, a redução da agregação de peptídeos/proteínas em conjuntos mieloides associados a doenças como Alzheimer e diabetes mellitus tipo 2 (STEFANI; RIGACCI, 2014).

Com relação aos efeitos anti-inflamatórios dos polifenóis, essa atividade se dá principalmente pela eliminação de radicais livres, regulação de atividades de células inflamatórias e modulação das atividades de enzimas envolvidas no metabolismo do AA como fosfolipase A2, LOX e Ciclo-oxigenases (COX), bem como modulando outras moléculas pró-inflamatórias como o NF-kB (SANTANGELO et al., 2007). Resveratrol e curcumina possuem fortes propriedades anti-inflamatórias e antioxidantes e exercem efeitos condroprotetores em culturas de condrócitos e explantes de cartilagem e modelos animais de osteoartrite. Foi demonstrado que esses polifenóis eliminam EROs e ativam o sistema de defesa antioxidante em condrócitos e suprimem a inflamação ao inibir as vias de sinalização pró-inflamatórias (ANSARI; AHMAD; HAQQI, 2020).

1.9. CURCUMINA

A curcumina foi descoberta cerca de dois séculos atrás, quando Vogel e Pelletier isolaram um composto amarelo dos rizomas da *Curcuma longa*, onde em 1842 conseguiram obter uma preparação pura do que antes era uma mistura de resina e óleo de açafrão (GUPTA et al., 2012; VOGEL, 1842). A estrutura química da curcumina foi identificada como diferuloilmetano, ou 1,6-heptadieno-3,5-diona-1,7-bis (4-hidroxi-3-metoxifenil)-(1E, 6E) em 1910 por Milobedzka e Lampe, posteriormente possibilitando a síntese do composto (GUPTA et al., 2012) (Figura 4).

Figura 4- Estrutura química da Curcumina.

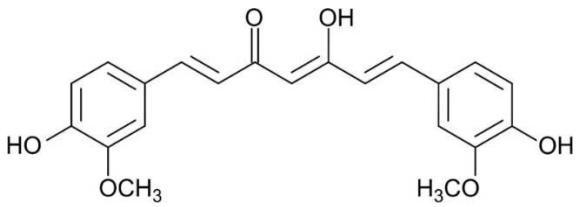

Fonte: (SHARIFI-RAD et al., 2020).

Embora tenha sido consumida por milhares de anos em países asiáticos como tempero dietético e para cura de doenças, as características biológicas da curcumina começaram a ser exploradas apenas a partir de 1949, onde Schraufstatter e colegas demonstraram que a curcumina era um componente

biológico ativo que possuía propriedades antibacterianas (SCHRAUFSTÄTTER; BERNT, 1949).

A curcumina é utilizada como suplemento em diversos países, por exemplo, no Japão é servido no chá, na Tailândia é usado em cosméticos, na China é usado como corante, na Coréia é servido em drinks, na Malásia é usado com antisséptico, e no Estados Unidos é usado como conservante e corante em molho de mostarda, queijo, manteiga e batata fritas. A sua comercialização é feita em diferentes formas, como cápsulas, comprimidos, pomadas, bebidas energéticas, sabonetes e cosméticos (GUPTA et al., 2012).

A curcumina foi definida como uma substância segura pelo FDA, demonstrando que não possui efeitos tóxicos aparentes. De acordo com comitês especialistas, o valor de digestão diária adequada da curcumina é 0 a 3 mg/kg. A ingestão de até 12g por dia de curcumina não demonstrou efeitos nocivos sobre indivíduos (LAO et al., 2006). Este composto é praticamente insolúvel em água, e sua estabilidade em solução aquosa depende do pH; a exposição à luz solar acelera sua degradação (PRIYADARSINI, 2009).

A curcumina mostrou regular diversas moléculas de sinalização celular, podendo causar regulação negativa ou positiva dependendo do alvo e do contexto celular (GUPTA et al., 2012). Dentre os principais alvos da curcumina podemos citar os fatores de transcrição pró-inflamatórios NF-κB, proteína ativadora-1 e transdutor de sinal e ativador de proteínas de transcrição (STAT), sendo responsáveis pela regulação da expressão de genes que contribuem para tumorigênese, sobrevivência celular, proliferação celular, angiogênese, dentro outras funções. A curcumina demonstrou regular negativamente esses fatores de transcrição (SHISHODIA; SINGH; CHATURVEDI, 2007).

Foi demonstrado o efeito citotóxico da curcumina em células tumorais pela indução do apoptose. Já foi elucidado também o efeito da curcumina na inibição da progressão do câncer em diversas etapas no processo de tumorigênese (DUVOIX et al., 2005). Curiosamente, a curcumina demonstrou sensibilizar tumores à quimioterapia, inibindo em partes, vias que levam à resistência ao tratamento (GOEL; AGGARWAL, 2010).

Alguns trabalhos demonstraram os efeitos anti-inflamatórios da curcumina pela redução do recrutamento de leucócitos e diminuição da ativação de NF-κB (FATTORI et al., 2015; WANG et al., 2018). Além de reduzir o edema articular

em artrite induzida por colágeno (WANG et al., 2019). A modulação de citocinas pró-inflamatórias como TNF-α e IL-1β também foi demonstrado em diferentes modelos (FATTORI et al., 2015; RINKUNAITE et al., 2021; WANG et al., 2019). Em modelo de inflamação induzida por partícula de titânio, foi observado que o tratamento com curcumina modula a polarização de macrófagos, aumentando o número macrófagos perfil M2, bem como os níveis de IL-10, reduzindo o número de macrófagos inflamatórios M1 e citocinas pró-inflamatórias IL-6 e TNF-α (LI et al., 2017).

O papel da curcumina na dor inflamatória foi explorado em modelo de dor induzida por ânion superóxido, onde 10mg/kg de curcumina reduziu a hiperalgesia térmica e mecânica, bem como o comportamento de dor espontânea (FATTORI et al., 2015). Além disso, tratamento com curcumina também reduziu a dor óssea induzida por câncer (ZHAO et al., 2021). No modelo de osteoartrite foi observado que a curcumina reduz a dor e a progressão da doença (ZHANG et al., 2016). O efeito analgésico da curcumina em modelo de colite induzida por sulfato sódico de dextrana (DSS) foi atribuído à redução da expressão de TRPV1 em GRDs (YANG et al., 2017).

Diversos estudos têm explorado o efeito antioxidante da curcumina, onde a eliminação de radicais livres foi demonstrada em vários estudos *in vitro*. A curcumina inibe completamente a produção *in vitro* de ânions superóxido, peróxido de hidrogênio e radical nitrito por macrófago de ratos (JOE; LOKESH, 1994). A inibição da peroxidação lipídica em preparação de microssomas de fígado de ratos também já foi demonstrada (PULLA REDDY; LOKESH, 1992). O efeito antioxidante da curcumina em modelo de nefropatia foi atribuído à diminuição do estresse oxidativo no rim, aumentando antioxidantes via Nrf2/HO-1 (DI TU et al., 2020). Essa via de sinalização já foi demonstrada ser regulada pela curcumina na medula espinal em modelo de injuria (JIN; BOTCHWAY; LIU, 2021). A administração de curcumina durante 28 dias demonstrou reduzir a dor neuropática por meio do aumento da enzima superóxido dismutase (SOD), glutationa peroxidase (GSH), bem como catalase, além disso, foi observado inibição da atividade de NF-κB e níveis de citocinas como TNF-α, IL-1β e IL-6 (ZHANG et al., 2020). Além dos trabalhos acerca do efeito terapêutico da curcumina em modelos animais, também tem sido explorado em testes clínicos,

principalmente para pacientes com osteoartrite (PAULTRE et al., 2021; ZENG et al., 2021).

2. OBJETIVOS

2.1. OBJETIVO GERAL

Avaliar os efeitos analgésicos, anti-inflamatórios e antioxidantes da curcumina e LXA_4 em modelo animal de artrite induzida por dióxido de titânio, um modelo de inflamação e dor induzida pelo uso de prótese.

2.2. OBJETIVOS ESPECÍFICOS

- Avaliar os efeitos do tratamento com LXA_4 na redução da Hiperalgesia mecânica, térmica e edema articular induzida por TiO_2;
- Analisar o efeito da LXA_4 nas alterações histopatológicas articulares e recrutamento leucocitário induzido por TiO_2;
- Verificar toxicidade hepática e renal, e lesão gástrica do tratamento crônico com LXA_4;
- Analisar o efeito da LXA_4 na modulação da produção de TNF-α, IL-1β, IL-6 e IL-10;
- Avaliar os efeitos do tratamento com LXA_4 no estresse oxidativo (ensaios de GSH e ABTS; expressão de Nrf2, níveis de EROs) induzido por TiO_2;
- Analisar o efeito da LXA_4 na ativação de NF-κB induzido por TiO_2;
- Verificar a expressão de ALXR/FPR2, TRPV1 e TRPA1, bem como ativação de NF-κB em neurônios do GRD no modelo e modulação após tratamento com LXA_4;
- Avaliar os efeitos do tratamento com curcumina na redução da hiperalgesia mecânica, térmica, edema e alterações histopatológicas no modelo de artrite induzida por TiO_2;
- Analisar os efeitos da curcumina na modulação do recrutamento leucocitário, estresse oxidativo (ensaios de TBARS e NBT; detecção de EROs e NO) e produção de IL-1β induzido por TiO_2;
- Avaliar o efeito da curcumina na expressão e ativação de TRPV1 e TRPA1, bem como ativação de NF-κB em neurônios do GRD;

3. REFERÊNCIAS

ABDELMOATY, S. et al. Spinal actions of lipoxin A4 and 17(R)-resolvin D1 attenuate inflammation-induced mechanical hypersensitivity and spinal TNF release. **PloS one**, v. 8, n. 9, 24 set. 2013.

AKIRA, S. Innate immunity and adjuvants. **Philosophical Transactions of the Royal Society B: Biological Sciences**, v. 366, n. 1579, p. 2748–2755, 12 out. 2011.

ALLEN, B. L. et al. Imbalance of proresolving lipid mediators in persistent allodynia dissociated from signs of clinical arthritis. **Pain**, v. 161, n. 9, p. 2155–2166, 1 set. 2020.

ALVES, R. R. N.; ROSA, I. M. L. Biodiversity, traditional medicine and public health: where do they meet? **Journal of ethnobiology and ethnomedicine**, v. 3, 21 mar. 2007.

ANSARI, M. Y.; AHMAD, N.; HAQQI, T. M. Oxidative stress and inflammation in osteoarthritis pathogenesis: Role of polyphenols. **Biomedicine & pharmacotherapy = Biomedecine & pharmacotherapie**, v. 129, 1 set. 2020.

ARDEN, N.; NEVITT, M. C. Osteoarthritis: epidemiology. **Best practice & research. Clinical rheumatology**, v. 20, n. 1, p. 3–25, fev. 2006.

ARNARDOTTIR, H. H. et al. Resolvin D3 Is Dysregulated in Arthritis and Reduces Arthritic Inflammation. **Journal of immunology (Baltimore, Md. : 1950)**, v. 197, n. 6, p. 2362–2368, 15 set. 2016.

AURSNES, M. et al. Synthesis of the 16S,17S-Epoxyprotectin Intermediate in the Biosynthesis of Protectins by Human Macrophages. **Journal of natural products**, v. 78, n. 12, p. 2924–2931, 24 dez. 2015.

BANNENBERG, G. L. et al. Molecular circuits of resolution: formation and actions of resolvins and protectins. **Journal of immunology (Baltimore, Md. : 1950)**, v. 174, n. 7, p. 4345–4355, 1 abr. 2005.

BERNARD, C.; TEDGUI, A. Cytokine network and the vessel wall. Insights into septic shock pathogenesis. **European cytokine network**, v. 3, n. 1, p. 19–33, 1992.

BÖRGESON, E. et al. Lipoxin A_4 and benzo-lipoxin A_4 attenuate experimental renal fibrosis. **FASEB journal : official publication of the Federation of American Societies for Experimental Biology**, v. 25, n. 9, p. 2967–2979, set. 2011.

BORGHI, S. M. et al. The flavonoid quercetin inhibits titanium dioxide (TiO2)-induced chronic arthritis in mice. **The Journal of nutritional biochemistry**, v. 53, p. 81–95, 1 mar. 2018.

BRAVO, L. Polyphenols: chemistry, dietary sources, metabolism, and nutritional significance. **Nutrition reviews**, v. 56, n. 11, p. 317–333, 1998.

BRAZ, J. et al. Transmitting pain and itch messages: a contemporary view of the spinal cord circuits that generate gate control. **Neuron**, v. 82, n. 3, p. 522–536, 7 maio 2014.

BRUYÈRE, O. et al. Health-related quality of life after total knee or hip replacement for osteoarthritis: a 7-year prospective study. **Archives of orthopaedic and trauma surgery**, v. 132, n. 11, p. 1583–1587, nov. 2012.

BUCKLEY, C. D.; GILROY, D. W.; SERHAN, C. N. Proresolving Lipid Mediators and Mechanisms in the Resolution of Acute Inflammation. **Immunity**, v. 40, n. 3, p. 315–327, 20 mar. 2014a.

BUCKLEY, C. D.; GILROY, D. W.; SERHAN, C. N. Proresolving lipid mediators and mechanisms in the resolution of acute inflammation. **Immunity**, v. 40, n. 3, p. 315–327, 20 mar. 2014b.

BUFFON, A. et al. Preprocedural serum levels of C-reactive protein predict early complications and late restenosis after coronary angioplasty. **Journal of the American College of Cardiology**, v. 34, n. 5, p. 1512–1521, 1 nov. 1999.

CALATI, R. et al. The impact of physical pain on suicidal thoughts and behaviors: Meta-analyses. **Journal of psychiatric research**, v. 71, p. 16–32, 1 dez. 2015.

CALLAHAN, C. M. et al. Patient outcomes following unicompartmental or bicompartmental knee arthroplasty. A meta-analysis. **The Journal of Arthroplasty**, v. 10, n. 2, p. 141–150, 1995.

CHEN, J. et al. In vivo acute toxicity of titanium dioxide nanoparticles to mice after intraperitioneal injection. **Journal of applied toxicology : JAT**, v. 29, n. 4, p. 330–337, maio 2009.

CHIANG, N. et al. The lipoxin receptor ALX: potent ligand-specific and stereoselective actions in vivo. **Pharmacological reviews**, v. 58, n. 3, p. 463–487, 2006.

CHIANG, N.; SERHAN, C. N. Structural elucidation and physiologic functions of specialized pro-resolving mediators and their receptors. **Molecular aspects of medicine**, v. 58, p. 114–129, 1 dez. 2017.

COBELLI, N. et al. Mediators of the inflammatory response to joint replacement devices. **Nature reviews. Rheumatology**, v. 7, n. 10, p. 600–608, out. 2011.

CONTE, F. P. et al. Lipoxin A(4) attenuates zymosan-induced arthritis by modulating endothelin-1 and its effects. **British journal of pharmacology**, v. 161, n. 4, p. 911–924, out. 2010.

CUI, K. et al. Lipoxin A4 improves erectile dysfunction in rats with type I diabetes by inhibiting oxidative stress and corporal fibrosis. **Asian journal of andrology**, v. 20, n. 2, p. 166, 2018.

CUNHA, F. Q. et al. The pivotal role of tumour necrosis factor alpha in the development of inflammatory hyperalgesia. **British journal of pharmacology**, v. 107, n. 3, p. 660–664, 1992.

CUNHA, T. M. et al. Crucial role of neutrophils in the development of mechanical inflammatory hypernociception. **Journal of leukocyte biology**, v. 83, n. 4, p. 824–832, 22 jan. 2008.

DALLI, J.; SERHAN, C. Macrophage Proresolving Mediators-the When and Where. **Microbiology spectrum**, v. 4, n. 3, 6 maio 2016.

DAR, G. I.; SAEED, M.; WU, A. Toxicity of TiO2 Nanoparticles. **TiO**, p. 67–103, 12 fev. 2020.

DE PETROCELLIS, L. et al. Actions of two naturally occurring saturated N-acyldopamines on transient receptor potential vanilloid 1 (TRPV1) channels. **British journal of pharmacology**, v. 143, n. 2, p. 251–256, set. 2004.

DESANTANA, J. M. et al. Revised definition of pain after four decades. **BrJP**, v. 3, n. 3, p. 197–198, 21 set. 2020.

DI TU, Q. et al. Curcumin Improves the Renal Autophagy in Rat Experimental Membranous Nephropathy via Regulating the PI3K/AKT/mTOR and Nrf2/HO-1 Signaling Pathways. **BioMed Research International**, v. 2020, 2020.

DIB-HAJJ, S. D.; WAXMAN, S. G. Translational pain research: Lessons from genetics and genomics. **Science translational medicine**, v. 6, n. 249, 13 ago. 2014.

D'MELLO, R.; DICKENSON, A. H. Spinal cord mechanisms of pain. **British journal of anaesthesia**, v. 101, n. 1, p. 8–16, 2008.

DÖRNER, T. et al. Implant-related inflammatory arthritis. **Nature clinical practice. Rheumatology**, v. 2, n. 1, p. 53–56, jan. 2006.

DUFTON, N. et al. Anti-inflammatory role of the murine formyl-peptide receptor 2: ligand-specific effects on leukocyte responses and experimental inflammation. **Journal of immunology (Baltimore, Md. : 1950)**, v. 184, n. 5, p. 2611–2619, 1 mar. 2010.

DUVOIX, A. et al. Chemopreventive and therapeutic effects of curcumin. **Cancer letters**, v. 223, n. 2, p. 181–190, 8 jun. 2005.

EDENIUS, C.; HAEGGSTRÖM, J.; LINDGREN, J. Å. Transcellular conversion of endogenous arachidonic acid to lipoxins in mixed human platelet-granulocyte suspensions. **Biochemical and biophysical research communications**, v. 157, n. 2, p. 801–807, 15 dez. 1988.

FATTORI, V. et al. Curcumin inhibits superoxide anion-induced pain-like behavior and leukocyte recruitment by increasing Nrf2 expression and reducing NF-κB activation. **Inflammation Research 2015 64:12**, v. 64, n. 12, p. 993–1003, 11 out. 2015.

FATTORI, V. et al. The specialised pro-resolving lipid mediator maresin 1 reduces inflammatory pain with a long-lasting analgesic effect. **British Journal of Pharmacology**, v. 176, n. 11, p. 1728–1744, 15 jun. 2019.

FATTORI, V.; AMARAL, F. A.; VERRI, W. A. Neutrophils and arthritis: Role in disease and pharmacological perspectives. **Pharmacological research**, v. 112, p. 84–98, 1 out. 2016.

FEI YIN, Z. et al. Recent progress in biomedical applications of titanium dioxide. **Physical chemistry chemical physics : PCCP**, v. 15, n. 14, p. 4844–4858, 14 abr. 2013.

FERNANDES, E. S.; FERNANDES, M. A.; KEEBLE, J. E. The functions of TRPA1 and TRPV1: moving away from sensory nerves. **British journal of pharmacology**, v. 166, n. 2, p. 510–521, 2012.

FERREIRA, S. H. The role of interleukins and nitric oxide in the mediation of inflammatory pain and its control by peripheral analgesics. **Drugs**, v. 46 Suppl 1, n. 1, p. 1–9, 1993.

FERREIRA, S. H.; NAKAMURA, M. I - Prostaglandin hyperalgesia, a cAMP/Ca2+ dependent process. **Prostaglandins**, v. 18, n. 2, p. 179–190, 1 ago. 1979.

FERREIRA, S. H.; ROMITELLI, M.; DE NUCCI, G. Endothelin-1 participation in overt and inflammatory pain. **Journal of cardiovascular pharmacology**, v. 13 Suppl 5, p. S220–S222, 1989.

FIORE, S.; SERHAN, C. N. Formation of lipoxins and leukotrienes during receptor-mediated interactions of human platelets and recombinant human granulocyte/macrophage colony-stimulating factor-primed neutrophils. **The Journal of experimental medicine**, v. 172, n. 5, p. 1451–1457, 1 nov. 1990.

FLOWER, R. J. Prostaglandins, bioassay and inflammation. **British journal of pharmacology**, v. 147 Suppl 1, n. Suppl 1, jan. 2006.

FOXMAN, E. F.; CAMPBELL, J. J.; BUTCHER, E. C. Multistep navigation and the combinatorial control of leukocyte chemotaxis. **The Journal of cell biology**, v. 139, n. 5, p. 1349–1360, 1 dez. 1997.

FRITZ, J. H. et al. Nod-like proteins in immunity, inflammation and disease. **Nature immunology**, v. 7, n. 12, p. 1250–1257, dez. 2006.

GARRISON, S. R.; STUCKY, C. L. Contribution of transient receptor potential ankyrin 1 to chronic pain in aged mice with complete Freund's adjuvant-induced arthritis. **Arthritis & rheumatology (Hoboken, N.J.)**, v. 66, n. 9, p. 2380–2390, 2014.

GHILARDI, J. R. et al. Selective blockade of the capsaicin receptor TRPV1 attenuates bone cancer pain. **The Journal of neuroscience : the official journal of the Society for Neuroscience**, v. 25, n. 12, p. 3126–3131, 23 mar. 2005.

GOEL, A.; AGGARWAL, B. B. Curcumin, the Golden Spice From Indian Saffron, Is a Chemosensitizer and Radiosensitizer for Tumors and Chemoprotector and Radioprotector for Normal Organs. **https://doi.org/10.1080/01635581.2010.509835**, v. 62, n. 7, p. 919–930, out. 2010.

GOLDSTEIN, J. L.; CRYER, B. Gastrointestinal injury associated with NSAID use: a case study and review of risk factors and preventative strategies. **Drug, healthcare and patient safety**, v. 7, p. 31–41, 22 jan. 2015.

GUPTA, S. C. et al. Discovery of curcumin, a component of golden spice, and its miraculous biological activities. **Clinical and experimental pharmacology & physiology**, v. 39, n. 3, p. 283–299, mar. 2012.

HAN, X. et al. Lipoxin A4 Preconditioning Attenuates Intestinal Ischemia Reperfusion Injury through Keap1/Nrf2 Pathway in a Lipoxin A4 Receptor Independent Manner. **Oxidative medicine and cellular longevity**, v. 2016, 2016.

HARDY, J. D.; WOLFF, H. G.; GOODELL, H. Experimental evidence on the nature of cutaneous hyperalgesia. **The Journal of clinical investigation**, v. 29, n. 1, p. 115–140, 1950.

HARRIS, W. H. Wear and periprosthetic osteolysis: the problem. **Clinical orthopaedics and related research**, v. 393, n. 393, p. 66–70, 2001.

HASHIMOTO, A. et al. Antiinflammatory mediator lipoxin A4 and its receptor in synovitis of patients with rheumatoid arthritis. **The Journal of rheumatology**, v. 34, n. 11, p. 2144–53, nov. 2007.

HEIM, K. E.; TAGLIAFERRO, A. R.; BOBILYA, D. J. Flavonoid antioxidants: Chemistry, metabolism and structure-activity relationships. **Journal of Nutritional Biochemistry**, v. 13, n. 10, p. 572–584, 1 out. 2002.

HENRY, J. L. Effects of substance P on functionally identified units in cat spinal cord. **Brain research**, v. 114, n. 3, p. 439–451, 24 set. 1976.

HUANG, L. et al. Enduring prevention and transient reduction of postoperative pain by intrathecal resolvin D1. **Pain**, v. 152, n. 3, p. 557–565, mar. 2011.

HUANG, S. M. et al. An endogenous capsaicin-like substance with high potency at recombinant and native vanilloid VR1 receptors. **Proceedings of the National Academy of Sciences of the United States of America**, v. 99, n. 12, p. 8400–8405, 11 jun. 2002.

HUANG, W. Y.; CAI, Y. Z.; ZHANG, Y. Natural phenolic compounds from medicinal herbs and dietary plants: potential use for cancer prevention. **Nutrition and cancer**, v. 62, n. 1, p. 1–20, jan. 2010.

INOHARA, N. et al. NOD-LRR proteins: role in host-microbial interactions and inflammatory disease. **Annual review of biochemistry**, v. 74, p. 355–383, 2005.

JACOBS, J. J. et al. Release and excretion of metal in patients who have a total hip-replacement component made of titanium-base alloy. **The Journal of bone and joint surgery. American volume**, v. 73, n. 10, p. 1475–86, dez. 1991.

JANCSÓ, N.; JANCSÓ-GÁBOR, A.; SZOLCSÁNYI, J. Direct evidence for neurogenic inflammation and its prevention by denervation and by pretreatment with capsaicin. **British Journal of Pharmacology and Chemotherapy**, v. 31, n. 1, p. 138, 1967.

JANEWAY, C. A. Approaching the asymptote? Evolution and revolution in immunology. **Cold Spring Harbor symposia on quantitative biology**, v. 54 Pt 1, n. 1, p. 1–13, 1989.

JIN, S. et al. Maresin 1 improves the Treg/Th17 imbalance in rheumatoid arthritis through miR-21. **Annals of the rheumatic diseases**, v. 77, n. 11, p. 1644–1652, 1 nov. 2018.

JIN, W.; BOTCHWAY, B. O. A.; LIU, X. Curcumin Can Activate the Nrf2/HO-1 Signaling Pathway and Scavenge Free Radicals in Spinal Cord Injury Treatment. **Neurorehabilitation and neural repair**, v. 35, n. 7, p. 576–584, 1 jul. 2021.

JOE, B.; LOKESH, B. R. Role of capsaicin, curcumin and dietary n — 3 fatty acids in lowering the generation of reactive oxygen species in rat peritoneal macrophages. **Biochimica et Biophysica Acta (BBA) - Molecular Cell Research**, v. 1224, n. 2, p. 255–263, 10 nov. 1994.

KAIDA, T. et al. Optical characteristics of titanium oxide interference film and the film laminated with oxides and their applications for cosmetics. **Journal of cosmetic science**, v. 55, n. 2, p. 219–20, 2004.

KANE, R. L. et al. The functional outcomes of total knee arthroplasty. **The Journal of bone and joint surgery. American volume**, v. 87, n. 8, p. 1719–1724, 2005.

KOIVISTO, A. et al. TRPA1: a transducer and amplifier of pain and inflammation. **Basic & clinical pharmacology & toxicology**, v. 114, n. 1, p. 50–55, jan. 2014.

KREMERS, H. M. et al. Prevalence of Total Hip and Knee Replacement in the United States. **The Journal of bone and joint surgery. American volume**, v. 97, n. 17, p. 1386–1397, 2 set. 2015.

KRÖNKE, G. et al. 12/15-lipoxygenase counteracts inflammation and tissue damage in arthritis. **Journal of immunology (Baltimore, Md. : 1950)**, v. 183, n. 5, p. 3383–3389, 1 set. 2009.

KUMAR, N.; PRUTHI, V.; GOEL, N. Structural, thermal and quantum chemical studies of p-coumaric and caffeic acids. **Journal of Molecular Structure**, v. 1085, p. 242–248, 5 abr. 2015.

KURTZ, S. et al. Projections of primary and revision hip and knee arthroplasty in the United States from 2005 to 2030. **The Journal of bone and joint surgery. American volume**, v. 89, n. 4, p. 780–785, 2007.

LAO, C. D. et al. Dose escalation of a curcuminoid formulation. **BMC complementary and alternative medicine**, v. 6, 17 mar. 2006.

LATORRE, R.; ZAELZER, C.; BRAUCHI, S. Structure-functional intimacies of transient receptor potential channels. **Quarterly reviews of biophysics**, v. 42, n. 3, p. 201–246, ago. 2009.

LAWRENCE, R. C. et al. Estimates of the prevalence of arthritis and other rheumatic conditions in the United States. Part II. **Arthritis and Rheumatism**, v. 58, n. 1, p. 26–35, jan. 2008.

LEE, C. H. Resolvins as new fascinating drug candidates for inflammatory diseases. **Archives of pharmacal research**, v. 35, n. 1, p. 3–7, jan. 2012.

LERI, M. et al. Healthy Effects of Plant Polyphenols: Molecular Mechanisms. **International journal of molecular sciences**, v. 21, n. 4, 1 fev. 2020.

LEVINE, J. D.; FIELDS, H. L.; BASBAUM, A. I. Peptides and the primary afferent nociceptor. **Journal of Neuroscience**, v. 13, n. 6, p. 2273–2286, 1 jun. 1993.

LEVY, B. D. et al. Lipid mediator class switching during acute inflammation: signals in resolution. **Nature immunology**, v. 2, n. 7, p. 612–619, 2001.

LEVY, B. D.; SERHAN, C. N. Resolution of acute inflammation in the lung. **Annual review of physiology**, v. 76, p. 467–492, fev. 2014.

LI, B. et al. Curcumin attenuates titanium particle-induced inflammation by regulating macrophage polarization in vitro and in vivo. **Frontiers in Immunology**, v. 8, n. JAN, p. 55, 31 jan. 2017.

LIAO, W. et al. Lipoxin A4 attenuates acute rejection via shifting TH1/TH2 cytokine balance in rat liver transplantation. **Transplantation proceedings**, v. 45, n. 6, p. 2451–2454, jul. 2013.

LIU, R. et al. Small-sized titanium dioxide nanoparticles mediate immune toxicity in rat pulmonary alveolar macrophages in vivo. **Journal of nanoscience and nanotechnology**, v. 10, n. 8, p. 5161–5169, ago. 2010.

LIUZZO, G. et al. Enhanced inflammatory response in patients with preinfarction unstable angina. **Journal of the American College of Cardiology**, v. 34, n. 6, p. 1696–1703, 15 nov. 1999.

MACIEJ SERDA et al. Artroplastia total de joelho e quadril: a preocupante realidade assistencial do Sistema Único de Saúde brasileiro. **Revista Brasileira de Ortopedia**, v. 53, n. 4, p. 432–440, 2018.

MADERNA, P.; GODSON, C. Lipoxins: resolutionary road. **British journal of pharmacology**, v. 158, n. 4, p. 947–959, out. 2009.

MAKUMIRE, S. et al. Immunomodulatory activity of zinc peroxide (ZnO_2) and titanium dioxide (TiO_2) nanoparticles and their effects on DNA and protein integrity. **Toxicology letters**, v. 227, n. 1, p. 56–64, 16 maio 2014.

MALAWISTA, S. E. et al. Tonic inhibition of chemotaxis in human plasma. **Proceedings of the National Academy of Sciences of the United States of America**, v. 105, n. 46, p. 17949–17954, 18 nov. 2008.

MARIATHASAN, S.; MONACK, D. M. Inflammasome adaptors and sensors: intracellular regulators of infection and inflammation. **Nature reviews. Immunology**, v. 7, n. 1, p. 31–40, jan. 2007.

MCDONALD, B. et al. Intravascular danger signals guide neutrophils to sites of sterile inflammation. **Science (New York, N.Y.)**, v. 330, n. 6002, p. 362–366, 15 out. 2010.

MEDZHITOV, R. Recognition of microorganisms and activation of the immune response. **Nature 2007 449:7164**, v. 449, n. 7164, p. 819–826, 17 out. 2007.

MEDZHITOV, R. Origin and physiological roles of inflammation. **Nature**, v. 454, n. 7203, p. 428–435, 24 jul. 2008.

MILLIGAN, E. D.; WATKINS, L. R. Pathological and protective roles of glia in chronic pain. **Nature reviews. Neuroscience**, v. 10, n. 1, p. 23–36, jan. 2009.

MINOZZI, S. et al. Risk of infections using anti-TNF agents in rheumatoid arthritis, psoriatic arthritis, and ankylosing spondylitis: a systematic review and meta-analysis. **Expert opinion on drug safety**, v. 15, n. sup1, p. 11–34, 2016.

MISHRA, A. et al. Bauhinia variegata leaf extracts exhibit considerable antibacterial, antioxidant, and anticancer activities. **BioMed research international**, v. 2013, 2013.

MORRIS, T. et al. Effects of low-dose aspirin on acute inflammatory responses in humans. **J Immunol**, v. 183, n. 3, p. 2089–2096, 2009.

NASH, M. S. et al. 7-tert-Butyl-6-(4-chloro-phenyl)-2-thioxo-2,3-dihydro-1H-pyrido[2,3-d]pyrimidin-4-one, a classic polymodal inhibitor of transient receptor potential vanilloid type 1 with a reduced liability for hyperthermia, is analgesic and ameliorates visceral hypersensitivity. **The Journal of pharmacology and experimental therapeutics**, v. 342, n. 2, p. 389–398, ago. 2012.

NATHAN, C.; DING, A. Nonresolving inflammation. **Cell**, v. 140, n. 6, p. 871–882, 2010.

NIJVELDT, R. J. et al. Flavonoids: a review of probable mechanisms of action and potential applications. **The American journal of clinical nutrition**, v. 74, n. 4, p. 418–425, 2001.

NORLING, L. V.; PERRETTI, M. The role of omega-3 derived resolvins in arthritis. **Current opinion in pharmacology**, v. 13, n. 3, p. 476–481, jun. 2013.

NÚÑEZ, M. et al. Health-related quality of life in patients with osteoarthritis after total knee replacement: factors influencing outcomes at 36 months of follow-up. **Osteoarthritis and cartilage**, v. 15, n. 9, p. 1001–1007, set. 2007.

ORTLIEB, M. White Giant or White Dwarf?: Particle Size Distribution Measurements of TiO2. **GIT laboratory journal Europe**, 2010.

PAMPLONA, F. A. et al. Anti-inflammatory lipoxin A4 is an endogenous allosteric enhancer of CB1 cannabinoid receptor. **Proceedings of the National Academy of Sciences of the United States of America**, v. 109, n. 51, p. 21134–21139, 18 dez. 2012.

PARK, C. K. Maresin 1 Inhibits TRPV1 in Temporomandibular Joint-Related Trigeminal Nociceptive Neurons and TMJ Inflammation-Induced Synaptic Plasticity in the Trigeminal Nucleus. **Mediators of inflammation**, v. 2015, 2015.

PARKINSON, J. F. Lipoxin and synthetic lipoxin analogs: an overview of anti-inflammatory functions and new concepts in immunomodulation. **Inflammation & allergy drug targets**, v. 5, n. 2, p. 91–106, abr. 2006.

PAULTRE, K. et al. Therapeutic effects of turmeric or curcumin extract on pain and function for individuals with knee osteoarthritis: a systematic review. **BMJ open sport & exercise medicine**, v. 7, n. 1, 2021.

PERVEEN, S. et al. Phenolic Compounds from the Natural Sources and Their Cytotoxicity. **Phenolic Compounds - Natural Sources, Importance and Applications**, 15 mar. 2017.

PINHO-RIBEIRO, F. A.; VERRI, W. A.; CHIU, I. M. Nociceptor Sensory Neuron-Immune Interactions in Pain and Inflammation. **Trends in immunology**, v. 38, n. 1, p. 5–19, 1 jan. 2017.

PRIYADARSINI, K. I. Photophysics, photochemistry and photobiology of curcumin: Studies from organic solutions, bio-mimetics and living cells. **Journal of Photochemistry and Photobiology C: Photochemistry Reviews**, v. 10, n. 2, p. 81–95, 1 jun. 2009.

PRÜSS, H. et al. Proresolution lipid mediators in multiple sclerosis - differential, disease severity-dependent synthesis - a clinical pilot trial. **PloS one**, v. 8, n. 2, 8 fev. 2013.

PULLA REDDY, A. C.; LOKESH, B. R. Studies on spice principles as antioxidants in the inhibition of lipid peroxidation of rat liver microsomes. **Molecular and cellular biochemistry**, v. 111, n. 1–2, p. 117–124, abr. 1992.

RANG, H. P.; BEVAN, S.; DRAY, A. Chemical activation of nociceptive peripheral neurones. **British medical bulletin**, v. 47, n. 3, p. 534–548, 1991.

RIBEIRO, R. A. et al. Involvement of resident macrophages and mast cells in the writhing nociceptive response induced by zymosan and acetic acid in mice. **European journal of pharmacology**, v. 387, n. 1, p. 111–118, 3 nov. 2000.

RINKUNAITE, I. et al. Anti-inflammatory effect of different curcumin preparations on adjuvant-induced arthritis in rats. **BMC complementary medicine and therapies**, v. 21, n. 1, 1 dez. 2021.

ROMANO, M. et al. Lipoxins and aspirin-triggered lipoxins in resolution of inflammation. **Eur J Pharmacol**, v. 760, p. 49–63, 2015.

RUPAREL, N. B. et al. Homologous and heterologous desensitization of capsaicin and mustard oil responses utilize different cellular pathways in nociceptors. **Pain**, v. 135, n. 3, p. 271–279, 2008.

SACHS, D. et al. Tumour necrosis factor-α, interleukin-1β and interleukin-8 induce persistent mechanical nociceptor hypersensitivity. **Pain**, v. 96, n. 1–2, p. 89–97, 2002.

SAMUELSSON, B. Role of basic science in the development of new medicines: examples from the eicosanoid field. **The Journal of biological chemistry**, v. 287, n. 13, p. 10070–10080, 23 mar. 2012a.

SAMUELSSON, B. Role of basic science in the development of new medicines: examples from the eicosanoid field. **The Journal of biological chemistry**, v. 287, n. 13, p. 10070–10080, 23 mar. 2012b.

SANTANGELO, C. et al. Polyphenols, intracellular signalling and inflammation. **Annali dell'Istituto superiore di sanita**, v. 43, n. 4, p. 394–405, 2007.

SCHMALSTIEG, F. C.; GOLDMAN, A. S. Ilya Ilich Metchnikoff (1845-1915) and Paul Ehrlich (1854-1915): the centennial of the 1908 Nobel Prize in Physiology or Medicine. **Journal of medical biography**, v. 16, n. 2, p. 96–103, 2008.

SCHOLZ, J.; WOOLF, C. J. Can we conquer pain? **Nature neuroscience**, v. 5 Suppl, n. 11s, p. 1062–1067, 2002.

SCHRAUFSTÄTTER, E.; BERNT, H. Antibacterial action of curcumin and related compounds. **Nature**, v. 164, n. 4167, p. 456–457, 1949.

SCHUMACHER, M. A. Transient receptor potential channels in pain and inflammation: therapeutic opportunities. **Pain practice : the official journal of World Institute of Pain**, v. 10, n. 3, p. 185–200, 2010.

SCHUMACHER, M.; GUAN, Z.; HELLMAN, J. Contemporary views on inflammatory pain mechanisms: TRPing over innate and microglial pathways. **F1000Research**, v. 5, 2016.

SERHAN, C. N. Lipoxin biosynthesis and its impact in inflammatory and vascular events. **Biochimica et Biophysica Acta (BBA) - Lipids and Lipid Metabolism**, v. 1212, n. 1, p. 1–25, 14 abr. 1994.

SERHAN, C. N. Lipoxins and novel aspirin-triggered 15-epi-lipoxins (ATL): A jungle of cell-cell interactions or a therapeutic opportunity? **Prostaglandins**, v. 53, n. 2, p. 107–137, fev. 1997.

SERHAN, C. N. et al. Novel Functional Sets of Lipid-Derived Mediators with Antiinflammatory Actions Generated from Omega-3 Fatty Acids via Cyclooxygenase 2–Nonsteroidal Antiinflammatory Drugs and Transcellular Processing. **Journal of Experimental Medicine**, v. 192, n. 8, p. 1197–1204, 16 out. 2000.

SERHAN, C. N. et al. Resolvins: a family of bioactive products of omega-3 fatty acid transformation circuits initiated by aspirin treatment that counter proinflammation signals. **The Journal of experimental medicine**, v. 196, n. 8, p. 1025–1037, 21 out. 2002.

SERHAN, C. N. et al. Reduced inflammation and tissue damage in transgenic rabbits overexpressing 15-lipoxygenase and endogenous anti-inflammatory lipid mediators. **Journal of immunology (Baltimore, Md. : 1950)**, v. 171, n. 12, p. 6856–6865, 15 dez. 2003.

SERHAN, C. N. Resolution phase of inflammation: novel endogenous anti-inflammatory and proresolving lipid mediators and pathways. **Annual review of immunology**, v. 25, p. 101–137, 2007.

SERHAN, C. N. et al. Maresins: novel macrophage mediators with potent antiinflammatory and proresolving actions. **Journal of Experimental Medicine**, v. 206, n. 1, p. 15–23, 16 jan. 2009.

SERHAN, C. N. Novel lipid mediators and resolution mechanisms in acute inflammation: to resolve or not? **The American journal of pathology**, v. 177, n. 4, p. 1576–1591, 2010.

SERHAN, C. N. et al. Macrophage proresolving mediator maresin 1 stimulates tissue regeneration and controls pain. **FASEB journal : official publication of the Federation of American Societies for Experimental Biology**, v. 26, n. 4, p. 1755–1765, abr. 2012a.

SERHAN, C. N. et al. Macrophage proresolving mediator maresin 1 stimulates tissue regeneration and controls pain. **The FASEB Journal**, v. 26, n. 4, p. 1755–1765, 1 abr. 2012b.

SERHAN, C. N. Pro-resolving lipid mediators are leads for resolution physiology. **Nature**, v. 510, n. 7503, p. 92–101, 2014.

SERHAN, C. N. et al. Lipid Mediators in the Resolution of Inflammation. **Cold Spring Harbor Perspectives in Biology**, v. 7, n. 2, 2015.

SERHAN, C. N. Treating inflammation and infection in the 21st century: new hints from decoding resolution mediators and mechanisms. **The FASEB Journal**, v. 31, n. 4, p. 1273–1288, 1 abr. 2017a.

SERHAN, C. N. Discovery of specialized pro-resolving mediators marks the dawn of resolution physiology and pharmacology. **Molecular aspects of medicine**, v. 58, p. 1–11, 1 dez. 2017b.

SERHAN, C. N.; CHIANG, N. Resolution phase lipid mediators of inflammation: agonists of resolution. **Current opinion in pharmacology**, v. 13, n. 4, p. 632–640, 2013.

SERHAN, C. N.; CHIANG, N.; DALLI, J. The resolution code of acute inflammation: Novel pro-resolving lipid mediators in resolution. **Seminars in immunology**, v. 27, n. 3, p. 200–215, 1 maio 2015.

SERHAN, C. N.; HAMBERG, M.; SAMUELSSON, B. Lipoxins: novel series of biologically active compounds formed from arachidonic acid in human leukocytes. **Proceedings of the National Academy of Sciences of the United States of America**, v. 81, n. 17, p. 5335–5339, 1984a.

SERHAN, C. N.; HAMBERG, M.; SAMUELSSON, B. Trihydroxytetraenes: a novel series of compounds formed from arachidonic acid in human leukocytes. **Biochemical and biophysical research communications**, v. 118, n. 3, p. 943–949, 14 fev. 1984b.

SERHAN, C. N.; SAVILL, J. Resolution of inflammation: the beginning programs the end. **Nat Immunol**, v. 6, n. 12, p. 1191–1197, 2005.

SHARIFI-RAD, J. et al. Turmeric and Its Major Compound Curcumin on Health: Bioactive Effects and Safety Profiles for Food, Pharmaceutical, Biotechnological and Medicinal Applications. **Frontiers in Pharmacology**, v. 11, p. 1021, 15 set. 2020.

SHELDON, I. M.; OWENS, S. E.; TURNER, M. L. Innate immunity and the sensing of infection, damage and danger in the female genital tract. **Journal of reproductive immunology**, v. 119, p. 67–73, 1 fev. 2017.

SHI, H. et al. Titanium dioxide nanoparticles: a review of current toxicological data. **Particle and Fibre Toxicology 2013 10:1**, v. 10, n. 1, p. 1–33, 15 abr. 2013a.

SHI, H. et al. Titanium dioxide nanoparticles: a review of current toxicological data. **Particle and fibre toxicology**, v. 10, n. 1, 15 abr. 2013b.

SHI, Y. et al. Lipoxin A4 mitigates experimental autoimmune myocarditis by regulating inflammatory response, NF-κB and PI3K/Akt signaling pathway in mice. **European review for medical and pharmacological sciences**, v. 21, n. 8, p. 1850–1859, abr. 2017.

SHIMIZU, T. Lipid mediators in health and disease: enzymes and receptors as therapeutic targets for the regulation of immunity and inflammation. **Annual review of pharmacology and toxicology**, v. 49, p. 123–150, 2009.

SHISHODIA, S.; SINGH, T.; CHATURVEDI, M. M. Modulation of transcription factors by curcumin. **Advances in experimental medicine and biology**, v. 595, p. 127–148, 2007.

SODIN-SEMRL, S. et al. Lipoxin A4 inhibits IL-1 beta-induced IL-6, IL-8, and matrix metalloproteinase-3 production in human synovial fibroblasts and

enhances synthesis of tissue inhibitors of metalloproteinases. **Journal of immunology (Baltimore, Md. : 1950)**, v. 164, n. 5, p. 2660–2666, 1 mar. 2000.

SPECTOR, W. G.; WILLOUGHBY, D. A. VASOACTIVE AMINES IN ACUTE INFLAMMATION. **Annals of the New York Academy of Sciences**, v. 116, n. 3, p. 839–846, 1964.

STEFANI, M.; RIGACCI, S. Beneficial properties of natural phenols: Highlight on protection against pathological conditions associated with amyloid aggregation. **BioFactors**, v. 40, n. 5, p. 482–493, 10 set. 2014.

STORY, G. M. et al. ANKTM1, a TRP-like channel expressed in nociceptive neurons, is activated by cold temperatures. **Cell**, v. 112, n. 6, p. 819–829, 21 mar. 2003.

SUL. Electrochemical growth behavior, surface properties, and enhanced in vivo bone response of TiO2 nanotubes on microstructured surfaces of blasted, screw-shaped titanium implants. **International Journal of Nanomedicine**, p. 87, fev. 2010.

SVENSSON, C. I.; ZATTONI, M.; SERHAN, C. N. Lipoxins and aspirin-triggered lipoxin inhibit inflammatory pain processing. **The Journal of experimental medicine**, v. 204, n. 2, p. 245–252, fev. 2007.

SZALLASI, A. et al. Vanilloid (capsaicin) receptors in the rat: distribution in the brain, regional differences in the spinal cord, axonal transport to the periphery, and depletion by systemic vanilloid treatment. **Brain Research**, v. 703, n. 1–2, p. 175–183, 12 dez. 1995.

SZOLCSANYI, J.; JANCSO GABOR, A. Sensory effects of capsaicin congeners. II. Importance of chemical structure and pungency in desensitizing activity of capsaicin type compounds. **Arzneimittel-Forschung/Drug Research**, v. 26, n. 1, p. 33–37, 1976.

SZOLCSÁNYI, J.; JANCSÓ-GÁBOR, A.; JOÓ, F. Functional and fine structural characteristics of the sensory neuron blocking effect of capsaicin. **Naunyn-Schmiedeberg's archives of pharmacology**, v. 287, n. 2, p. 157–169, jun. 1975.

TAKEUCHI, O.; AKIRA, S. Pattern recognition receptors and inflammation. **Cell**, v. 140, n. 6, p. 805–820, 2010.

TOMINAGA, M. et al. The cloned capsaicin receptor integrates multiple pain-producing stimuli. **Neuron**, v. 21, n. 3, p. 531–543, 1998.

VERRI, W. A. et al. IL-15 mediates immune inflammatory hypernociception by triggering a sequential release of IFN-gamma, endothelin, and prostaglandin. **Proceedings of the National Academy of Sciences of the United States of America**, v. 103, n. 25, p. 9721–9725, 20 jun. 2006a.

VERRI, W. A. et al. Hypernociceptive role of cytokines and chemokines: Targets for analgesic drug development? **Pharmacology & Therapeutics**, v. 112, n. 1, p. 116–138, 1 out. 2006b.

VOGEL, M. On curcumine. **The London, Edinburgh, and Dublin Philosophical Magazine and Journal of Science**, v. 21, n. 137, p. 233–234, set. 1842.

WANG, C. T. et al. Over-expression of receptor activator of nuclear factor-kappaB ligand (RANKL), inflammatory cytokines, and chemokines in periprosthetic osteolysis of loosened total hip arthroplasty. **Biomaterials**, v. 31, n. 1, p. 77–82, jan. 2010.

WANG, J. J.; SANDERSON, B. J. S.; WANG, H. Cyto- and genotoxicity of ultrafine TiO2 particles in cultured human lymphoblastoid cells. **Mutation research**, v. 628, n. 2, p. 99–106, 2 abr. 2007.

WANG, J. X. et al. TiO2 nanoparticles translocation and potential toxicological effect in rats after intraarticular injection. **Biomaterials**, v. 30, n. 27, p. 4590–4600, set. 2009.

WANG, Q. et al. Curcumin attenuates collagen-induced rat arthritis via anti-inflammatory and apoptotic effects. **International immunopharmacology**, v. 72, p. 292–300, 1 jul. 2019.

WANG, Y. et al. Curcumin as a therapeutic agent for blocking NF-κB activation in ulcerative colitis. **https://doi.org/10.1080/08923973.2018.1469145**, v. 40, n. 6, p. 476–482, 2 nov. 2018.

WATKINS, L. R. et al. Mechanisms of tumor necrosis factor-alpha (TNF-alpha) hyperalgesia. **Brain research**, v. 692, n. 1–2, p. 244–250, 18 set. 1995.

WINTER, J. et al. Nerve growth factor (NGF) regulates adult rat cultured dorsal root ganglion neuron responses to the excitotoxin capsaicin. **Neuron**, v. 1, n. 10, p. 973–981, 1 dez. 1988.

WOLF, R. et al. Sunscreens--the ultimate cosmetic. **Acta dermatovenerologica Croatica : ADC**, v. 11, n. 3, p. 158–62, 2003.

WOOLEY, P. H. et al. Inflammatory responses to orthopaedic biomaterials in the murine air pouch. **Biomaterials**, v. 23, n. 2, p. 517–526, 2002.

WOOLF, C. J.; SALTER, M. W. Neuronal plasticity: increasing the gain in pain. **Science (New York, N.Y.)**, v. 288, n. 5472, p. 1765–1768, 9 jun. 2000.

WU, L. et al. Lipoxin A4 ameliorates cerebral ischaemia/reperfusion injury through upregulation of nuclear factor erythroid 2-related factor 2. **Neurological research**, v. 35, n. 9, p. 968–975, nov. 2013.

WU, T.; TANG, M. The inflammatory response to silver and titanium dioxide nanoparticles in the central nervous system. **Nanomedicine (London, England)**, v. 13, n. 2, 2018.

XU, Z. Z. et al. Resolvins RvE1 and RvD1 attenuate inflammatory pain via central and peripheral actions. **Nature medicine**, v. 16, n. 5, p. 592–597, maio 2010.

YANG, M. et al. Oral administration of curcumin attenuates visceral hyperalgesia through inhibiting phosphorylation of TRPV1 in rat model of ulcerative colitis. **Molecular pain**, v. 13, 1 ago. 2017.

ZENG, L. et al. The efficacy and safety of Curcuma longa extract and curcumin supplements on osteoarthritis: a systematic review and meta-analysis. **Bioscience reports**, v. 41, n. 6, 1 maio 2021.

ZHANG, L. et al. BML-111, a lipoxin receptor agonist, modulates the immune response and reduces the severity of collagen-induced arthritis. **Inflammation research : official journal of the European Histamine Research Society ... [et al.]**, v. 57, n. 4, p. 157–162, abr. 2008.

ZHANG, X. et al. Curcumin Alleviates Oxaliplatin-Induced Peripheral Neuropathic Pain through Inhibiting Oxidative Stress-Mediated Activation of NF-κB and Mitigating Inflammation. **Biological & pharmaceutical bulletin**, v. 43, n. 2, p. 348–355, 2020.

ZHANG, Z. et al. Curcumin slows osteoarthritis progression and relieves osteoarthritis-associated pain symptoms in a post-traumatic osteoarthritis mouse model. **Arthritis Research and Therapy**, v. 18, n. 1, p. 1–12, 3 jun. 2016.

ZHAO, G. et al. Curcumin Exerts Antinociceptive Effects in Cancer-Induced Bone Pain via an Endogenous Opioid Mechanism. **Frontiers in Neuroscience**, v. 15, p. 967, 3 set. 2021.

ZHAO, Y. N. et al. Resveratrol improves learning and memory in normally aged mice through microRNA-CREB pathway. **Biochemical and biophysical research communications**, v. 435, n. 4, p. 597–602, 14 jun. 2013.

ZOBDEH, F. et al. Pharmacogenetics and Pain Treatment with a Focus on Non-Steroidal Anti-Inflammatory Drugs (NSAIDs) and Antidepressants: A Systematic Review. **Pharmaceutics**, v. 14, n. 6, 1 jun. 2022.

4. ARTIGO 1

Como trabalho de qualificação de doutorado apresentado ao programa de pós graduação em Patologia experimental, é apresentado artigo realizado no Laboratório de Dor, Inflamação, Neuropatia e Câncer (LADINC) intitulado "*Therapeutic activity of Lipoxin A4 in TiO_2-induced arthritis in mice: NF-κB and Nrf2 in synovial fluid leukocytes and neuronal TRPV1 mechanisms*" submetido na revista Frontiers in immunology (IF:8.786) sob autoria de Telma Saraiva-Santos, Tiago H. Zaninelli, Marília F. Manchope, Ketlem C. Andrade, Camila R. Ferraz, Mariana M. Bertozzi, Nayara A. Artero, Anelise Franciosi, Stephanie Badaro-Garcia, Larissa Staurengo-Ferrari, Sérgio M. Borghi, Graziela S. Ceravolo, Avacir Casanova Andrello, Janaína Menezes Zanoveli, Rúbia Casagrande e Waldiceu A. Verri Jr.

Therapeutic activity of Lipoxin A_4 in TiO_2-induced arthritis in mice: NF-κB and Nrf2 in synovial fluid leukocytes and neuronal TRPV1 mechanisms

Telma Saraiva-Santos[1], Tiago H. Zaninelli[1], Marília F. Manchope[1], Ketlem C. Andrade[1], Camila R. Ferraz[1], Mariana M. Bertozzi[1], Nayara A. Artero[1], Anelise Franciosi[1], Stephanie Badaro-Garcia[1], Larissa Staurengo-Ferrari[1], Sérgio M. Borghi[2], Graziela S. Ceravolo[3], Avacir Casanova Andrello[4], Janaína Menezes Zanoveli[5], Rúbia Casagrande[6] and Waldiceu A. Verri Jr[1*]

[1]Laboratory of Pain, Inflammation, Neuropathy, and Cancer, Department of Pathology, Londrina State University, Londrina, Paraná, Brazil.
[2]Laboratory of Pain, Inflammation, Neuropathy, and Cancer, Department of Pathology, Londrina State University, Londrina, Paraná, Brazil; Center for Research in Health Sciences, University of Northern Paraná, Londrina, Paraná, Brazil.
[3]Department of Physiological Sciences, Center for Biological Sciences, Londrina State University, Londrina, Paraná, Brazil.
[4]Department of Physics, Londrina State University, Londrina, Paraná, Brazil.
[5]Department of Pharmacology, Biological Sciences Sector, Federal University of Parana, Curitiba, Parana, Brazil.
[6]Department of Pharmaceutical Sciences, Centre of Health Sciences, Londrina State University, Londrina, Paraná, Brazil.

*** Correspondence:**
Waldiceu A. Verri Jr
waverri@uel.br

Abstract

Lipoxin A4 (LXA_4) is a specialized pro-resolving mediator (SPM) with anti-inflammatory and pro-resolutive roles in inflammation. We evaluated the effects and mechanisms of action of LXA_4 in titanium dioxide (TiO_2) arthritis, a model of prosthesis-induced joint inflammation and pain. This aim was not pursued before, as far as we know. Mice were stimulated with TiO_2 (3mg) in the knee joint followed by LXA_4 (0.1, 1, or 10ng/animal) or vehicle (ethanol 3.2% in saline) administration. Pain-like behavior, inflammation, and dosages were performed to assess the effects of LXA_4 in vivo. LXA_4 reduced mechanical and thermal hyperalgesia, histopathological damage, edema, and recruitment of leukocytes without liver, kidney, or stomach toxicity. LXA_4 reduced leukocyte migration and modulated cytokine production (TNF-α, IL-1β, IL-6, and IL-10). These effects were explained by reduced nuclear factor kappa B (NF-κB) activation in macrophages recruited. LXA_4 improved antioxidant parameters [reduced glutathione (GSH) and 2,2-azino-bis 3-ethylbenzothiazoline-6-sulfonate (ABTS) levels, nuclear factor erythroid 2-related factor 2 (Nrf2) mRNA and Nrf2 protein expression] reducing reactive oxygen species (ROS) fluorescent detection induced by TiO_2 in synovial fluid leukocytes. We show the increase of lipoxin receptor (ALX/FPR2) in transient receptor potential cation channel subfamily V member 1 $(TRPV1)^+$ DRG nociceptive neurons upon TiO_2 inflammation. LXA_4 reduced TiO_2-induced TRPV1 and transient receptor potential ankyrin 1 (TRPA1) mRNA expression and protein detection, as well TRPV1

co-stained with p-NF-κB, indicating neuronal activation. The treatment with LXA_4 down-modulated neuronal activation and response to capsaicin (a TRPV1 agonist) and AITC (a TRPA1 agonist) of DRG neurons. Concluding, LXA_4 might target recruited leukocytes and primary afferent nociceptive neurons to exert analgesic and anti-inflammatory activities in an inflammation model resembling that observed in patients with prosthesis inflammation.

Keywords: Lipoxin A4, TiO_2, ALX/FPR2, inflammation, TRPV1, and ROS.

1 Introduction

Total joint replacement recovers joint function, reduces pain, and improves life quality (1–4). Total knee arthroplasty is a recurrent procedure for joint replacement, which is expected to increase in the coming years (5,6). In Europe, 2.5 million knee arthroplasties were recorded from 1975 to 2018 (7), and by the year 2030, 3.5 million procedures are expected in the United States (8). Despite the success of arthroplasty, deterioration of prosthetic components is the most associated complication. This event is characterized by the release of metallic nanoparticles that promote osteolysis and, thus, arthroplasty revision (8–10).

TiO_2 is widely used in the production of orthopedic prostheses (11). However, these molecules are the main triggers in prosthesis wear process-induced arthritis. Resident macrophages are activated and release tumor necrosis factor-alpha (TNF-α) and interleukin-1 beta (IL-1β) upon TiO_2 phagocytosis (12). Intra-articular (i.a.) administration of TiO_2 induces chronic arthritis and phenocopies the articular inflammation and pain caused by the release of prosthesis components upon the wearing process (13). The available therapies for prosthesis-induced arthritis patients lay on non-steroidal anti-inflammatory drugs (NSAIDs), corticosteroids, and opioids. These drugs promote tolerance and offer several adverse effects or addiction (14,15), affecting life quality and economic expenses (16,17). Therefore, investigating novel candidates for prosthesis-induced arthritis treatment is crucial. If a novel therapy presents different side effects, it might benefit patients that current treatments and their side effects cannot cover.

Lipoxin A4 (LXA_4) is a specialized pro-resolving lipid mediator (SPM) derived from arachidonic acid (18). This endogenous molecule plays anti-inflammatory and resolutive roles in inflammation (19,20). LXA_4 acts on the range of nanograms, diminishing cellular recruitment, chemotaxis, and polymorphonuclear adhesion, thus, controlling inflammatory tissue damage (21). LXA_4 properties depend on reducing pro-inflammatory cytokine levels, and inhibiting apoptosis in acute liver failure model for example (22). LXA_4 reduces inflammatory pain by suppressing mechanical and thermal hyperalgesia (23,24). LXA_4 is a potent antioxidant via nuclear factor erythroid 2-related factor 2 (Nrf2)-dependent antioxidant mechanisms in several animal models resulting in blockade of reactive oxygen species (ROS) generation (25–29). Furthermore, LXA_4 inhibits nuclear factor kappa B (NF-κB), accounting for an essential anti-inflammatory mechanism (22,30–32). LXA_4 acts through G protein coupled receptors (GPCR) for LXA_4 (ALXR), also known as FPRL1 and FPR2 (33–35) The activation of ALX/FPR2 receptor explain most of the anti-inflammatory, pro-resolving, and protective actions of

LXA_4 (21,34,36). The multiple sites of actions and cellular mechanisms demonstrate that LXA_4 has relevant properties for therapeutic development (21). Some of the LXA_4 mechanisms are relevant in the disease development in TiO_2 articular inflammation such as oxidative stress and cytokine production (13). Therefore, we reason that LXA_4 merits investigation of its anti-inflammatory and analgesic activities in the context of prosthesis wearing process released components like TiO_2, which we pursued in the present study.

2 Materials and Methods

2.1 Animals

Male Swiss (20-25 g) mice were used. Mice were housed in standard clear plastic cages with free access to water and food, a light/dark cycle of 12/12h, and a controlled temperature (21°±1°C). Animals were acclimated to the testing room at least one hour before the experiments, and all behavioral testing was performed between 9 a.m. and 5 p.m. Animal care and handling procedures were developed accordingly to the International Association for Study of Pain (IASP) guidelines and with the approval of the Londrina State University Ethics Committee on Animal Research and Welfare (process number 11147.2016.40). All efforts were made to minimize the number of animals used and their suffering.

2.2 Experimental procedures

The experiments dedicated to determining the disease phenotype upon LXA_4 treatment were summarized in Fig. 1; protocol 1. Parameters were pain, inflammation, oxidative stress, and histopathological alterations. Mice (n=6 per group per experiment) were stimulated in the right knee joint with an i.a. injection of TiO_2 (3 mg/10 µl/ knee joint), as previously described (13). Twenty-four hours after (post-treatment) TiO_2 stimulus, mice were treated with LXA_4 (0.1, 1, or 10 ng) or vehicle (3.2% ethanol/saline) [100µl per animal, intraperitoneal (i.p.)]. Mechanical hyperalgesia and edema were evaluated twenty-four hours after TiO_2 stimulus, before and after LXA_4 treatment (1, 3, 5, 7, and twenty-four hours after LXA_4 treatment on the first day and every other day from the 2nd to the 30th day). The dose and treatment time were chosen based on the results of mechanical hyperalgesia. After defining the most effective dose of LXA_4 (10 ng/animal), the thermal hyperalgesia was evaluated every three days for 30 days. Articular edema was analyzed for 30 days, and knee joint lavages were collected on the 30th day for leukocyte recruitment analysis. The stomach was collected to determine toxicity after chronic treatment, on the 30th-day post-induction, assess myeloperoxidase (MPO) activity (stomach ulceration), and blood samples were used to assess serum levels of aspartate transaminase (AST), alanine transaminase (ALT) (liver damage), urea, and creatinine (renal damage). The knee joints of 12 mice per group were collected for histopathology analysis [hematoxylin-eosin stain (HE)].

The 2nd day after stimulus injection was chosen to elucidate the potential mechanisms of this lipid mediator in the early stages of TiO_2-induced pain and inflammation (Fig. 1; protocol 2). The peak of inflammation was already achieved by the 2nd day, and higher leukocyte numbers omparing with the 30th day post-TiO_2 injection. Therefore, on the 2nd day, the knee joint was used to determine leukocyte recruitment; cytokine levels as per enzyme-linked immunosorbent assay (ELISA) (TNF-α, IL-1β, IL-

6, and IL-10); oxidative stress as per GSH and 2,2-azino-bis(3-ethylbenzothiazoline-6-sulfonate) (ABTS) measurement and Nrf2 mRNA expression by reverse transcriptase-quantitative real-time polymerase chain reaction (RT-qPCR). Synovial fluid leukocytes were also collected for p-NF-κB and Nrf2 staining by immunofluorescence; and total ROS using the probe 2',7'–dichlorofluorescein diacetate (DCF-DA) assay. Ipsilateral dorsal root ganglia (DRG) (corresponding to L4-L6 segments) were also dissected 2 days after TiO_2 to determine calcium influx imaging using confocal microscopy: transient receptor potential cation channel subfamily V member 1 (TRPV1) mRNA expression by RT-qPCR and TRPV1, transient receptor potential ankyrin 1 (TRPA1), ALX/FPR2 receptor, and p-NF-κB staining by immunofluorescence. All experimental conditions were standardized by our laboratory as previously published (13,37–39) and in preliminary experiments performed for this manuscript.

The peritonitis model induced by TiO_2 was used to mimetic the inflammation and evaluate the NF-κB activation in macrophage and if the treatment with LXA_4 could modulate this activation (Fig. 1; protocol 3). For this, mice were injected intraperitoneally with TiO_2 (30 mg/500 µl) and, twenty-four hours after (post-treatment) TiO_2 stimulus, mice were treated with LXA_4 (10 ng) or vehicle (saline) (100µl per animal, i.p.). After twenty-four hours, peritoneal washes were collected in FACS buffer (10mL per animal), and the cells were used to count leukocyte recruitment and cytokine production by adhered macrophage and flow cytometry.

2.3 Drugs, Reagents, and Antibodies

Materials were obtained from the following sources: saline solution (NaCl 0.9%; Frenesius Kabi Brasil Ltda, Aquiraz, CE, Brazil), LXA_4, ≥ 95% purity, was purchased from Cayman Chemical (Ann Arbor, MI, USA) and pure TiO_2, MW 79.90, was purchased from Synth (Diadema, SP, Brazil). ELISA kits for measurement of TNF-α, IL-1β, IL-6, and IL-10 were from eBioscience (Thermo Fisher Scientific, VIE, Austria). DCF-DA was purchased from Sigma-Aldrich (#D6883; San Luis, MO, EUA). Hank's Balanced Salt Solution (HBSS) was from Thermo Fisher Scientific (Waltham, MA, USA). The fluorescent antibodies were: anti-phospho NF-κB p65 (#sc-136548; Mouse, Santa Cruz Biotechnology, Dallas, TX, USA); anti-Nrf2 (#sc-722; Rabbit, Santa Cruz Biotechnology, Dallas, TX, USA); FcR Blocking Reagent (Miltenyi Biotec, Cambridge, MA, USA); Ghost Dye™ Red 780 (Tombo, San Diego, CA, USA); PE anti-mouse CD45 antibody (#103106; Rat, BioLegend, San Diego, CA, USA); FITC anti-mouse CD45 antibody (103107; Rat, BioLegend, San Diego, CA, USA); FITC anti-mouse CD4 (#100406; Rat, BioLegend, San Diego, CA, USA); PerCP anti-mouse F4/80 antibody (#123126; Rat, BioLegend, San Diego, CA, USA); anti-capsaicin receptor antibody (#ab5566; Guinea pig, Merck Millipore, Burlington, MA, USA); anti-FPRL1/FPR2 antibody (#NLS1878ss; Rabbit, Novus biologicals, Englewood, CO, USA); anti-TRPA1/TSA antibody (#ab58844; Rabbit, Abcam, Cambridge, MA, USA); anti-mouse secondary antibody (Alexa Fluor 647-Goat, #115-605-003; Jackson ImmunoResearch, West Grove, PA, USA) and (Alexa Fluor 488-Goat anti-mouse; #A11001, Thermo Fisher Scientific, Waltham, MA, USA); anti-rabbit secondary antibody (Alexa fluor 488-Goat, #A-11008; Thermo Fisher Scientific, Waltham, MA, USA); anti-rabbit secondary antibody (Alexa fluor 647- Goat, #A32733; Thermo Fisher Scientific, Waltham, MA, USA); anti-Guinea pig secondary antibody (Alexa Fluor 488- Goat, #A11073, Thermo

Fisher Scientific, Waltham, MA, USA). Hoechst 33342, trihydrochloride trihydrate was from Thermo Fisher Scientific (Waltham, MA, USA). 4′,6-Diamidine-2′-phenylindole dihydrochloride (DAPI) was from Thermo Fisher Scientific (Waltham, MA, USA). The panoptic kit for differential counts of recruited leukocytes was from Laborclin (Pinhais, PR, Brazil). Neurobasal-A medium (NBM) was purchased from Life Technologies (Thermo Fisher Scientific); Dispase II was from RocheApplied Sciences (Indianapolis, IN, USA); 4-(2-hydroxyethyl)-1- piperazine ethane sulfonic acid (HEPES)-buffered saline was from Millipore Sigma (Burlington, MA, USA); and Fluo-4 a.m. was from Invitrogen (#F14201, Carlsbad, CA, USA).

2.4 Evaluation of articular mechanical hyperalgesia

The knee joint mechanical hyperalgesia was evaluated. Mice were allowed to habituate to the apparatus for at least one h during three consecutive days before the measurements. Animals are placed in acrylic cages with a wire grid floor, and the stimulation was performed when the animals were quiet and with the four paws on the grid floor. This method consists of an electronic pressure meter with a force transducer fitted with a polypropylene tip (Electronic von Frey aesthesiometer; Insight instruments, Ribeirao Preto, SP, Brazil). We used a large tip (4.15mm2) to evaluate knee joint pain to exclude the subcutaneous effect (40). An increased perpendicular force was applied to the central area of the plantar surface to induce flexion of the tibiofemoral joint, followed by hind paw withdrawal. A digital aesthesiometer recorded the maximal intensity of the force applied [in grams (g)] when the paw was withdrawn. The test was performed in the time points of 1, 3, 5, 7, and twenty-four hours on the first day after LXA_4 treatment and every other day from the 2nd to the 30th. The investigators were blinded to the treatment groups. The results were expressed as the mechanical withdrawal threshold in g.

2.5 Evaluation of articular thermal hyperalgesia

For the heat hyperalgesia test, mice were allowed to habituate to the apparatus for at least two hours during three consecutive days before the measurements. After habituation, a baseline measurement was obtained. To measure pain sensitivity to a heat stimulus (heat hyperalgesia), we placed mice on a glass plate of a Hargreaves apparatus (Model 390G, IITC Life Science, Woodland Hills, CA, USA). A radiant heat source was used to stimulate the paw by gradually increasing the temperature of the plantar surface. The test was performed after LXA_4 treatment and every three days until the 30th. The pain threshold was determined as the latency (in seconds) to evoke a response of paw withdrawal: paw flinches or licking. In this experiment, the device was set to 30% radiant heat source intensity and a cut-off time of 15s of exposure to prevent tissue damage.

2.6 Articular edema measurements

Articular edema of the tibiofemoral joint was assessed through measurements of the transverse diameters using a caliper (Digmatic Caliper, Mitutoyo Corporation, Kanagawa, Japan). The edema was determined for each mouse knee joint by the difference indicated times post-stimulus and zero time. The test was performed at the time points of 1, 3, 5, 7, and twenty-four hours on the first day after LXA_4 treatment and every other day from the 2nd to the 30th. The results were expressed as Δ mm/joint.

2.7 Leukocyte migration

The total and differential counts of recruited leukocytes to the knee joint cavity were determined on the 2nd, and 30th day, as previously described (14). Briefly, knee joint cavities were washed with saline containing EDTA (50µl of solution/ 3 washes of 3.33µl), which was recovered to evaluate total and differential cell counts. The peritonitis model collected the peritoneal washes (10mL of FACS buffer) on the 2nd day after stimulis to evaluate the counts. Total cell counts were performed in the Neubauer chamber using Turk's solution, and differential cell counts (100 cells per slide) were performed in slices stained with the panoptic kit under a light microscope (Olympus CX31RTSF, Tokyo, Japan). Results were expressed as total leukocytes, polymorphonuclear, and mononuclear cells (cells × 10^3/ synovial cavity and cells × 10^6/ cavity).

2.8 Liver and kidney toxicity assay

Blood samples were collected on the 30th day post TiO_2 stimulus, centrifuged (0.4 rcf, 20 min, 4°C), and the serum was separated to assess the safety of treatment with LXA_4. AST and ALT were used as markers of hepatotoxicity, and acetaminophen was used as a positive drug control (650 mg/kg, i.p.), diluted in sterile saline once). Urea and creatinine levels were used to evaluate nephrotoxicity, and diclofenac was a positive drug control (200 mg/kg, orally, diluted in sterile saline, once) (41). The samples were processed according to the manufacturer's instructions (Labtest Diagnóstico S. A., Brazil). Results were presented as U/mL (AST and ALT) or mg/dL (urea and creatinine) of serum.

2.9 MPO activity

On the 30th-day post-TiO_2 injection, samples of the stomach were harvested in 50 mM K_2HPO_4 buffer (pH 6.0) containing 0.5% hexadecyl trimethylammonium bromide (HTAB) and kept at – 80 °C until use. Frozen samples were homogenized using a tissue turrax (Tissue-Tearor 985370, BioSpec Products, Bartlesville, OK, USA) and centrifuged (2 min, 16,000g, 4 °C), and the resulting supernatant was assayed using a spectrophotometer (Multiskan GO Microplate Spectrophotometer, Thermo Fisher Scientific, Vantaa, Finland) for MPO activity determination at 450 nm. Briefly, 15µL of the sample was mixed with 200µL of 50 mM phosphate buffer (pH 6.0) containing 0.167 mg/mL O-dianisidine dihydrochloride and 0.0005% hydrogen peroxide. The MPO activity of samples was compared to a standard curve of neutrophils. Indomethacin (2.5 mg/kg, i.p., diluted in tris/HCl buffer, for 7 days) was used as positive drug control for stomach damage (42). The results were presented as MPO activity (number of neutrophils × 10^6/ mg of tissue).

2.10 Histopathological analysis

Joints were collected on the 30th day and fixed in 10% buffered formaldehyde. After decalcification in 20% EDTA disodium salt solution (pH 7,4) for 48 hours, the samples were processed for paraffin embedding. The tibiofemoral joint tissues were cut (10 µm) and stained with HE. The sections were examined, blinded, and scored by a pathologist in light microscopy. The score was determined by summing of synovial hyperplasia, inflammatory infiltrate, and vascular proliferation score, as described

previously (39) Briefly, the degrees of the following parameters were: (a) synovial hyperplasia (from 0 = no pannus formation, to 3 = most severe pannus formation); (b) inflammatory infiltrate (from 0 = no inflammation, to 3 = most severe inflammation; and (c) angiogenesis (from 0 = no vascular proliferation, to 3 = most severe proliferation). Vascular proliferation was considered the number of capillary blood vessels. The final score was determined by summating all three parameters (a–c), resulting in a score for each sample expressed as the mean of six samples accordingly to the groups.

2.11 Cytokine measurement

Knee joint samples collected on the 2nd day were homogenized in 500µL of buffer containing protease inhibitors. Samples were centrifuged (3000 rpm × 15 min × 4°C). TNF-α, IL-1β, IL-6, and IL-10 levels were determined from the supernatant by ELISA. The results were expressed as pg of cytokine/mg of protein.

2.12 Synovial fluid leukocytes immunofluorescence

Knee joint cavities were washed in the 2nd day with FACS buffer (PBS and 0.5% BSA) containing EDTA (2mM), which was recovered to immunofluorescence assay as previously described with modifications (43). Samples were fixed with 4% paraformaldehyde for 30 min on ice. Then, samples were centrifuged (10 min, 4°C, 300g) and incubated with blocking buffer (PBS, 0.3% Triton) with bovine serum albumin (BSA) 3% for 1h and incubated with primary antibodies [anti-p-NF-κB p65 (1:200) or anti-Nrf2 (1:200)] overnight (4°C). On the following day, samples were washed and incubated with secondary antibodies conjugated with Alexa Fluor 647-Goat anti-mouse (1:500) or Alexa Fluor 647-Goat anti-rabbit (1:500), and DAPI (1:500) was used as a nucleus marker. The samples were resuspended in PBS, placed on slides, and let to dry out at room temperature overnight. Imaging was performed using a confocal microscope (Leica TCS SP8, Leica, Wetzlar, Germany) with a 63x objective (p-NF-κB p65) and a 63x objective with a zoom-in of 1.5 (Nrf2). Images were processed using Leica EL6000 software (Leica, Wetzlar, Germany). The fluorescence intensity of p-NF-κB p65 of the different groups was quantified in randomly selected fields and analyzed from the mean fluorescence measured with the LAS X software (Leica Microsystems). The percentage of positive cells per field of Nrf2 was quantitated manually considering the following equation: total number of Nrf2+ cells times 100, divided by the total number of $DAPI^{+}$ cells. Results were expressed as fluorescence intensity (p-NF-κB p65) and percentage of positive cells per field (Nrf2).

2.13 Flow cytometry

Mice have injected an i.p. injection of TiO_2 (30 mg/500 µl), and twenty-four hours after (post-treatment) TiO_2 stimulus, mice were treated with LXA_4 (10 ng) or vehicle (saline) (100µl per animal, i.p.). After twenty-four hours, peritoneal washes were collected in FACS buffer (10mL per animal), and cells were centrifuged for 10 min at 300 g; the supernatant was discarded, and the pellet was resuspended in 200 µl of FACS buffer. The cell suspension was incubated on ice with mouse FcR Blocking Reagent for 10 min and then incubated for 30 min on ice with the following antibodies: anti-CD45-PE (1:200), anti-CD45-FITC (1:200), anti-F4/80-PerCP (1:200), anti-CD4 FITC (1:200) and ghost dye red (1:200). After the incubation, cells were fixed with 2% PFA for 30

minutes at room temperature followed by permeabilization with FACs with 0,5% de Triton and the intracellular staining with anti-p-NF-κB p65 (1:200) overnight. On the following day, cells were washed and incubated with secondary antibody Alexa Fluor 488 Goat anti-Mouse (1:500) for 1h. Cells were centrifuged for 10 min at 300 g, and the pellet was resuspended in 200 µl of FACS 2% PFA. FACS assay was performed using Guava® easyCyte™. Data were analysed and plotted using FCS express software .Results were expressed as cells × 10^6/ cavity.

2.14 Antioxidant capacity measurement

The knee joint collection on the 2nd day was processed as previously described (44–46), and the levels of synovial GSH were determined using a spectrophotometric method. Frozen samples of knee joints were homogenized in cold 0.02 M EDTA. The homogenate was treated with 50% trichloroacetic acid and centrifuged (15 min x 1,500 g). The resulting supernatant received 0.4 M Tris-HCl, pH 8.9; next, samples were vortex-mixed, and 10 mM dithiobis nitrobenzoic acid was added, followed by vortex-mixing. After these procedures, samples could stand for 5 minutes before being read at 412 nm. The standard curves requested in the test were prepared using different concentrations of GSH. The results were presented as nmols of GSH / mg of protein. The free-radical scavenging ability was determined using the ABTS assay (44,46). ABTS was diluted with phosphate buffer saline at pH 7.4 to an absorbance of 0.80 at 730 nm. Subsequently, 1.0 mL of diluted ABTS solution was mixed with 20µL of the supernatant. After 6 min, the absorbance was measured at 730 nm. The results were equated against a standard Trolox curve (1.5-30 µmol/L, final concentrations). The results are expressed as Trolox equivalents per milligram of protein.

2.15 Total intracellular ROS detection

The DCF-DA fluorescent probe was used to determine the presence of ROS. Knee joint cavities were washed on the 2nd day with FACS buffer (PBS and 0.5% BSA) containing EDTA, which was recovered to DCF-DA assay. The recovered articular fluids were seeded on Nunc™ Glass Bottom Dishes for 30 min at 37°C. Samples were then loaded with 10 µM of DCF-DA for 30 min 37°C, washed with HBSS, and imaged in a Confocal Microscope (TCS SP8, Leica Microsystems) with a 63x objective. Total intracellular ROS detection was analyzed from the mean fluorescence measured with the LAS X software (Leica Microsystems).

2.16 RT-qPCR

Total RNA was extracted from knee joints and DRGs (L4-L6) on the 2nd day using the SV Total RNA Isolation System (Promega). The purity of total RNA was measured using a spectrophotometer (Multiskan GO Microplate Spectrophotometer, Thermo Fisher Scientific, Vantaa, Finland), and the wavelength absorption relationship (260/280) was between 1.8 and 2.0 for all preparations. Reverse transcription of total RNA to cDNA and qPCR was carried out using GoTaq® 2-Step RT-qPCR System (Promega) and specific primers. The qPCR reaction was performed in a StepOnePlus™ Real-Time PCR System (Applied Biosystems®). The relative gene expression was measured using the comparative $2^{-(\Delta\Delta Cq)}$ method. Table 1 shows the primer sequences. The expressions of

β-actin mRNA were used as the reference gene, and the results were expressed as mRNA expression (normalized to β-actin).

2.17 Calcium imaging experiments

DRGs samples (L4-L6) were collected on the 2nd day, and calcium imaging was performed as previously described (37) DRGs were dissected into NBM, dissociated in 1 mg/ml collagenase A and 2,4 U/ml de dispase II in HEPES for 20 minutes at 37˚C. After trituration with decreasing size glass Pasteur pipettes, DRG cells were centrifuged over a 10% BSA gradient, plated on laminin-coated cell culture dishes. DRGs were then loaded with 1.2 μM of Fluo-4 a.m. in NBM, incubated for 30 min 37°C, washed with HBSS, and imaged in a Confocal Microscope (TCS SP8, Leica Microsystems). DRG plates were recorded for 6 min to evaluate TRPV1 and TRPA1 activation, which was divided into 2 min of initial reading (0-120s, baseline values), followed by stimulation with 100 nM capsaicin (a TRPV1 agonist, 120-240s) or 100 μM AITC (a TRPA1 agonist, 120-240s), and 40 mM of KCl (240-360s), activates all neurons. Only the KCl-responsive cells were considered in the analyses of capsaicin-responsive or allyl isothiocyanate (AITC)-responsive cells. Calcium flux was analyzed from the mean fluorescence (KCl responsive neurons) measured with the LAS X software (Leica Microsystems).

2.18 DRG immunofluorescence

For immunofluorescence, DRGs of L4–L6 segments from Swiss were collected on 2nd day and maintained in 4% paraformaldehyde (PFA, for twenty-four hours), then in 30% sucrose (twenty-four hours) and 30% sucrose + OCT (1:1) (twenty-four hours) before inclusion with Optimum cutting temperature reagent (Tissue-Tek 1, O.C.T. Compound, IA018, ProSciTech, Australia) and 10 μm sections were cut in a cryostat and processed for immunofluorescence. After that, the slides were incubated with blocking buffer (PBS, 0.3% Triton) with bovine serum albumin (BSA) 3% for 1h and incubated with primary antibodies anti-TRPV1 (1:500); anti-FPRL1/FPR2 antibody (ALX/FPR2 receptor; 1:200); anti-TRPA1/TSA (1:100); anti-p-NF-κB p65 (1:200)] overnight (4°C). On the following day, the slides were washed and incubated with secondary antibodies conjugated with Alexa Fluor 488- Goat Anti-Guinea pig (1:500); Alexa Fluor 647 Goat anti-Rabbit (1:500); Alexa Fluor 488 Goat anti-Rabbit (1:500); Alexa Fluor Goat anti-Mouse (1:500). Hoechst 33342, trihydrochloride trihydrate (1:500) and DAPI (1:500) was used for nuclear staining. Imaging was performed using a confocal microscope (Leica TCS SP8, Leica, Wetzlar, Germany) with a 20x objective with a zoom-in of 1.0. Images were processed using Leica EL6000 software (Leica, Wetzlar, Germany). The results are expressed as the number of positive cells per area and percent of positive cells (double stained), manually quantitated.

2.19 Statistical analysis

Data were analyzed using GraphPad Prism statistical software (GraphPad Software, Inc., USA-500.288, version 8.0). The results were presented as means ± SEM for parametric data and medians and interquartile ranges for non-parametric data. To this end, we used Shapiro–Wilk normality test and Brown-Forsythe homogeneity test. For in vivo experiments, an of 6, 8, or 10 mice in each group per experiment and represent two

separate experiments depending on the methodology (indicated in the figure legends). *In vitro* experiments with DRG samples were performed using an n of 4 pools [DRGs (L4-L6) of 10 mice to form 1 pool] per group and represent two separate experiments. Two-way repeated-measures analysis of variance (ANOVA) followed by Tukey's post-test was used to compare all groups and doses when responses were measured at different times after the stimulus injection. The analyzed factor were treatments, time, and time versus treatment interaction. Parametric results were evaluated by one-way ANOVA followed by Tukey's post-test for data from a single time point. Kruskal–Wallis followed by Dunn post-test or two-way were used for non-parametric results. $P<0.05$ was considered significant.

3. Results

3.1. Treatment with LXA_4 reduces TiO_2-induced articular mechanical hyperalgesia, thermal hyperalgesia, and edema in mice

A dose-response curve was performed to assess the potential analgesic and anti-inflammatory effects of LXA_4 in TiO_2-induced arthritis. Treatment started twenty-four after TiO_2 i.a. injection. We could still observe significant analgesia by the 24th hours after LXA_4 treatment, which was reduced by the 48th hours (data not shown). Therefore, treatments with LXA_4 were performed every 48h. The injection of 3 mg/joint of TiO_2 induced mechanical hyperalgesia, and treatment with LXA_4 reduced the mechanical hyperalgesia in a dose-dependent (0.1, 1, or 10 ng/ animal, 100µl i.p.) manner. The most effective dose was 10 ng/animal, which was chosen for the following experiments (Fig. 2A). TiO_2 also induced thermal hyperalgesia, which was reduced by LXA_4 10 ng/animal treatment. The reduction of thermal hyperalgesia was observed from the 4th day onwards, with complete inhibition from the 7th to the 30th day (Fig. 2B).

We also investigated if the treatment with LXA_4 reduces knee joint edema. The dose of 10 ng/animal of LXA_4 significantly reduced TiO_2-induced articular edema 24h after the first treatment, with persistent anti-inflammatory effect until the 30th day of arthritis (Fig. 2C). The saline-injected group did not develop edema (Fig. 2C).

3.2 LXA_4 reduces TiO_2-induced joint histopathology changes and inhibits leukocyte recruitment to the articular space

Mice were treated with LXA_4 (10ng/ animal, i.p., every 48h) or vehicle (ethanol 3.2% in saline) twenty-four hours after TiO_2 (3mg) i.a. injection. On the 30th day, the knee joint was collected for HE histopathology evaluation (Fig. 3A-G). LXA_4 reduced TiO_2-induced synovial hyperplasia, inflammatory infiltrates, and vascular proliferation observed in the histopathological index analyses (Fig. 3A). Treatment with a vehicle showed no effect on TiO_2-induced histopathological changes.

Leukocyte recruitment to the knee joint is a hallmark of arthritis (47). To investigate the effect of LXA_4 on leukocyte recruitment 30 days post-TiO_2 stimulus, knee joint washes were collected to evaluate the total number of leukocytes, mononuclear and

polymorphonuclear cells. The injection of TiO_2 significantly increases the number of leukocytes recruited to the knee joint 30th day after the stimulus (Fig. 3H-J). Our results show that the treatment with LXA_4 at 10 ng/animal reduced TiO_2-induced recruitment of total leukocyte (Fig. 3H), mononuclear (Fig. 3I), and polymorphonuclear cells (Fig. 3J).

3.3 LXA_4 does not induce liver, kidney, or stomach damage

Thirty days after TiO_2 stimulis, serum samples and stomach were collected to evaluate whether the chronic treatment with LXA_4 would induce gastric, hepatic, or renal damage, which are common side effects of non-steroidal anti-inflammatory drugs (48). Toxicity was assessed through the concentrations of AST, ALT, urea, creatinine, and MPO activity (Fig. 4). The treatment with 10 ng/animal of LXA_4 did not modify the serum concentration of AST, ALT (Fig. 4A and B), urea, creatinine (Fig. 4C and D), or MPO activity in the stomach compared with positive controls (Fig. 4E). Therefore, our data suggest that chronic treatment does not induce detectable gastric, hepatic, or renal lesion/damage.

3.4 LXA_4 reduces TiO_2-induced macrophage recruitment, cytokines production, and NF-κB activation in mice

In the following experiments, we opted to reduce the treatment period to investigate the inflammatory and pain mechanisms of LXA_4. We considered that figures 2-4 established the beneficial effect of LXA_4 treatment during a chronic period and that inflammation and pain achieved significant development by the second day of arthritis. This approach allowed us to reduce the suffering of animals and, investigate the mechanisms involved in LXA_4 post-treatment of ongoing TiO_2 arthritis.

Given the role of recruited leukocytes in inflammatory pain and oxidative burst (49), we next assessed the efficacy of LXA_4 in modulating TiO_2-induced leukocyte recruitment after a single treatment. In this case, recruitment was evaluated on the 2nd day (Fig. 5A-C) to further support that this time point is adequate and mimics all inflammatory features of TiO_2 arthritis together with the pain and edema observed in Fig. 2. The injection of TiO_2 significantly increased the number of total leukocytes recruited on the 2nd day after the stimulus (Fig. 5A-C). Our results show that the treatment with LXA_4 at 10 ng/animal reduced TiO_2-induced recruitment of total leukocyte (Fig. 5A), mononuclear (Fig. 5B), and polymorphonuclear cells (Fig. 5C). These data show that most leukocytes recruited to the joint were mononuclear cells (90%). Compared with the 30th day data (Fig. 5A-C), 10.6-fold more leukocytes migrated in the knee joint on the 2nd day, indicating that this time point is suitable for investigating inflammatory mechanisms. It was noticeable that on the 2nd day, higher mononuclear cells than neutrophil counts were already established, which is an unusual cellular profile and deserves further investigation of the pathophysiological mechanisms underlying it in future studies.

The potential of LXA_4 to modulate pro-inflammatory cytokine (TNF-α, IL-1β, and IL-6) and anti-inflammatory cytokine (IL-10) production in the joint tissue was evaluated on the 2nd day (Fig. 5D-G). The i.a. injection of TiO_2 induced a significant increase in the levels of TNF-α (Fig. 5D), IL-1β (Fig. 5E), and IL-6 (Fig. 5F). A single treatment with LXA_4 was enough to reduce the levels of these pro-inflammatory cytokines induced by TiO_2 (Fig. 5D-F). Thus, the role of LXA_4 in reducing the production of essential cytokines

unveils one of its mechanisms, reducing pain, edema, and recruitment of leukocytes (50). Besides, IL-10 production was also increased by LXA_4 (Fig. 5G), evidencing this lipid mediator's anti-inflammatory and immunoregulatory capacity with a single treatment.

Synovial fluid leukocytes were collected on the 2nd day, and the phosphorylated (p) form of NF-κB was determined by immunofluorescence assay (Fig. 5H). Treatment with LXA_4 inhibited the fluorescence intensity of the p-NF-κB p65 subunit induced by TiO_2 (Fig. 5H). Therefore, these data suggest that inhibition of NF-κB activation is, at least, one of the mechanisms by which LXA_4 ameliorates TiO_2-induced inflammation and pain due to the importance of this transcription factor to cytokine production (Fig. 5D-G) and leukocyte recruitment (Fig. 5A-C).

The number of recovered cells in synovial washes was insufficient to perform a flow cytometry to demonstrate the mainly recruited cellular type, so, to enable this explanation, we standardized a peritonitis model to mimic the TiO_2-induced inflammation. We performed a dose-response of TiO_2 (data not shown), and the dose of 30 mg per animal was sufficient to induce leukocyte recruitment to the cavity. We performed a single treatment with 10 ng of LXA_4, sufficient to reduce the leukocyte recruitment (Fig. 6A-C). The following experiments were performed to elucidate the macrophage roles in TiO_2-induced inflammation and the number of cells with NF-κB activation. To this, we performed flow cytometry, demonstrating the total leukocyte recruited (CD45+ cells) (Fig. 6D) cells induced by TiO2. We show that TiO_2 increased NF-κB activation in macrophage cells ($NF\text{-}\kappa B^+$ $F4/80^+$ cells) (Fig. 6F and G), which represents 85% of the total ($NF\text{-}\kappa B^+$ $CD45^+$ cells) cells (Fig. 6E and G), and the LXA_4 treatment reduced this activation.

Our previous results demonstrated that mononuclear cells were the most recruited leukocyte after TiO2 injection is mononuclear cells. Therefore, we evaluated the ratio of macrophages and lymphocytes recruited, and the modulation by LXA_4. Our data shows that TiO_2 increased the number of macrophages [$CD45^+$ $F480^+$ (Fig.7A)] and lymphocytes $CD45^+$ $CD4^+$ (Fig. 7B)], and the treatment with LXA_4 reduced the number of macrophages (Fig. 7A), but not the lymphocytes (Fig. 7B) recruited. The proportion of macrophages represents 70% of the total leukocyte recruited, and lymphocytes represents 10% of total population (Fig. 7C). This data corroborated with the elucidation of macrophage roles in TiO2-induced inflammation and pain, and the modulation by LXA_4.

3.5 LXA_4 inhibits oxidative stress improving antioxidant capacity in mice

Knee joint samples were collected on the 2nd day, and the parameters of the antioxidant capacity were determined by GSH and ABTS assay (Fig. 8A and B). It has already been demonstrated in other models that TiO_2 induces the production of ROS and, consequently, oxidative stress in various organs (51–53). Herein, we show that TiO_2 stimulus reduced the levels of endogenous antioxidants as observed in free radical scavenging ability and GSH levels (Fig. 8A and B) in the knee joint tissues. On the 2nd day, a single treatment with LXA_4 significantly restored the levels of ABTS and GSH (Fig. 8A and B), demonstrating that treatment with LXA_4 reestablished the antioxidant ability to scavenge free radicals such as ABTS cationic radical and positively up-regulates the endogenous antioxidant GSH. GSH is up-regulated by the transcription factor Nrf2 (54), and we observed that LXA_4 increases the Nrf2 mRNA expression (Fig. 8C). Then,

as these phenomena were observed in the knee joint tissue and recruited leukocytes have a major role in those alterations, we analyzed the recruited leukocytes.

ROS production was measured in the synovial fluid leukocytes using DCF-DA probe, which, when oxidized, generates a fluorescence product (DCF) proportional to overall intracellular ROS levels. We observed that treatment with LXA_4 inhibited DCF fluorescence intensity (Fig. 8D), demonstrating that treatment with LXA_4 inhibits TiO_2-induced production of ROS (Fig. 8D). Articular fluids were collected on the 2nd day, and Nrf2 was determined by immunofluorescence assay (Fig. 8E). Supporting the qPCR data, we observed that treatment with LXA_4 increased the percentage of positive cells per field of Nrf2 (Fig. 8E).

3.6 TiO_2 increases the ALX/FPR2 receptor expression on nociceptive $TRPV1^+$ neurons.

LXA_4 acts through ALX/FPR2 receptor in peripheral tissues and regulates cellular responses of interest in inflammation and resolution (21). ALX/FPR2 receptor is expressed in tissues and cell types such as immune cells, fibroblasts, epithelial cells, and astrocytes (21,24). The effect of LXA_4 in reducing mechanical and thermal hyperalgesia indicates that it could, eventually, act on nociceptor neurons. To suggest a neuronal effect of LXA_4 it was necessary to determine if TiO_2 increse the expression of ALX/FPR2 receptor and whether the expression in TRPV1 nociceptive neurons. These were our next steps. We investigated the expression of ALX/FPR2 receptor in the DRG by performing an immunofluorescence staining for ALX/FPR2 receptor and TRPV1, which is a TRP channel expressed by nociceptive C-fibers (Fig. 9). Our data show that TiO_2 incresed the expression of ALX/FPR2 receptor in the DRG of mice (Fig. 9A and C). We also found that TiO_2 increases the percent of double positive ALXR/TRPV1 cells, indicating nociceptor sensory neurons express ALX/FPR2 receptor, which is enhanced in this population in TiO_2 inflammation (Fig. 9B and C). Thus, suggesting that nociceptive $TRPV1^+$ neurons are targets to the action of LXA_4 during TiO_2-induced arthritis. The treatment with LXA_4 didn't modifed the expression of ALX receptor in DRG.

3.7 LXA_4 reduces TiO_2-induced TRPV1 activation and expression on DRG neurons

Considering the results of Fig. 9, our next step was to assess neuronal activation, which was performed using calcium influx quantitation by a fluorescent probe in DRG neurons (55). We investigated whether DRG neurons from TiO_2-stimulated mice would present an increase in the baseline calcium levels and response to capsaicin (TRPV1 agonist) stimulation compared to saline-injected controls mice, and the ability of LXA_4 to modulate this response (Fig. 10). DRG neurons from vehicle-treated mice presented a higher baseline level of calcium influx than saline mice or LXA_4-treated DRGs (Fig. 10A-C). These data suggest that LXA_4 reduces the activation of DRG neurons in TiO_2-induced inflammation because the increase in calcium influx is indicative of DRG neuron activation (Fig. 10A-C). Notably, in addition to the diminished basal level of calcium, LXA_4 treatment also reduced the responsiveness of DRG neurons to capsaicin, which is a TRPV1 agonist (Fig. 10A-C). The treatment reduced 50% of of the number of responsiveness neurons to capsaicin, increased by TiO_2 (Fig. 10D). Corroborating with

the reduction of neuronal activation and diminished response to capsaicin, we demonstrated that treatment with LXA_4 inhibited the increase of TRPV1 (Fig. 11B) mRNA expression induced by TiO_2, as wells as TRPV1 staining in the DRG (Fig. 11A and C). Therefore, LXA_4 inhibits TiO_2-induced DRG protein detection, mRNA expression, and activity of a critical ion channel (TRPV1) to nociceptor sensory neurons sensitization (56), which resulted in a functional outcome of reduced neuronal responsiveness and pain upon LXA_4 treatment.

We also investigated whether $TRPV1^+$ neurons co-expressed p-NF-κB in the TiO_2-induced DRG as a marker of neuronal activation. The immunofluorescence assay shows that the intra-articular injection of TiO_2 increased the percent of $TRPV1^+$ neurons co-stained with p-NF-κB, and the treatment with LXA_4 can reduce it (Fig. 12A and B). Thus, it further corroborates that $TRPV1^+$ neurons are activated in TiO_2 inflammation, and LXA_4 treatment reduces their activation.

3.8 LXA_4 reduces TiO_2-induced TRPA1 activation on DRG neurons

$TRPA1^+$ neurons in dorsal root ganglion are involved in inflammation-induced hyperalgesia in peripheral tissues (57–60). Therefore, to further explore the neuronal mechanism involved in the model and the role of LXA_4 we investigated whether LXA_4 modulates TRPA1 channels in TiO_2-induced arthritis. For this, we investigated whether DRG neurons from stimulated mice would increase calcium levels in response to AITC (a TRPA1 agonist) stimulation and the modulation by LXA_4 (Fig. S1). We observed that LXA_4 treatment reduced the responsiveness of DRG neurons to AITC induced by TiO_2 (Fig. S1A-C). The treatment reduced 37% of the number of responsiveness neurons to AITC, increased by TiO_2 (Fig. S1D). Moreover, TRPA1 staining was enhanced in DRG neurons in the TiO_2 group, and one treatment with LXA_4 reduced the TRPA1 stained neurons (Fig. S2A and S2C). The co-staining of TRPA1 with p-NF-κB showed that TiO_2 did not induce the TRPA1 nociceptive neurons activation (Fig. S2B and S2C). These data show the importance of both ion channels in this model of inflammatory pain and that expression and activation of TRPV1 and TRPA1 channels and inflammatory pain.

4 Discussion

LXA_4 administration reduced chronic ongoing TiO_2-induced joint edema, mechanical and thermal hyperalgesia, leukocyte recruitment, and histopathological changes. LXA_4 activity was explained by reducing pro-inflammatory cytokines (TNF-α, IL-1β, and IL-6) and increasing anti-inflammatory cytokine IL-10. Corroborating with these data, LXA_4 reduced NF-κB activation in synovial fluid leukocytes. In the inflammatory context, we demonstrated that macrophages are mainly recruited cell induced by TiO_2, and the NF-κB activation is majority in these cells. The IL-10 production *in vivo* by macrophage is increased after LXA_4 treatment. In the disease context, a single treatment with LXA_4 significantly restored free-radical scavenging ability (ABTS) and GSH levels. It reduced the production of ROS, accompanied by increased Nrf2 mRNA expression in the knee joint tissue and protein staining in synovial fluid leukocytes supporting an antioxidant effect. Thus, demonstrating that LXA_4 has anti-inflammatory and antioxidant effects in TiO_2-induced arthritis. Moreover, we show

that TiO2 injection increased ALX/FPR2 receptor expression on TRPV1 neurons. LXA_4 decreased TiO_2-induced DRG mRNA expression and protein staining of pain-related ion channel TRPV1. In terms of neuronal function, LXA_4 reduced the activation of DRG neurons, observed by low baseline levels of calcium influx in DRG, and lessened responsiveness to TRPV1 activation by capsaicin stimulation.

Intra-articular administration of TiO_2 induces a response that resembles prosthesis joint inflammation and pain (13). Pain is a cardinal symptom of joint inflammation and is directly related to the decision to seek medical care, limitation of limb function, and quality of life (61). Therefore, the development of novel therapeutics effective for optimal pain management is critical in prosthesis wear process-induced arthritis. TiO_2 arthritis is, in principle, an aseptic inflammation and the opposite of septic arthritis as that induced by intraarticular injection of *Staphylococcus aureus*. Evidence demonstrates that limiting the endogenous production and action of LXA_4 by genetic deletion of 5-lipoxygenase and antagonizing the ALX/FPR2 receptor with BOC-2, respectively, improve the immune response against *S. aureus* by avoiding the down-regulation of dendritic cells' recruitment by LXA_4 (62). However, we are demonstrating a beneficial effect of exogenous LXA_4 treatment in aseptic prosthesis arthritis, and endogenous LXA_4 has a detrimental role in septic arthritis. Further exemplifying aseptic inflammatory conditions, LXA_4 levels were decreased in synovial fluid patients with rheumatoid arthritis and osteoarthritis, suggesting that downmodulation of LXA_4 is a permissive factor to chronic joint diseases with high and low inflammation profiles (63).

Prosthesis wear process particles, such as TiO_2, activate macrophages to produce various pro-inflammatory mediators, growth factors, and pro-inflammatory lipids (49,64), and these molecules orchestrate the inflammatory response (65). LXA_4 and agonists of ALX/FPR2 receptors can down-regulate those inflammatory mechanisms. LXA_4 inhibited synoviocyte proliferation as well as decreased the levels of IL-6, IL-1β, and TNF-α in rheumatoid arthritis (66). Of interest, LXA_4 downregulates TNF-α–directed neutrophil trafficking (67). ALX/FPR2 agonist (AT-01-KG) reduced neutrophilic inflammation, CXCL1, and IL-1β production and enhanced neutrophil apoptosis in a model of gout arthritis (68). LXA_4 diminishes pain in the non-compressive lumbar disc herniation model through inhibition of pro-inflammatory cytokines (TNF-α, and IL-1β) up-regulation of IL-10 and transforming growth factor-beta (TGF-β) (30). Treatment with LXA_4 also increases anti-inflammatory cytokine (TGF-β and IL-10) levels after exposition to ultra-violet light (69). IL-10 restricts the polarization of M1 macrophages and blocks the IL-33/ST2 axis during arthritis (70), inhibits neutrophil recruitment, matrix metalloproteinases activity, edema (71) and pain (72). We show that LXA_4 reduced TNF-α, IL-1β, and IL-6 levels and increased IL-10 levels in TiO_2-induced arthritis, and that production is by macrophages recruited during the inflammatory process. Thus, reducing pro-inflammatory cytokines and increasing anti-inflammatory cytokines, which orchestrate the inflammatory and nociceptive responses, might contribute to LXA_4 alleviation of leukocyte recruitment, edema, and mechanical and thermal hyperalgesia.

Oxidative stress has an essential role in inflammatory pain (73). Reactive oxygen and nitrogen species (ROS and RNS, respectively) produced during inflammation contribute directly to nociceptor neuron activation (74). TiO_2 induces lipid peroxidation, DNA damage, and protein breakdown, corroborating there is oxidative stress (75). LXA_4

increases antioxidant capacity via Nrf2 in varied models (25,29,69,76). Herein we demonstrated the in vivo antioxidant effect of LXA_4 and induction of Nrf2, explaining the mechanism of protection against oxidative stress by increasing endogenous antioxidants as per GSH and ABTS assays. GSH is a downstream target of Nrf2 activity (77), and our data on GSH together with the literature (25,69), guided the choice of investigating Nrf2. Furthermore, LXA_4 did not induce gastric, hepatic, or renal damage indicating its safety compared to common side effects of non-steroidal anti-inflammatory drugs.

Administration of TiO_2 particles bypasses the chronic awaiting of prosthesis wearing and reduces the number of animals used to investigate this condition in terms of mechanisms and novel treatments. Chronic inflammation is responsible for peri-prosthetic osteolysis and aseptic loosening of the prosthesis (78,79). Macrophage-like synoviocytes are resident cells in the synovium lining. They are responsible for the phagocytosis of prosthetic wear particles, production of pro-inflammatory cytokines, such as IL-1β and TNF-α, triggering inflammation, recruitment of immune cells, and activation of fibroblast-like synoviocytes (80,81). There are a significant number of macrophages infiltrate into peri-implant tissues during aseptic loosening (82). Total leukocytes in the synovial cavity were higher in the early stage (2nd day) than in late stage (30th day). We also observed higher counts of mononuclear cells than neutrophils on the 2nd day post-TiO_2 administration, which is unexpected, considering the leukocyte recruitment kinetics of most inflammatory responses. We show that the macrophage is mainly recruited cell in the TiO_2-inflammation and apper to be a crutial target to the LXA_4 anti-inflammatory effects. Further studies are necessary to investigate the underlying mechanisms for this specific leukocyte kinetics in TiO_2 arthritis. LXA_4 reduced inflammatory cytokines production induced by TiO_2, which lined up well with the reduced p-NF-κB staining in synovial fluid leukocytes. NF-κB exerts its transcription factor activity and regulates the expression of various genes encoding pro-inflammatory cytokines, which have been shown to play essential roles in inflammation. Diminished NF-κB activation reduces the production of pro-inflammatory cytokines and downmodulates inflammatory reactions (83). Our findings corroborate prior evidence that LXA_4 inhibits NF-κB in other disease models (22,30,84). Furthermore, LXA_4 suppresses the LPS-induced proliferation of RAW264.7 macrophages by targeting the NF-κB pathway (85). The treatment with LXA_4 reduced LPS-evoked TNF-α production and inhibited NF-κB activation in a coculture system using RAW264.7 cells and human colon carcinoma cell line (Caco-2) (86). We confirm that this NF-κB activation is increased in macrophage, that represent the major-activated cell and is inhibed by LXA_4 treatment.

In arthritis, synovial fluid cells are crucial in the production of ROS, which can increase the level of NF-κB-dependent pro-inflammatory cytokines and promote the formation of an amplification loop that feeds back to further elevation of additional ROS (87). Prosthesis wear particles can induce oxidative stress in macrophage culture (88). On the other hand, LXA_4 treatment increases nuclear translocation of Nrf2 in cardiomyocytes (89). In cultured cortical astrocytes exposed to oxygen-glucose deprivation/ recovery insults, LXA_4 reduced oxidative stress by enhancing Nrf2 pathway (29). We show that LXA_4 inhibits TiO_2-triggered ROS generation and enhances Nrf2 in synovial fluid leukocytes. Altogether, these data indicate that LXA_4 enhances Nrf2, and reduces cytokine, ROS production, and, importantly, NF-κB activation, which TiO2 triggered.

The modulation of p-NF-κB and Nrf2 by LXA_4 can also involve their competition to bind to CREB (cAMP-responsive element-binding protein) (54).

LXA_4 has an analgesic effect in various conditions, ranging from acute inflammation (23,24) to neuropathic pain (90). Our data show that LXA_4 has an analgesic effect over ongoing prothesis-wearing-like chronic arthritis (30 days) at 10 ng/animal dose. LXA_4 reduced mechanical and thermal hyperalgesia and provided a 2-days long-lasting analgesia per treatment. The lipid mediator maresin 1 (MaR1) reduces the activation of DRG neurons and TRPV1 mRNA expression in Complete Freund's Adjuvant paw inflammation (37). In inflammatory pain, resolving D2 (RvD2) is a potent TRPV1 and TRPA1 inhibitor in DRG neurons (91). Thus, some SPM can modulate ion channels to induce analgesia suggesting this mechanism should also be investigated for LXA_4 in TiO_2-induced arthritis. However, to that end, we first needed to ascertain if the expression of ALX/FPR2 receptor was increased in TiO_2-induced arhtritis. We observed that ALX/FPR2 receptor staining was increased in TiO_2-induced arthritis, and more specifically, $TRPV1^+$ nociceptive neurons express ALX/FPR2 receptor and that TiO_2 inflammation enhances the $ALXR^+/TRPV1^+$ neurons. Thus, DRG $TRPV1^+$ neurons are likely more susceptible to LXA_4 action during TiO_2 arthritis than uninflamed conditions, supporting the analgesic effect. A single post-treatment with LXA_4 reduced ongoing DRG neuronal activation (baseline calcium levels) and prevented capsaicin-induced TRPV1 activation of DRG neurons. Explaining the diminished neuronal activation by LXA_4, this SPM reduced TiO_2-induced TRPV1 mRNA expression and protein staining (and co-stained with p-NF-κB p65) in DRG neurons. To our knowledge, this is the first work to demonstrate that LXA_4 reduces TRPV1 channel mRNA expression and protein staining in DRG neurons, which resulted in diminished TRPV1 activity, causing analgesia. TRPV1 is expressed by approximately 54% of DRG neurons, and TRPA1 is expressed by approximately 22% of DRG neurons. Most of the TRPA1 channels are co-expressed with TRPV1 in DRG neurons (92), and there is evidence that they can also dimerize as a mechanism of nociceptor sensitization (93). Those TRPA1 channels that are not co-expressed with TRPV1 represent a sub-population of neurons involved in neuropathic pain and not in inflammatory pain (93). Corroborating the literature about the role of TRPA1 in pain and its interaction with TRPV1(58,92,93), as well as the present results on TRPV1, and we also observed that TiO_2 enhances the neuronal activation to TRPA1 agonist, and TRPA1 staining, but not indicate neuronal activation. The activation of TRPA1 agonist and TRPA1 staining were inhibited by LXA_4 treatment. Thus, the mechanism of action of LXA_4 depends, at least in part, on the down-modulation of essential ion channels involved in nociceptor neuronal sensitization and chronic pain (94), and the neuronal activation of $TRPV1^+$ neurons. Our study also contributes to building the concept that targeting ion channels is part of the mechanisms of action of SPM.

We demonstrated that LXA_4 has therapeutic effects against ongoing chronic TiO_2 arthritis, favorably altering knee joint pathology. Figure 13 is a schematic representation of the mechanism of action of LXA_4 in TiO_2-induced arthritis. TiO_2 triggered the production of cytokines and ROS to induce inflammation and pain. The activation of NF-κB in macrophage cells and down-modulation of Nrf2 are mechanisms occurring, at least, in synovial fluid leukocytes that amplify inflammatory cytokines and oxidative stress pathways in response to TiO_2, which LXA_4 targets. We further observed that LXA_4

attenuated the staining of nociceptor neuron sensitization-related ion channels named TRPV1 and TRPA1, unveiling a hitherto unknown nociceptor neuron mechanism of LXA_4. To sum up, this study demonstrated that LXA_4 is a promising approach to treating complications related to prosthesis-induced inflammation and pain by inhibiting the activation of synovial fluid leukocytes and primary afferent nociceptor sensory neurons.

5 Acknowledgments

This study was supported by grants from Conselho Nacional de Desenvolvimento Científico e Tecnológico (CNPq); Financiadora de Estudos e Projetos-Apoio à Infraestrutura (FINEP CT-INFRA); Coordenação de Aperfeiçoamento de Pessoal de Nível Superior (CAPES; finance code 001); Programa de Pesquisa para o Sistema Único de Saúde (PPSUS) grant supported by Ministério da Ciência, Tecnologia e Inovação (MCTI), Secretaria da Saúde do Estado do Paraná (SESA-PR), and Parana State Government (Brazil) (agreements 041/2017); and Programa de Apoio a Grupos de Excelência (PRONEX) grant supported by SETI/Fundação Araucária and MCTI/CNPq, and Governo do Estado do Paraná (agreement 014/2017). The Authors thank the core facility CMLP-UEL for access to equipment free of charge.

Conflicts of Interest: The authors declare no conflict of interest.

6 References

Bruyere O, Ethgen O, Neuprez A, Zegels B, Gillet P, Huskin JP, Reginster JY. Health-related quality of life after total knee or hip replacement for osteoarthritis: a 7-year prospective study. *Arch Orthop Trauma Surg* (2012) 132:1583–1587. doi: 10.1007/s00402-012-1583-7

Dailiana ZH, Papakostidou I, Varitimidis S, Liaropoulos L, Zintzaras E, Karachalios T, Michelinakis E, Malizos KN. Patient-reported quality of life after primary major joint arthroplasty: a prospective comparison of hip and knee arthroplasty. *BMC Musculoskelet Disord* (2015) 16:366. doi: 10.1186/s12891-015-0814-9

Fortin PR, Clarke AE, Joseph L, Liang MH, Tanzer M, Ferland D, Phillips C, Partridge AJ, Belisle P, Fossel AH, et al. Outcomes of total hip and knee replacement: preoperative functional status predicts outcomes at six months after surgery. *Arthritis Rheum* (1999) 42:1722–1728. doi: 10.1002/1529-0131(199908)42:8<1722::AID-ANR22>3.0.CO;2-R

Jones CA, Voaklander DC, Johnston DW, Suarez-Almazor ME. The effect of age on pain, function, and quality of life after total hip and knee arthroplasty. *Arch Intern Med* (2001) 161:454–460. doi: 10.1001/archinte.161.3.454

Canovas F, Dagneaux L. Quality of life after total knee arthroplasty. *Orthop Traumatol Surg Res* (2018) 104:S41–S46. doi: 10.1016/j.otsr.2017.04.017

6.1 van Onna M, Ozturk B, Starmans M, Peeters R, Boonen A. Disease and management
2 beliefs of elderly patients with rheumatoid arthritis and comorbidity: a qualitative study.
3 *Clin Rheumatol* (2018) 37:2367–2372. doi: 10.1007/s10067-018-4167-2

7.4 Lubbeke A, Silman AJ, Barea C, Prieto-Alhambra D, Carr AJ. Mapping existing hip
5 and knee replacement registries in Europe. *Health Policy* (2018) 122:548–557. doi:
6 10.1016/j.healthpol.2018.03.010

8.7 Kurtz S, Ong K, Lau E, Mowat F, Halpern M. Projections of primary and revision hip
8 and knee arthroplasty in the United States from 2005 to 2030. *J Bone Joint Surg Am*
9 (2007) 89:780–785. doi: 10.2106/JBJS.F.00222

9.0 Hellman EJ, Capello WN, Feinberg JR. Omnifit cementless total hip arthroplasty. A 10-
11 year average followup. *Clin Orthop Relat Res* (1999)164–174. doi: 10.1097/00003086-
12 199907000-00022

10.3. Sansone V, Pagani D, Melato M. The effects on bone cells of metal ions released from
14 orthopaedic implants. A review. *Clin Cases Miner Bone Metab* (2013) 10:34–40. doi:
15 10.11138/ccmbm/2013.10.1.034

11.6. Grande F, Tucci P. Titanium Dioxide Nanoparticles: a Risk for Human Health? *Mini*
17 *Rev Med Chem* (2016) 16:762–769. doi: 10.2174/1389557516666160321114341

11.8. Dorner T, Haas J, Loddenkemper C, von Baehr V, Salama A. Implant-related
19 inflammatory arthritis. *Nat Clin Pract Rheumatol* (2006) 2:53–6; quiz 57. doi:
20 10.1038/ncprheum0087

12.1. Borghi SM, Mizokami SS, Pinho-Ribeiro FA, Fattori V, Crespigio J, Clemente-
22 Napimoga JT, Napimoga MH, Pitol DL, Issa JPM, Fukada SY, et al. The flavonoid
23 quercetin inhibits titanium dioxide (TiO2)-induced chronic arthritis in mice. *J Nutr*
24 *Biochem* (2018) 53:81–95. doi: 10.1016/j.jnutbio.2017.10.010

12.5. Cobelli N, Scharf B, Crisi GM, Hardin J, Santambrogio L. Mediators of the
26 inflammatory response to joint replacement devices. *Nat Rev Rheumatol* (2011) 7:600–
27 608. doi: 10.1038/nrrheum.2011.128

12.8. Wooley PH, Morren R, Andary J, Sud S, Yang SY, Mayton L, Markel D, Sieving A,
29 Nasser S. Inflammatory responses to orthopaedic biomaterials in the murine air pouch.
30 *Biomaterials* (2002) 23:517–526. doi: 10.1016/s0142-9612(01)00134-x

13.1. Ferreira CC, Ricci VP, Sousa LL de, Mariano NA, Campos MGN. Improvement of
32 titanium corrosion resistance by coating with poly-caprolactone and poly-
33 caprolactone/titanium dioxide: potential application in heart valves. *Materials Research*
34 (2018) 20:126–133.

13.5. Verri Jr. WA, Souto FO, Vieira SM, Almeida SC, Fukada SY, Xu D, Alves-Filho JC,
36 Cunha TM, Guerrero AT, Mattos-Guimaraes RB, et al. IL-33 induces neutrophil
37 migration in rheumatoid arthritis and is a target of anti-TNF therapy. *Ann Rheum Dis*
38 (2010) 69:1697–1703. doi: 10.1136/ard.2009.122655

13.9. Brennan EP, Nolan KA, Borgeson E, Gough OS, McEvoy CM, Docherty NG, Higgins
40 DF, Murphy M, Sadlier DM, Ali-Shah ST, et al. Lipoxins attenuate renal fibrosis by

inducing let-7c and suppressing TGFbetaR1. *J Am Soc Nephrol* (2013) 24:627–637. doi: 10.1681/ASN.2012060550

3. Chandrasekharan JA, Sharma-Walia N. Lipoxins: nature's way to resolve inflammation. *J Inflamm Res* (2015) 8:181–192. doi: 10.2147/JIR.S90380

5. Serhan CN. Pro-resolving lipid mediators are leads for resolution physiology. *Nature* (2014) 510:92–101. doi: 10.1038/nature13479

7. Serhan CN. Lipoxins and aspirin-triggered 15-epi-lipoxins are the first lipid mediators of endogenous anti-inflammation and resolution. *Prostaglandins Leukot Essent Fatty Acids* (2005) 73:141–162. doi: 10.1016/j.plefa.2005.05.002

10. Jiang X, Li Z, Jiang S, Tong X, Zou X, Wang W, Zhang Z, Wu L, Tian D. Lipoxin A4 exerts protective effects against experimental acute liver failure by inhibiting the NF-kappaB pathway. *Int J Mol Med* (2016) 37:773–780. doi: 10.3892/ijmm.2016.2483

13. Abdelmoaty S, Wigerblad G, Bas DB, Codeluppi S, Fernandez-Zafra T, El-Awady el S, Moustafa Y, Abdelhamid Ael D, Brodin E, Svensson CI. Spinal actions of lipoxin A4 and 17(R)-resolvin D1 attenuate inflammation-induced mechanical hypersensitivity and spinal TNF release. *PLoS One* (2013) 8:e75543. doi: 10.1371/journal.pone.0075543

17. Svensson CI, Zattoni M, Serhan CN. Lipoxins and aspirin-triggered lipoxin inhibit inflammatory pain processing. *J Exp Med* (2007) 204:245–252. doi: 10.1084/jem.20061826

20. Han X, Yao W, Liu Z, Li H, Zhang ZJ, Hei Z, Xia Z. Lipoxin A4 Preconditioning Attenuates Intestinal Ischemia Reperfusion Injury through Keap1/Nrf2 Pathway in a Lipoxin A4 Receptor Independent Manner. *Oxid Med Cell Longev* (2016) 2016:9303606. doi: 10.1155/2016/9303606

24. Jin W, Jia Y, Huang L, Wang T, Wang H, Dong Y, Zhang H, Fan M, Lv P. Lipoxin A4 methyl ester ameliorates cognitive deficits induced by chronic cerebral hypoperfusion through activating ERK/Nrf2 signaling pathway in rats. *Pharmacol Biochem Behav* (2014) 124:145–152. doi: 10.1016/j.pbb.2014.05.023

27. Wu SH, Wang MJ, Lu J, Chen XQ. Signal transduction involved in lipoxin A4induced protection of tubular epithelial cells against hypoxia/reoxygenation injury. *Mol Med Rep* (2017) 15:1682–1692. doi: 10.3892/mmr.2017.6195

31. Ye W, Zheng C, Yu D, Zhang F, Pan R, Ni X, Shi Z, Zhang Z, Xiang Y, Sun H, et al. Lipoxin A4 Ameliorates Acute Pancreatitis-Associated Acute Lung Injury through the Antioxidative and Anti-inflammatory Effects of the Nrf2 Pathway. *Oxid Med Cell Longev* (2019) 2019:2197017. doi: 10.1155/2019/2197017

35. Wu L, Li HH, Wu Q, Miao S, Liu ZJ, Wu P, Ye DY. Lipoxin A4 Activates Nrf2 Pathway and Ameliorates Cell Damage in Cultured Cortical Astrocytes Exposed to Oxygen-Glucose Deprivation/Reperfusion Insults. *J Mol Neurosci* (2015) 56:848–857. doi: 10.1007/s12031-015-0525-6

39. Miao GS, Liu ZH, Wei SX, Luo JG, Fu ZJ, Sun T. Lipoxin A4 attenuates radicular pain possibly by inhibiting spinal ERK, JNK and NF-kappaB/p65 and cytokine signals, but

not p38, in a rat model of non-compressive lumbar disc herniation. *Neuroscience* (2015) 300:10–18. doi: 10.1016/j.neuroscience.2015.04.060

36. Walker J, Dichter E, Lacorte G, Kerner D, Spur B, Rodriguez A, Yin K. Lipoxin a4 increases survival by decreasing systemic inflammation and bacterial load in sepsis. *Shock* (2011) 36:410–416. doi: 10.1097/SHK.0b013e31822798c1

37. Wu SH, Liao PY, Dong L, Chen ZQ. Signal pathway involved in inhibition by lipoxin A(4) of production of interleukins induced in endothelial cells by lipopolysaccharide. *Inflamm Res* (2008) 57:430–437. doi: 10.1007/s00011-008-7147-1

38. McMahon B, Mitchell S, Brady HR, Godson C. Lipoxins: revelations on resolution. *Trends in Pharmacological Sciences* (2001) 22:391–395. doi: 10.1016/S0165-6147(00)01771-5

39. Fiore S, Maddox JF, Perez HD, Serhan CN. Identification of a human cDNA encoding a functional high affinity lipoxin A4 receptor. *The Journal of Experimental Medicine* (1994) 180:253. doi: 10.1084/JEM.180.1.253

40. Chiang N, Fierro IM, Gronert K, Serhan CN. Activation of Lipoxin a4 Receptors by Aspirin-Triggered Lipoxins and Select Peptides Evokes Ligand-Specific Responses in Inflammation. *The Journal of Experimental Medicine* (2000) 191:1197. doi: 10.1084/JEM.191.7.1197

41. Takano T, Fiore S, Maddox JF, Brady HR, Petasis NA, Serhan CN. Aspirin-triggered 15-epi-lipoxin A4 (LXA4) and LXA4 stable analogues are potent inhibitors of acute inflammation: evidence for anti-inflammatory receptors. *J Exp Med* (1997) 185:1693–1704. doi: 10.1084/JEM.185.9.1693

42. Fattori V, Pinho-Ribeiro FA, Staurengo-Ferrari L, Borghi SM, Rossaneis AC, Casagrande R, Verri Jr. WA. The specialised pro-resolving lipid mediator maresin 1 reduces inflammatory pain with a long-lasting analgesic effect. *Br J Pharmacol* (2019) 176:1728–1744. doi: 10.1111/bph.14647

43. Ferraz CR, Carvalho TT, Fattori V, Saraiva-Santos T, Pinho-Ribeiro FA, Borghi SM, Manchope MF, Zaninelli TH, Cunha TM, Casagrande R, et al. Jararhagin, a snake venom metalloproteinase, induces mechanical hyperalgesia in mice with the neuroinflammatory contribution of spinal cord microglia and astrocytes. *Int J Biol Macromol* (2021) 179:610–619. doi: 10.1016/j.ijbiomac.2021.02.178

44. Manchope MF, Artero NA, Fattori V, Mizokami SS, Pitol DL, Issa JPM, Fukada SY, Cunha TM, Alves-Filho JC, Cunha FQ, et al. Naringenin mitigates titanium dioxide (TiO2)-induced chronic arthritis in mice: role of oxidative stress, cytokines, and NFkappaB. *Inflamm Res* (2018) 67:997–1012. doi: 10.1007/s00011-018-1195-y

45. Guerrero AT, Verri Jr. WA, Cunha TM, Silva TA, Rocha FA, Ferreira SH, Cunha FQ, Parada CA. Hypernociception elicited by tibio-tarsal joint flexion in mice: a novel experimental arthritis model for pharmacological screening. *Pharmacol Biochem Behav* (2006) 84:244–251. doi: 10.1016/j.pbb.2006.05.008

46. Fattori V, Borghi SM, Guazelli CFS, Giroldo AC, Crespigio J, Bussmann AJC, Coelho-Silva L, Ludwig NG, Mazzuco TL, Casagrande R, et al. Vinpocetine reduces

diclofenac-induced acute kidney injury through inhibition of oxidative stress, apoptosis, cytokine production, and NF-kappaB activation in mice. *Pharmacol Res* (2017) 120:10–22. doi: 10.1016/j.phrs.2016.12.039

24. Wallace JL, McKnight GW, Bell CJ. Adaptation of rat gastric mucosa to aspirin requires mucosal contact. *Am J Physiol* (1995) 268:G134-8. doi: 10.1152/ajpgi.1995.268.1.G134

37. Bussmann AJC, Borghi SM, Zaninelli TH, dos Santos TS, Guazelli CFS, Fattori V, Domiciano TP, Pinho-Ribeiro FA, Ruiz-Miyazawa KW, Casella AMB, et al. The citrus flavanone naringenin attenuates zymosan-induced mouse joint inflammation: induction of Nrf2 expression in recruited CD45(+) hematopoietic cells. *Inflammopharmacology* (2019) 27:1229–1242. doi: 10.1007/s10787-018-00561-6

42. Borghi SM, Carvalho TT, Staurengo-Ferrari L, Hohmann MS, Pinge-Filho P, Casagrande R, Verri Jr. WA. Vitexin inhibits inflammatory pain in mice by targeting TRPV1, oxidative stress, and cytokines. *J Nat Prod* (2013) 76:1141–1149. doi: 10.1021/np400222v

45. Casagrande R, Georgetti SR, Verri Jr. WA, Jabor JR, Santos AC, Fonseca MJ. Evaluation of functional stability of quercetin as a raw material and in different topical formulations by its antilipoperoxidative activity. *AAPS PharmSciTech* (2006) 7:E10. doi: 10.1208/pt070110

46. Hohmann MS, Cardoso RD, Pinho-Ribeiro FA, Crespigio J, Cunha TM, Alves-Filho JC, da Silva R v, Pinge-Filho P, Ferreira SH, Cunha FQ, et al. 5-lipoxygenase deficiency reduces acetaminophen-induced hepatotoxicity and lethality. *Biomed Res Int* (2013) 2013:627046. doi: 10.1155/2013/627046

47. Fattori V, Amaral FA, Verri Jr. WA. Neutrophils and arthritis: Role in disease and pharmacological perspectives. *Pharmacol Res* (2016) 112:84–98. doi: 10.1016/j.phrs.2016.01.027

48. Bindu S, Mazumder S, Bandyopadhyay U. Non-steroidal anti-inflammatory drugs (NSAIDs) and organ damage: A current perspective. *Biochem Pharmacol* (2020) 180:114147. doi: 10.1016/j.bcp.2020.114147

49. Chen O, Donnelly CR, Ji RR. Regulation of pain by neuro-immune interactions between macrophages and nociceptor sensory neurons. *Curr Opin Neurobiol* (2020) 62:17–25. doi: 10.1016/j.conb.2019.11.006

50. Zhang JM, An J. Cytokines, inflammation, and pain. *Int Anesthesiol Clin* (2007) 45:27–37. doi: 10.1097/AIA.0b013e318034194e

51. Huang KT, Wu CT, Huang KH, Lin WC, Chen CM, Guan SS, Chiang CK, Liu SH. Titanium nanoparticle inhalation induces renal fibrosis in mice via an oxidative stress up-regulated transforming growth factor-beta pathway. *Chem Res Toxicol* (2015) 28:354–364. doi: 10.1021/tx500287f

52. Hwang YJ, Jeung YS, Seo MH, Yoon JY, Kim DY, Park JW, Han JH, Jeong SH. Asian dust and titanium dioxide particles-induced inflammation and oxidative DNA damage

in C57BL/6 mice. *Inhal Toxicol* (2010) 22:1127–1133. doi: 10.3109/08958378.2010.528805

53. Sang X, Zheng L, Sun Q, Li N, Cui Y, Hu R, Gao G, Cheng Z, Cheng J, Gui S, et al. The chronic spleen injury of mice following long-term exposure to titanium dioxide nanoparticles. *J Biomed Mater Res A* (2012) 100:894–902. doi: 10.1002/jbm.a.34024

54. Staurengo-Ferrari L, Badaro-Garcia S, Hohmann MSN, Manchope MF, Zaninelli TH, Casagrande R, Verri Jr. WA. Contribution of Nrf2 Modulation to the Mechanism of Action of Analgesic and Anti-inflammatory Drugs in Pre-clinical and Clinical Stages. *Front Pharmacol* (2018) 9:1536. doi: 10.3389/fphar.2018.01536

55. Chiu IM, Heesters BA, Ghasemlou N, von Hehn CA, Zhao F, Tran J, Wainger B, Strominger A, Muralidharan S, Horswill AR, et al. Bacteria activate sensory neurons that modulate pain and inflammation. *Nature* (2013) 501:52–57. doi: 10.1038/nature12479

56. Caterina MJ, Rosen TA, Tominaga M, Brake AJ, Julius D. A capsaicin-receptor homologue with a high threshold for noxious heat. *Nature* (1999) 398:436–441. doi: 10.1038/18906

57. Bandell M, Story GM, Hwang SW, Viswanath V, Eid SR, Petrus MJ, Earley TJ, Patapoutian A. Noxious cold ion channel TRPA1 is activated by pungent compounds and bradykinin. *Neuron* (2004) 41:849–857. doi: 10.1016/S0896-6273(04)00150-3

58. Bautista DM, Jordt SE, Nikai T, Tsuruda PR, Read AJ, Poblete J, Yamoah EN, Basbaum AI, Julius D. TRPA1 mediates the inflammatory actions of environmental irritants and proalgesic agents. *Cell* (2006) 124:1269–1282. doi: 10.1016/J.CELL.2006.02.023

59. Silverman HA, Chen A, Kravatz NL, Chavan SS, Chang EH. Involvement of Neural Transient Receptor Potential Channels in Peripheral Inflammation. *Front Immunol* (2020) 11: doi: 10.3389/FIMMU.2020.590261

60. McMahon SB, Wood JN. Increasingly irritable and close to tears: TRPA1 in inflammatory pain. *Cell* (2006) 124:1123–1125. doi: 10.1016/J.CELL.2006.03.006

61. Hadler NM. Knee pain is the malady--not osteoarthritis. *Ann Intern Med* (1992) 116:598–599. doi: 10.7326/0003-4819-116-7-598

62. Boff D, Oliveira VLS, Queiroz Junior CM, Galvao I, Batista N v, Gouwy M, Menezes GB, Cunha TM, Verri Junior WA, Proost P, et al. Lipoxin A4 impairs effective bacterial control and potentiates joint inflammation and damage caused by Staphylococcus aureus infection. *FASEB J* (2020) 34:11498–11510. doi: 10.1096/fj.201802830RR

63. Hashimoto A, Hayashi I, Murakami Y, Sato Y, Kitasato H, Matsushita R, Iizuka N, Urabe K, Itoman M, Hirohata S, et al. Anti-inflammatory mediator lipoxin A4 and its receptor in synovitis of patients with rheumatoid arthritis. *J Rheumatol* (2007) 34:2144–2153. http://www.ncbi.nlm.nih.gov/pubmed/17918787

64. Nich C, Takakubo Y, Pajarinen J, Ainola M, Salem A, Sillat T, Rao AJ, Raska M, Tamaki Y, Takagi M, et al. Macrophages-Key cells in the response to wear debris from

joint replacements. *J Biomed Mater Res A* (2013) 101:3033–3045. doi: 10.1002/jbm.a.34599

63. Montecucco F, Mach F. Common inflammatory mediators orchestrate pathophysiological processes in rheumatoid arthritis and atherosclerosis. *Rheumatology (Oxford)* (2009) 48:11–22. doi: 10.1093/rheumatology/ken395

66. Li J, Sun Q, Zheng C, Bai C, Liu C, Zhao X, Deng P, Chai L, Jia Y. Lipoxin A4-Mediated p38 MAPK Signaling Pathway Protects Mice Against Collagen-Induced Arthritis. *Biochem Genet* (2021) 59:346–365. doi: 10.1007/s10528-020-10016-9

67. Hachicha M, Pouliot M, Petasis NA, Serhan CN. Lipoxin (LX)A4 and aspirin-triggered 15-epi-LXA4 inhibit tumor necrosis factor 1alpha-initiated neutrophil responses and trafficking: regulators of a cytokine-chemokine axis. *J Exp Med* (1999) 189:1923–1930. doi: 10.1084/jem.189.12.1923

68. Galvao I, Melo EM, de Oliveira VLS, Vago JP, Queiroz-Junior C, de Gaetano M, Brennan E, Gahan K, Guiry PJ, Godson C, et al. Therapeutic potential of the FPR2/ALX agonist AT-01-KG in the resolution of articular inflammation. *Pharmacol Res* (2021) 165:105445. doi: 10.1016/j.phrs.2021.105445

69. Martinez RM, Fattori V, Saito P, Melo CBP, Borghi SM, Pinto IC, Bussmann AJC, Baracat MM, Georgetti SR, Verri Jr. WA, et al. Lipoxin A4 inhibits UV radiation-induced skin inflammation and oxidative stress in mice. *J Dermatol Sci* (2018) doi: 10.1016/j.jdermsci.2018.04.014

70. Chen S, Chen B, Wen Z, Huang Z, Ye L. IL-33/ST2-mediated inflammation in macrophages is directly abrogated by IL-10 during rheumatoid arthritis. *Oncotarget* (2017) 8:32407–32418. doi: 10.18632/oncotarget.16299

71. Sodin-Semrl S, Taddeo B, Tseng D, Varga J, Fiore S. Lipoxin A4 inhibits IL-1 beta-induced IL-6, IL-8, and matrix metalloproteinase-3 production in human synovial fibroblasts and enhances synthesis of tissue inhibitors of metalloproteinases. *J Immunol* (2000) 164:2660–2666. doi: 10.4049/jimmunol.164.5.2660

72. Poole S, Cunha FQ, Selkirk S, Lorenzetti BB, Ferreira SH. Cytokine-mediated inflammatory hyperalgesia limited by interleukin-10. *Br J Pharmacol* (1995) 115:684–688. doi: 10.1111/j.1476-5381.1995.tb14987.x

73. Salvemini D, Little JW, Doyle T, Neumann WL. Roles of reactive oxygen and nitrogen species in pain. *Free Radic Biol Med* (2011) 51:951–966. doi: 10.1016/j.freeradbiomed.2011.01.026

74. Maioli NA, Zarpelon AC, Mizokami SS, Calixto-Campos C, Guazelli CF, Hohmann MS, Pinho-Ribeiro FA, Carvalho TT, Manchope MF, Ferraz CR, et al. The superoxide anion donor, potassium superoxide, induces pain and inflammation in mice through production of reactive oxygen species and cyclooxygenase-2. *Braz J Med Biol Res* (2015) 48:321–331. doi: 10.1590/1414-431X20144187

75. Dubey A, Goswami M, Yadav K, Chaudhary D. Oxidative Stress and Nano-Toxicity Induced by TiO2 and ZnO on WAG Cell Line. *PLoS One* (2015) 10:e0127493. doi: 10.1371/journal.pone.0127493

76. Zong H, Li X, Lin H, Hou C, Ma F. Lipoxin A4 pretreatment mitigates skeletal muscle ischemia-reperfusion injury in rats. *Am J Transl Res* (2017) 9:1139–1150. http://www.ncbi.nlm.nih.gov/pubmed/28386340

77. Tonelli C, Chio IIC, Tuveson DA. Transcriptional Regulation by Nrf2. *Antioxid Redox Signal* (2018) 29:1727–1745. doi: 10.1089/ars.2017.7342

78. Gallo J, Goodman SB, Konttinen YT, Raska M. Particle disease: biologic mechanisms of periprosthetic osteolysis in total hip arthroplasty. *Innate Immun* (2013) 19:213–224. doi: 10.1177/1753425912451779

79. Ulrich SD, Seyler TM, Bennett D, Delanois RE, Saleh KJ, Thongtrangan I, Kuskowski M, Cheng EY, Sharkey PF, Parvizi J, et al. Total hip arthroplasties: what are the reasons for revision? *Int Orthop* (2008) 32:597–604. doi: 10.1007/s00264-007-0364-3

80. Landgraeber S, Jager M, Jacobs JJ, Hallab NJ. The pathology of orthopedic implant failure is mediated by innate immune system cytokines. *Mediators Inflamm* (2014) 2014:185150. doi: 10.1155/2014/185150

81. Tu J, Hong W, Zhang P, Wang X, Korner H, Wei W. Ontology and Function of Fibroblast-Like and Macrophage-Like Synoviocytes: How Do They Talk to Each Other and Can They Be Targeted for Rheumatoid Arthritis Therapy? *Front Immunol* (2018) 9:1467. doi: 10.3389/fimmu.2018.01467

82. Jamsen E, Pajarinen J, Lin TH, Lo CW, Nabeshima A, Lu L, Nathan K, Eklund KK, Yao Z, Goodman SB. Effect of Aging on the Macrophage Response to Titanium Particles. *J Orthop Res* (2020) 38:405–416. doi: 10.1002/jor.24461

83. Liu T, Zhang L, Joo D, Sun SC. NF-kappaB signaling in inflammation. *Signal Transduct Target Ther* (2017) 2: doi: 10.1038/sigtrans.2017.23

84. Song Y, Yang Y, Cui Y, Gao J, Wang K, Cui J. Lipoxin A4 Methyl Ester Reduces Early Brain Injury by Inhibition of the Nuclear Factor Kappa B (NF-kappaB)-Dependent Matrix Metallopeptidase 9 (MMP-9) Pathway in a Rat Model of Intracerebral Hemorrhage. *Med Sci Monit* (2019) 25:1838–1847. doi: 10.12659/MSM.915119

85. Huang YH, Wang HM, Cai ZY, Xu FY, Zhou XY. Lipoxin A4 inhibits NF-kappaB activation and cell cycle progression in RAW264.7 cells. *Inflammation* (2014) 37:1084–1090. doi: 10.1007/s10753-014-9832-2

86. Kure I, Nishiumi S, Nishitani Y, Tanoue T, Ishida T, Mizuno M, Fujita T, Kutsumi H, Arita M, Azuma T, et al. Lipoxin A(4) reduces lipopolysaccharide-induced inflammation in macrophages and intestinal epithelial cells through inhibition of nuclear factor-kappaB activation. *J Pharmacol Exp Ther* (2010) 332:541–548. doi: 10.1124/jpet.109.159046

87. Morgan MJ, Liu ZG. Crosstalk of reactive oxygen species and NF-kappaB signaling. *Cell Res* (2011) 21:103–115. doi: 10.1038/cr.2010.178

88. Luo G, Li Z, Wang Y, Wang H, Zhang Z, Chen W, Zhang Y, Xiao Y, Li C, Guo Y, et al. Resveratrol Protects against Titanium Particle-Induced Aseptic Loosening Through

Reduction of Oxidative Stress and Inactivation of NF-kappaB. *Inflammation* (2016) 39:775–785. doi: 10.1007/s10753-016-0306-6

Chen XQ, Wu SH, Zhou Y, Tang YR. Lipoxin A4-induced heme oxygenase-1 protects cardiomyocytes against hypoxia/reoxygenation injury via p38 MAPK activation and Nrf2/ARE complex. *PLoS One* (2013) 8:e67120. doi: 10.1371/journal.pone.0067120

Martini AC, Berta T, Forner S, Chen G, Bento AF, Ji RR, Rae GA. Lipoxin A4 inhibits microglial activation and reduces neuroinflammation and neuropathic pain after spinal cord hemisection. *J Neuroinflammation* (2016) 13:75. doi: 10.1186/s12974-016-0540-8

Park CK, Xu ZZ, Liu T, Lu N, Serhan CN, Ji RR. Resolvin D2 is a potent endogenous inhibitor for transient receptor potential subtype V1/A1, inflammatory pain, and spinal cord synaptic plasticity in mice: distinct roles of resolvin D1, D2, and E1. *J Neurosci* (2011) 31:18433–18438. doi: 10.1523/JNEUROSCI.4192-11.2011

Bautista DM, Movahed P, Hinman A, Axelsson HE, Sterner O, Högestätt ED, Julius D, Jordt SE, Zygmunt PM. Pungent products from garlic activate the sensory ion channel TRPA1. *Proc Natl Acad Sci U S A* (2005) 102:12248–12252. doi: 10.1073/PNAS.0505356102

Patil MJ, Salas M, Bialuhin S, Boyd JT, Jeske NA, Akopian AN. Sensitization of small-diameter sensory neurons is controlled by TRPV1 and TRPA1 association. *FASEB Journal* (2020) 34:287–302. doi: 10.1096/FJ.201902026R

Julius D. TRP channels and pain. *Annu Rev Cell Dev Biol* (2013) 29:355–384. doi: 10.1146/annurev-cellbio-101011-155833

Figures and legends

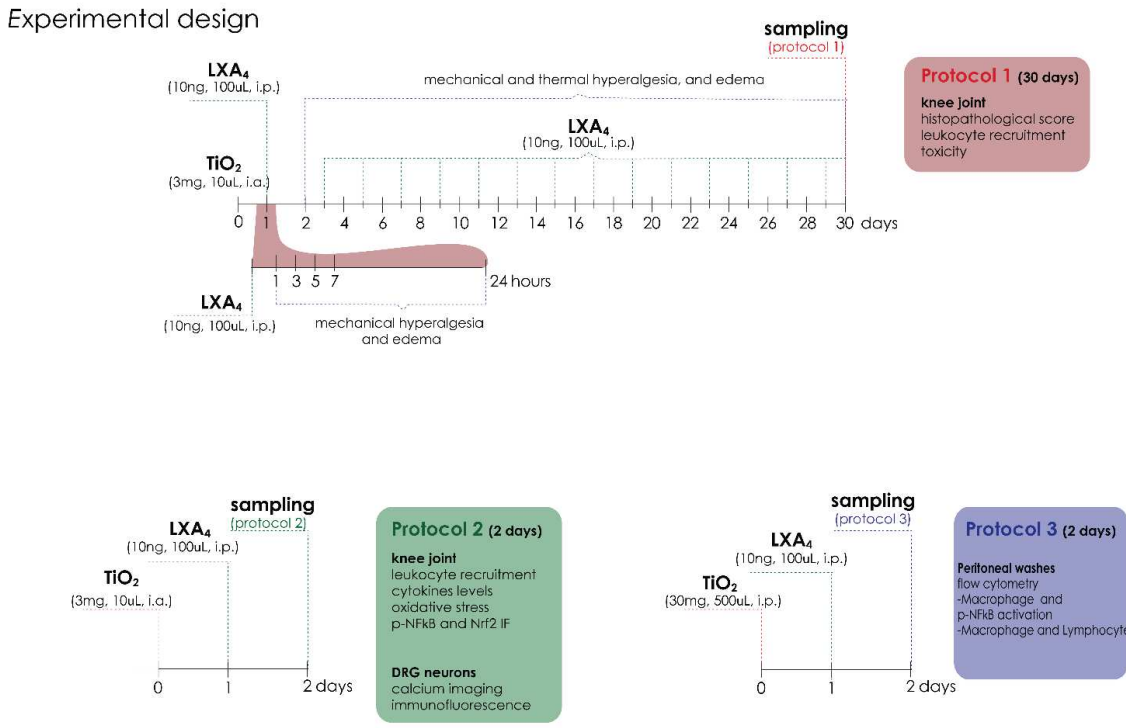

Figure 1. Experimental design. Protocol 1 of 30 days experimental design. Mice were treated for 30 days with LXA_4 (0.1, 1, 10 ng/ animal, i.p.) or vehicle (ethanol) starting twenty-four hours after i.a. injection of TiO_2 (3mg/ joint), and mechanical hyperalgesia and edema were evaluated 1, 3, 5, 7, 24 h (day 1) and subsequently every two days until the 30th day. Thermal hyperalgesia was evaluated on day one and every three days until the 30th. On the 30th day, the knee joint was collected for histopathological analysis and toxicity assay, and the knee joint washes to leukocyte recruitment. Protocol 2 of 2 days experimental design. Mice were treated with a single treatment of LXA_4 (10ng/ animal) starting twenty-four hours after i.a., injection of TiO_2 (3mg/ joint), and on the 2nd day, knee joint wash was collected for leukocyte recruitment, knee joint cytokine levels, NF-κB phosphorylation, and oxidative stress (GSH, ABTS, ROS assay, and Nrf2 expression and activation). On the 2nd day of the model, DRGs samples (L4-L6) were collected for calcium imaging (TRPV1 and TRPA1 agonists) and dissected for immunofluorescence (ALX/FPR2 receptor co-stained with TRPV1; TRPV1 and p-NF-κB co-staining with TRPV1 and TRPA1), and RT-qPCR. Protocol 3 of TiO_2-induced peritonitis. Mice were induced with an i.p. injection of TiO_2 (30 mg/500 µl), and after twenty-four hours, the animals received treatment with LXA_4 (10 ng/animal) or vehicle (saline) (100µl per animal, i.p.). Peritoneal washes were collected on the 2nd day to count total leukocytes recruited and flow cytometry for lymphocytes, macrophages and p-NF-κB activation.

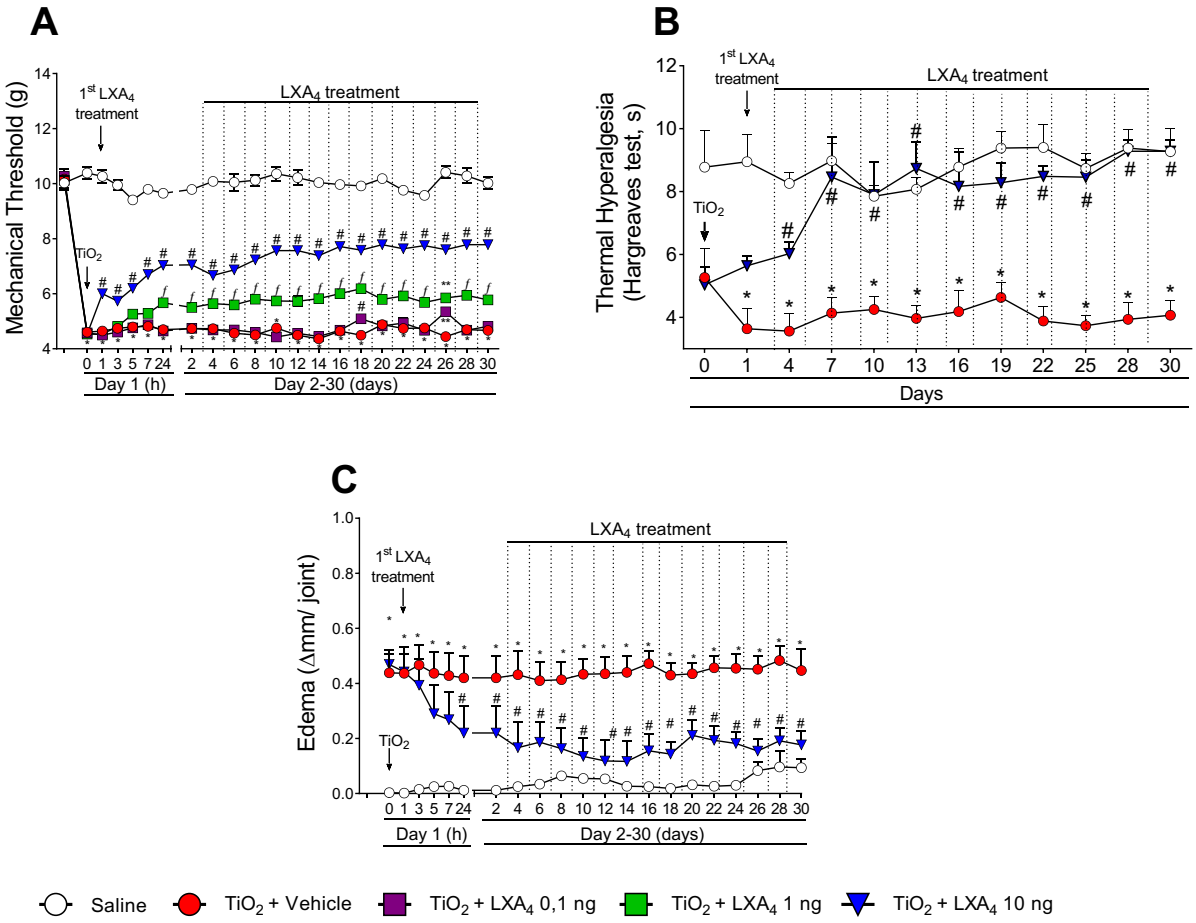

Figure 2. LXA_4 inhibits TiO_2-induced articular mechanical hyperalgesia, thermal hyperalgesia, and edema in the knee joint. Mice were treated for 30 days with LXA_4 (0.1, 1, 10 ng/ animal, i.p.; 48 h intervals) or vehicle (ethanol) starting twenty-four hours after i.a. injection of TiO_2 (3mg/ joint) and mechanical hyperalgesia **(A)** was evaluated 1, 3, 5, 7, 24 h (day 1) and subsequently every two days until the 30th day. Thermal hyperalgesia **(B)** was evaluated on day one and every three days until the 30th. Results are expressed as mean ± SEM, n= 6 mice per group per experiment and are representative of two separate experiments (*p< 0.05 vs. saline group; #p<0.05 vs. TiO_2 group; **p < 0.05 vs. TiO_2 and LXA_4 (10ng) groups; *f*p< 0.05 vs. TiO_2 and LXA_4 (10 and 1 ng) groups), repeated measures two-way ANOVA followed by Tukey's post-test. Edema **(C)** was evaluated 1, 3, 5, 7, 24 h (day 1) and subsequently every two days until the 30th day.

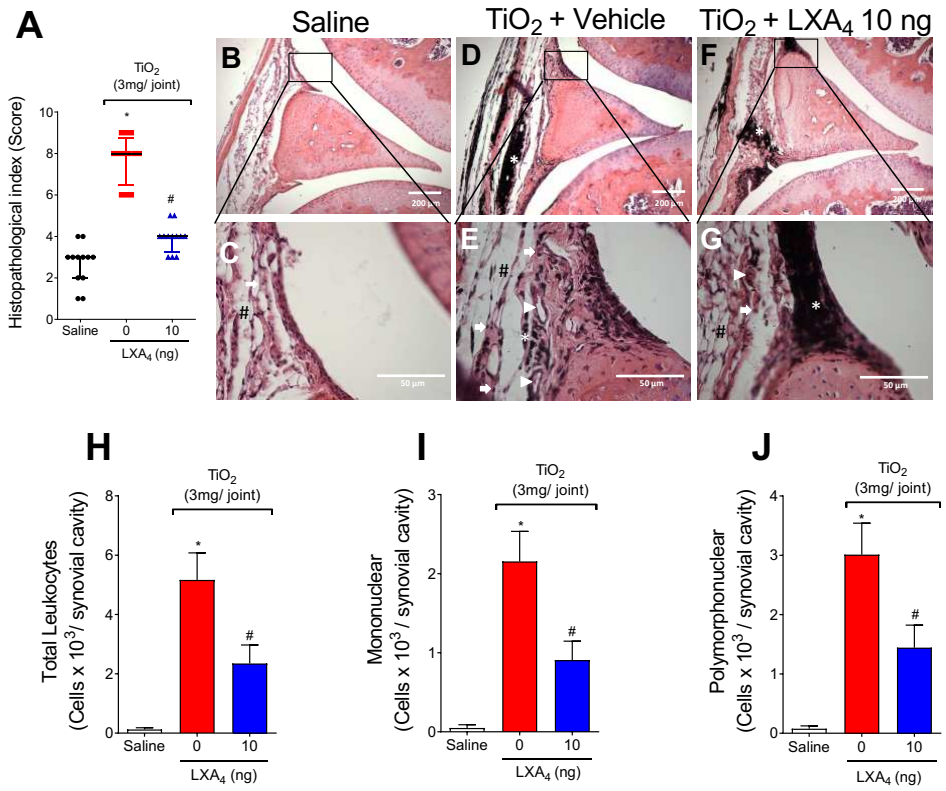

Figure 3. LXA_4 reduces TiO_2-induced histopathological damage and recruitment in the knee joint. Mice were treated with LXA_4 (10ng/ animal, i.p.) or vehicle (ethanol) twenty-four hours after TiO_2 (3mg) i.a. injection and on alternate days for 30 days. On the 30th day, the knee joint was collected and stained with HE. Histopathological index **(A)** and analysis **(B-G)**. The panel shows: saline **(B and C)**, TiO_2 treated with vehicle **(D and E)**, and TiO_2 treated with LXA_4 **(F and G)**. The representative image demonstrated the invasive pannus (arrowhead); leukocyte infiltration (arrow), and angiogenesis (asterisk). Original magnification 10x **(B, D and F)** and 40x **(C, E and G)**. Results are expressed as mean ± SEM, n=12 mice per group per experiment, two independent experiments (*$p<0.05$ vs. saline group; #$p<0.05$ vs. TiO_2 group, Kruskal-Wallis followed by Dunn's post-test). On the 30th day, knee joint washes were collected to count total leukocytes **(H)**, mononuclear **(I)**, and polymorphonuclear cells **(J)**. Results are expressed as mean ± SEM, n=6 mice per group per experiment, two independent experiments (*$p<0.05$ vs. saline group; #$p<0.05$ vs. TiO_2 group, one-way ANOVA followed by Tukey's post-test).

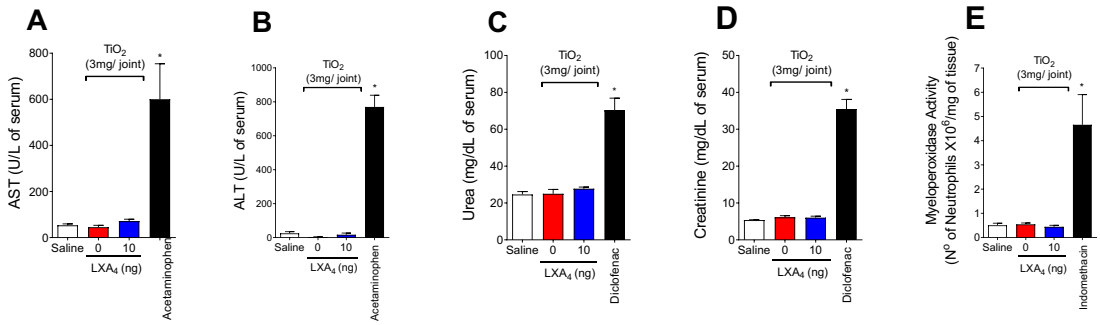

Figure 4. LXA_4 chronic treatment does not induce toxicity. Mice were treated for 30 days with LXA_4 (10 ng/ animal, i.p.) starting twenty-four hours after i.a. injection of TiO_2 (3 mg/ joint), and serum and stomach were collected. AST **(A)**, ALT **(B)**, urea **(C)**, and creatinine **(D)** serum levels and MPO activity in the stomach **(E)** were determined to evaluate treatment toxicity. As positive drug control for gastric, hepatic, and renal toxicity, indomethacin (2.5 mg/kg, i.p., diluted in tris/HCl buffer, for 7 days), acetaminophen (650 mg/kg, i.p., diluted in saline), and diclofenac (200 mg/kg, p.o., diluted in saline) were used, respectively. Results are expressed as mean ± SEM, n=6 mice per group per experiment, two independent experiments (*$p<0.05$ vs. all groups, one-way ANOVA followed by Tukey's post-test).

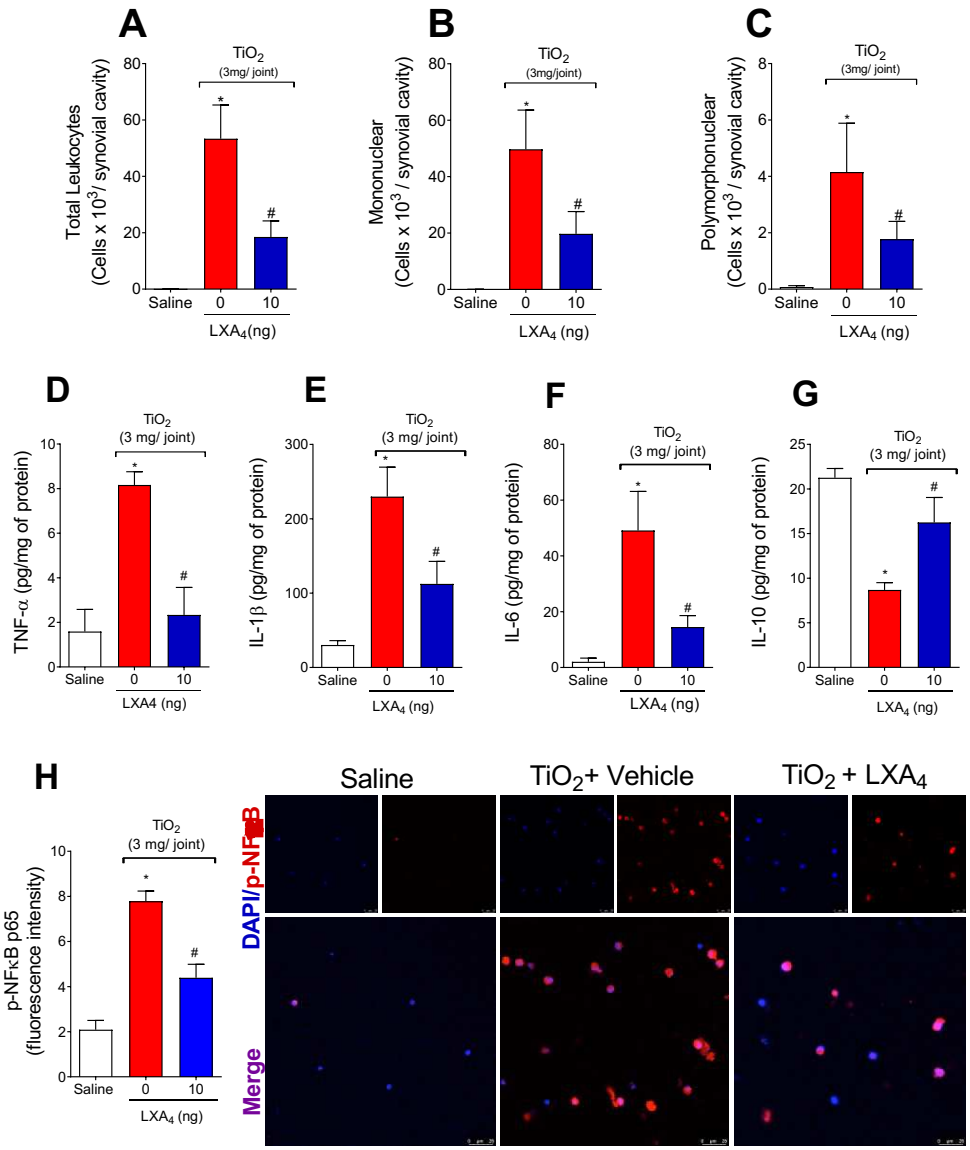

Figure 5. LXA_4 modulates TiO_2-induced mononuclear cells and cytokine production, reducing NF-κB activation. Mice received a single treatment of LXA_4 (10ng/ animal) starting twenty-four hours after i.a. injection of TiO_2 (3mg/ joint), and on the 2nd day, knee joint washes were collected to count total leukocytes **(A)**, mononuclear **(B)**, and polymorphonuclear cells **(C)**. The knee joint was collected, and TNF-α **(D)**, IL-1β **(E)**, IL-6 **(F)**, and IL-10 **(G)** were measured by ELISA. Knee joint washes were used to perform an immunofluorescence assay. Panel **(E)** show the representative images of p-NF-κB p65 (red) with nuclear staining by DAPI, and the quantitation. Fluorescence intensity **(E)** was analyzed by a confocal microscope at 63x magnification. Results are expressed as mean ± SEM, n=6 mice per group per experiment, two independent experiments (*$p<0.05$ vs. saline group; #$p<0.05$ vs. TiO_2 group, one-way ANOVA followed by Tukey's post-test).

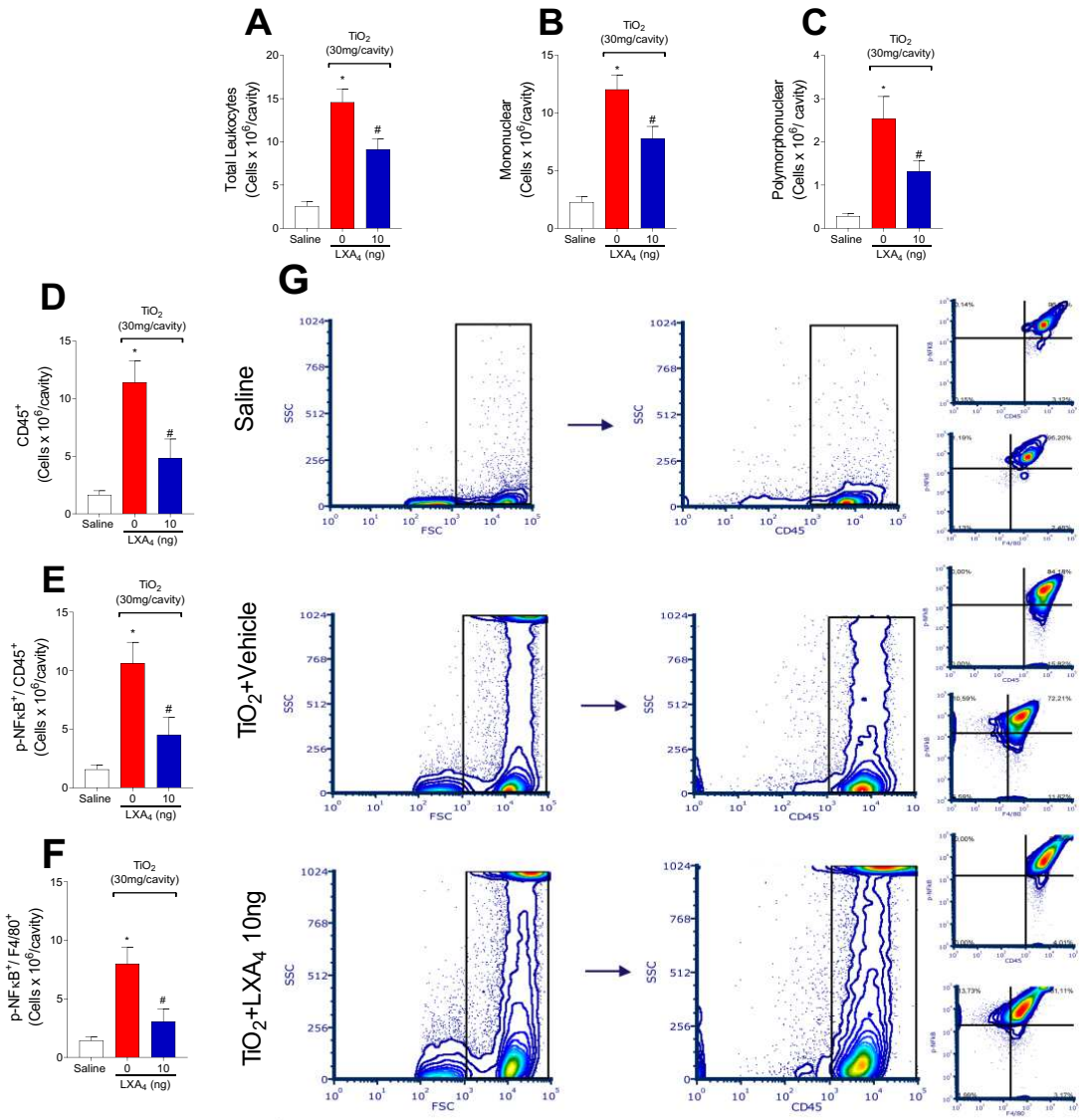

Figure 6. Treatment with LXA_4 reduces NF-κB activation in macrophages induced by TiO_2. TiO_2-induced peritonitis was induced with an i.p. injection of TiO_2 (30 mg/500 µl), and after twenty-four hours, the animals received treatment with LXA_4 (10 ng) or vehicle (saline) (100µl per animal, i.p.). Peritoneal washes were collected on the 2nd to count total leukocytes recruited **(A)**, mononuclear **(B),** and polymorphonuclear cells **(C)**. Flow cytometry for total leukocyte cells [$CD45^+$ cells **(D)**], macrophages ($CD45^+$ $F4/80^+$ cells), and p-NF-κB p65 [$CD45^+$ p-NF-κB $^+$ cells and $F4/80^+$ p-NF-κB $^+$ cells **(E and F)**]. Panel (**G**) shows the gates. Results are expressed as mean ± SEM, n=10 mice per group per experiment, two independent experiments (*p<0.05 vs. saline group; #p<0.05 vs. TiO_2 group, ** p<0.05 vs. all groups) one-way ANOVA followed by Tukey's post-test).

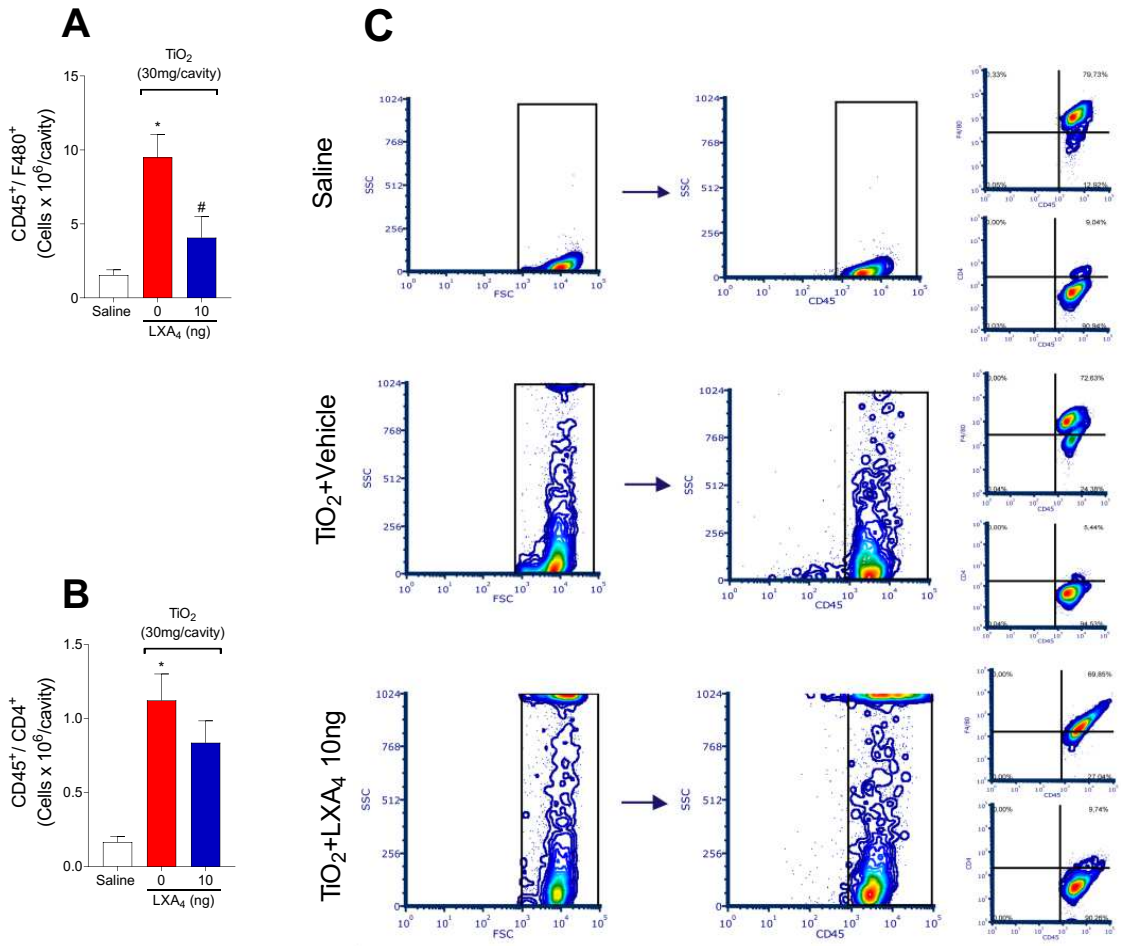

Figure 7. TiO_2 increases macrophage and lymphocyte cells that, in part, are modulated by LXA_4. TiO_2-induced peritonitis was induced with an i.p. injection of TiO_2 (30 mg/500 µl), and after twenty-four hours, the animals received treatment with LXA_4 (10 ng) or vehicle (saline) (100µl per animal, i.p.). Peritoneal washes were collected on the 2nd to flow cytometry for total leukocyte cells [$CD45^+$ cells, macrophages [$CD45^+$ $F4/80^+$ cells (**A**)], and lymphocyte [$CD45^+$ $CD4^+$ cells **(B)**]. Panel (**C**) shows the gates. Results are expressed as mean ± SEM, n=10 mice per group per experiment, two independent experiments (*$p<0.05$ vs. saline group; #$p<0.05$ vs. TiO_2 group, ** $p<0.05$ vs. all groups) one-way ANOVA followed by Tukey's post-test).

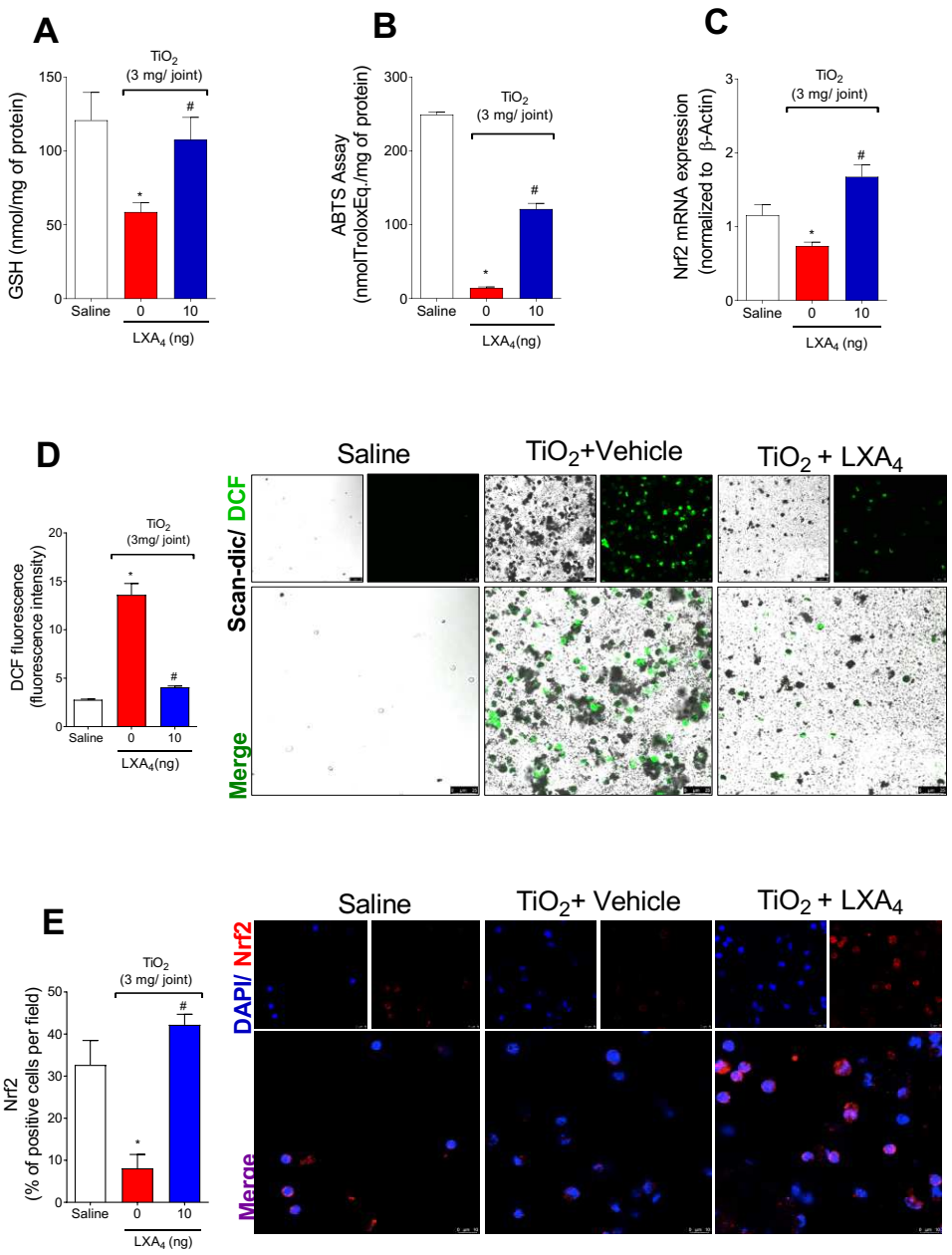

Figure 8. LXA_4 inhibits TiO_2-induced oxidative stress improving antioxidant capacity. Mice received a single treatment of LXA_4 (10ng/ animal) twenty-four hours after i.a. injection of TiO_2 (3mg/ joint), and on the 2nd day, the knee joint was collected, and the antioxidant capacity of LXA_4 was measured by GSH levels **(A)** and ABTS **(B)**. Nrf2 mRNA expression was quantitated by RT-qPCR **(C)**. Dihydrofluorescein diacetate (DCF-DA) was added to knee joint wash cells for 30 min, and intracellular ROS levels from intact cells were analyzed using the scan-dic and green channel in a confocal microscope at 63x magnification. DCF fluorescence intensity **(D)** indicates ROS production, which was quantitated. Representative images show DCF fluorescence for the negative control, TiO_2, and LXA_4 groups **(D)**. Knee joint washes were used to perform an immunofluorescence assay. Panel **(E)** show the representative images of Nrf2 (red) with nuclear staining by DAPI, and the quantitation by % of positive cells per field. The data **(E)** was analyzed by a confocal microscope at 63x magnification with 1.5 zoom in.

Results are expressed as mean ± SEM, n=6 mice per group per experiment, two independent experiments (*p<0.05 vs. saline group; #p<0.05 vs. TiO_2 group, one-way ANOVA followed by Tukey's post-test).

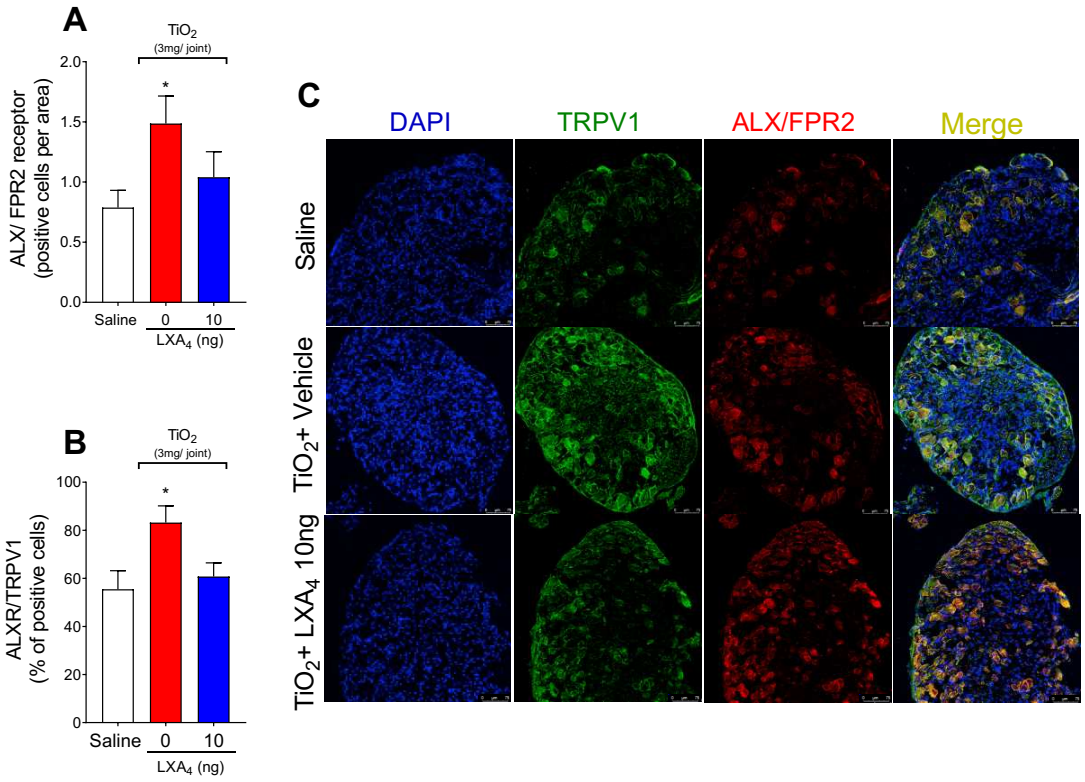

Figure 9. TiO_2 increases the ALX/FPR2 receptor expression on nociceptive neurons. On the 2nd day of the model, DRGs samples (L4-L6) were dissected for TRPV1 and ALX/FPR2 receptor staining by immunofluorescence technique. Panels **(A and B)** shows the quantitation analyses by the number of ALX/FPR2 receptor-positive cells per area **(A)** and co-stained with TRPV1 (as a percent of positive cells) **(B)**. Panel **(C)** shows the representative images of $TRPV1^+$ cells (green), ALX/FPR2 receptor-positive cells (red), and the merge of double labeling of TRPV1 and ALX/FPR2 receptor on DRG (20x magnification with 1.0 zoom in). Results are expressed as mean ± SEM, n=8 mice per group per experiment, two independent experiments (*p<0.05 vs. saline group; #p<0.05 vs. TiO_2 group, one-way ANOVA followed by Tukey's post-test).

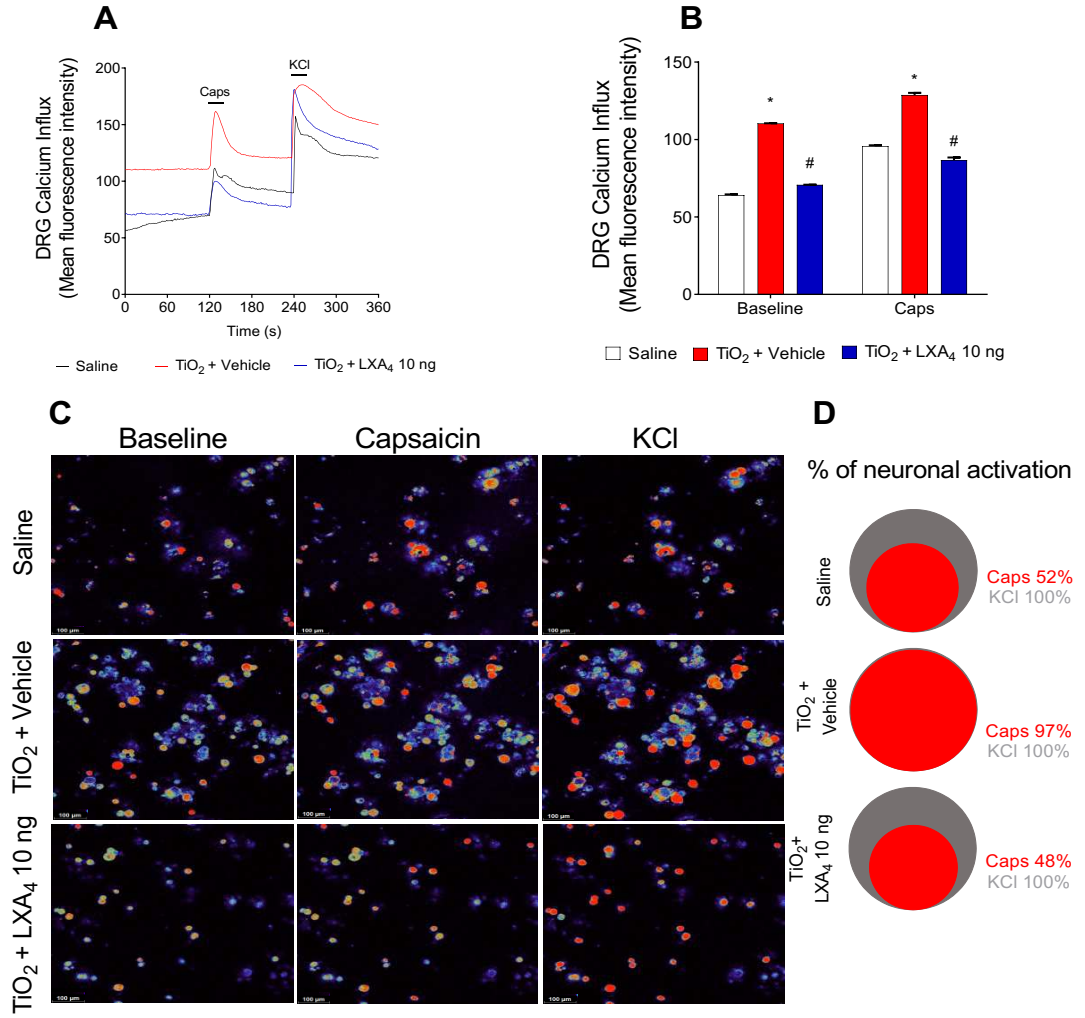

Figure 10. LXA_4 reduces TiO_2-induced TRPV1 activation on DRG neurons. Mice received a single treatment of LXA_4 (10ng/ animal) starting twenty-four hours after i.a. injection of TiO_2 (3mg/ joint), and on the 2nd day, the DRGs samples (L4-L6) were collected for calcium imaging using Fluo-4 a.m. probe. The fluorescence intensity traces of calcium influx from the representative DRG fields, responsive for KCl (240-s mark, activates all neurons), during the 6 min of recording was shown in panel **(A)**. Panel **(B)** displays the mean fluorescence intensity of calcium influx of the baseline (0-s mark) and that following the stimulus with capsaicin (120-s mark, a TRPV1 agonist). Panel **(C)** shows representative fields of DRG neurons (baseline fluorescence, the fluorescence after capsaicin, and after KCl). Panel (**D**) shows Venn Diagram comparing the percent of neurons population with capsaicin activation (red) that had responded to KCl stimulation (grey). Results are expressed as mean ± SEM, n = 4 DRG seeded plates (each plate is a neuronal culture pooled from 10 mice) per group per experiment, two independent experiments (*$p<0.05$ vs. saline group; #$p<0.05$ vs. TiO_2 group, two-way ANOVA followed by Tukey's post-test).

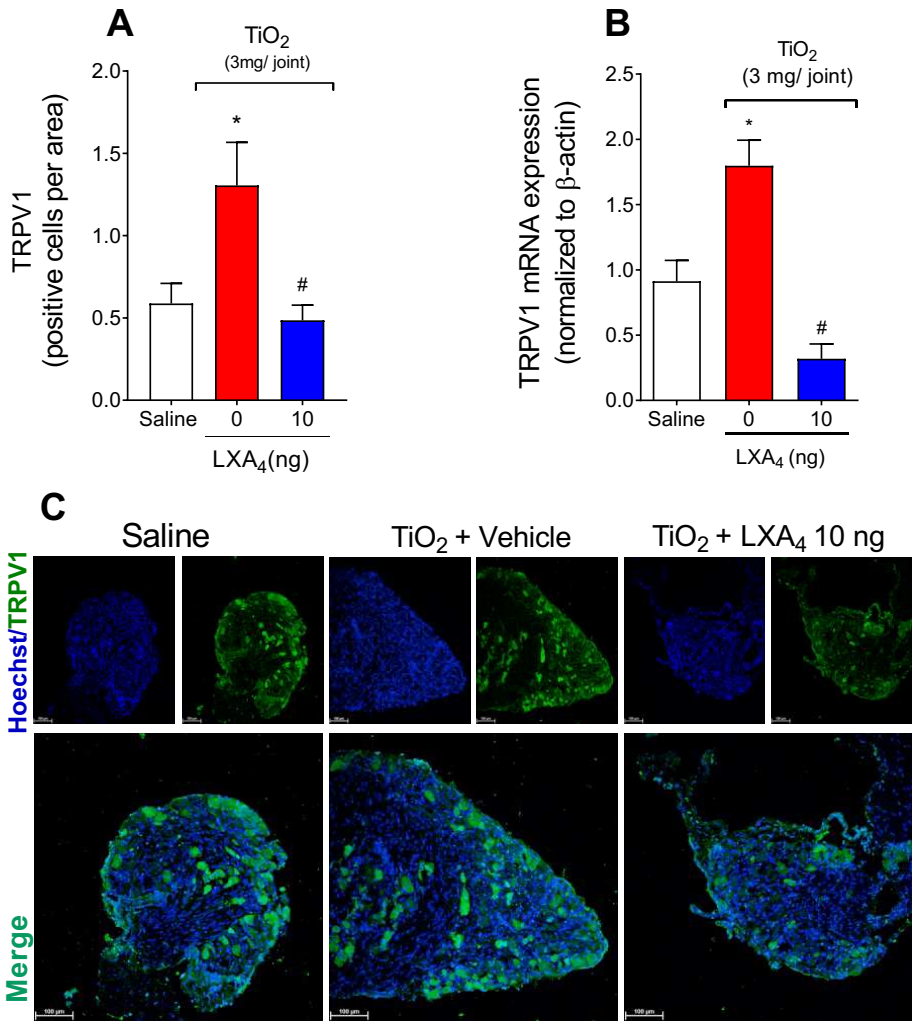

Figure 11. LXA_4 inhibits TiO_2-induced TRPV1 expression in DRG neurons. On the 2nd day of the model, DRGs samples (L4-L6) were dissected for TRPV1 staining by immunofluorescence analysis and mRNA expression by RT-qPCR. Panels [**(A)** - quantitation and **(C)** – representative images] show the number of positive cells per area TRPV1 (green) with nuclear staining by Hoechst 33342 on DRGs (20x magnification with 1.0 zoom in). Panel **(B)** shows the DRG RT-qPCR data, demonstrating that LXA_4 reduced TiO_2-induced TRPV1 mRNA expression. Results are expressed as mean ± SEM, n=8 mice per group per experiment, and RT-qPCR used n=6 mice per group per experiment, two independent experiments (*$p<0.05$ vs. saline group; #$p<0.05$ vs. TiO_2 group, one-way ANOVA followed by Tukey's post-test).

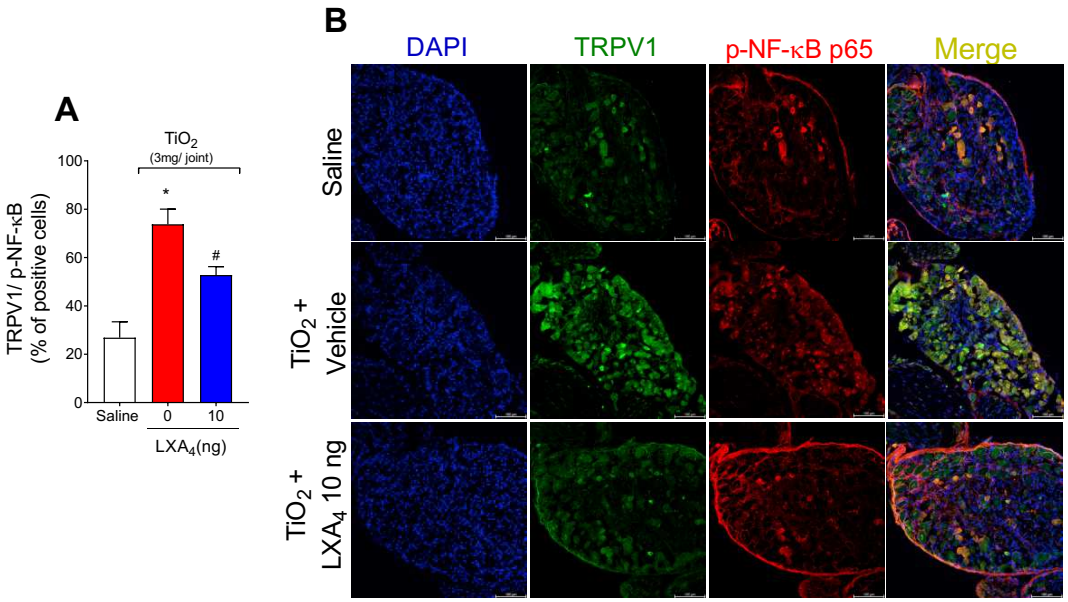

Figure 12. LXA_4 reduces NF-κB activation in TRPV1 positive neurons induced by TiO_2. On the 2nd day of the model, DRGs samples (L4-L6) were dissected for TRPV1 and p65 p-NF-κB staining by immunofluorescence technique. Panel **(A)** shows the quantitation analyses by percent of positive cells co-stained with p65 p-NF-κB. Panel **(B)** shows the representative images of TRPV1+ cells (green), p65 p-NF-κB positive cells (red), and the merge of double labeling of TRPV1 and NF-κB in DRG samples (20x magnification with 1.0 zoom in). DAPI performed the nuclear staining. Results are expressed as mean ± SEM, n=8 mice per group per experiment, two independent experiments (*$p<0.05$ vs. saline group; #$p<0.05$ vs. TiO_2 group, one-way ANOVA followed by Tukey's post-test).

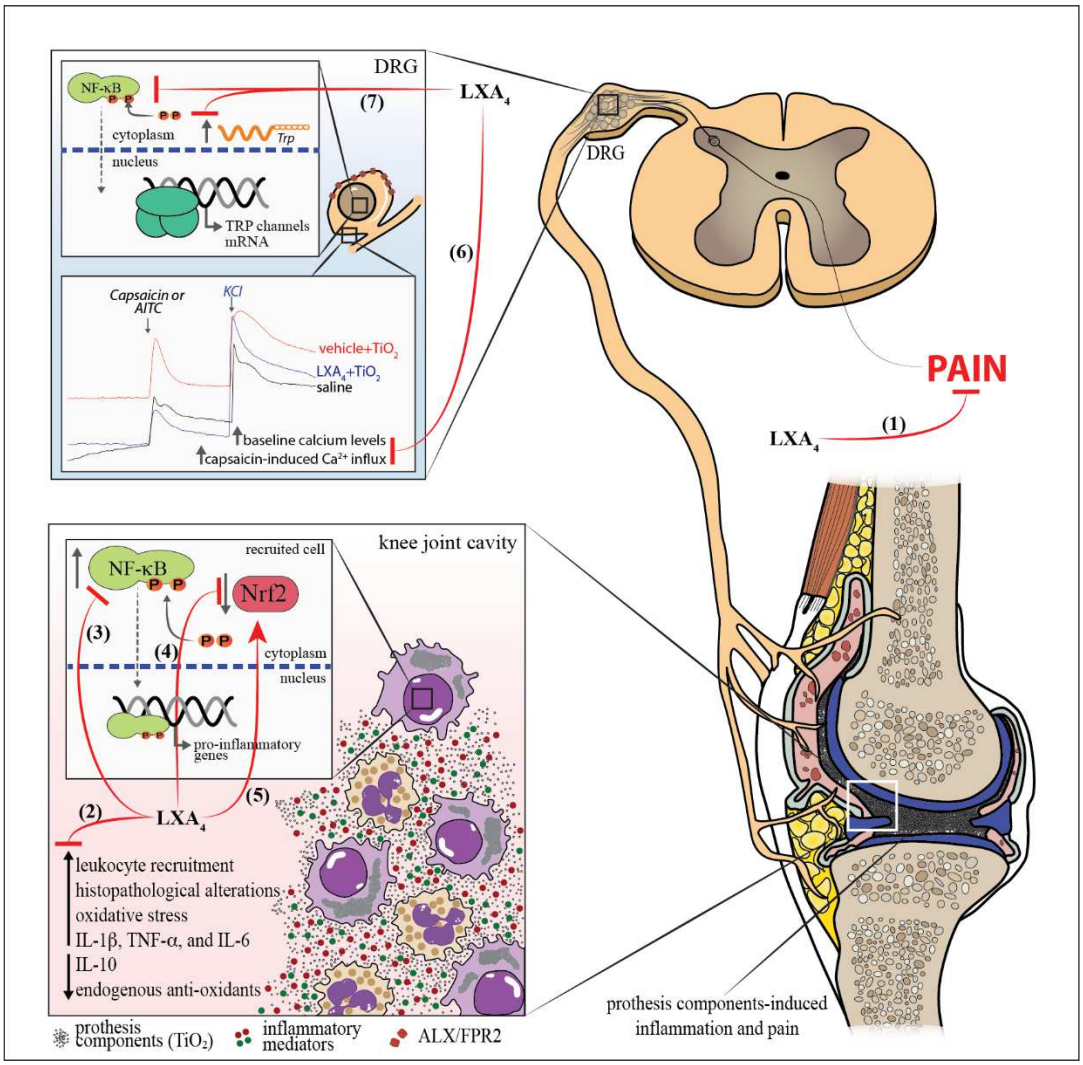

Figure 13. Mechanism of action of LXA_4 in TiO_2-induced arthritis. **(1)** LXA_4 treatment reduces chronic articular pain induced by TiO_2. **(2)** LXA_4 reduces leukocyte recruitment to the knee joint at early and late TiO_2-induced arthritis stages, histopathological alterations, oxidative stress, and IL-1β, TNF-α, and IL-6 production, and increases endogenous antioxidants and IL-10 production. These anti-inflammatory findings were supported by the **(3)** decreased NF-κB activation in macrophage cells. **(4 and 5)** LXA_4 increases the Nrf2 mRNA expression and activation, which were reduced by TiO_2. **(6)**. We also demonstrated that LXA_4 reduces the activation of DRG neurons in TiO_2-inflammation by decreasing the baseline neuronal activation and capsaicin/AITC-induced calcium influx **(7)** and increasing TRPV1 mRNA expression and protein staining (and co-stained with p-NF-κB$^+$), and TRPA1 staining induced by TiO_2. TRPV1$^+$ nociceptive neurons express ALX/FPR2 receptor, and that TiO_2 inflammation enhances the ALXR$^+$/TRPV1$^+$. Finally, all these mechanisms explain the analgesic **(1)** and anti-inflammatory **(2)** effects of LXA_4 in this animal model of prosthesis-wearing process released components (e.g., TiO_2)-induced arthritis.

Table 1. Primer sequences for RT-qPCR

Gene	Sense	Antisense
Nrf2	5′-TCACACGAGATGACGTTAGGGCAA-3′	5′-TACAGTTCTGGGCGGCGGACTTTAT-3′
Trpv1	5′-TTCCTGCAGAAGAGCAAGAAGC-3′	5′-CCCATTGTGCAGATTGAGCAT-3′
β-actin	5′-AGCTGC GTTTTACACCCTTT-3′	5′-AAGCCATGCCAATGTTGTCT-3′

Supplementary Material

1. Supplementary Figures

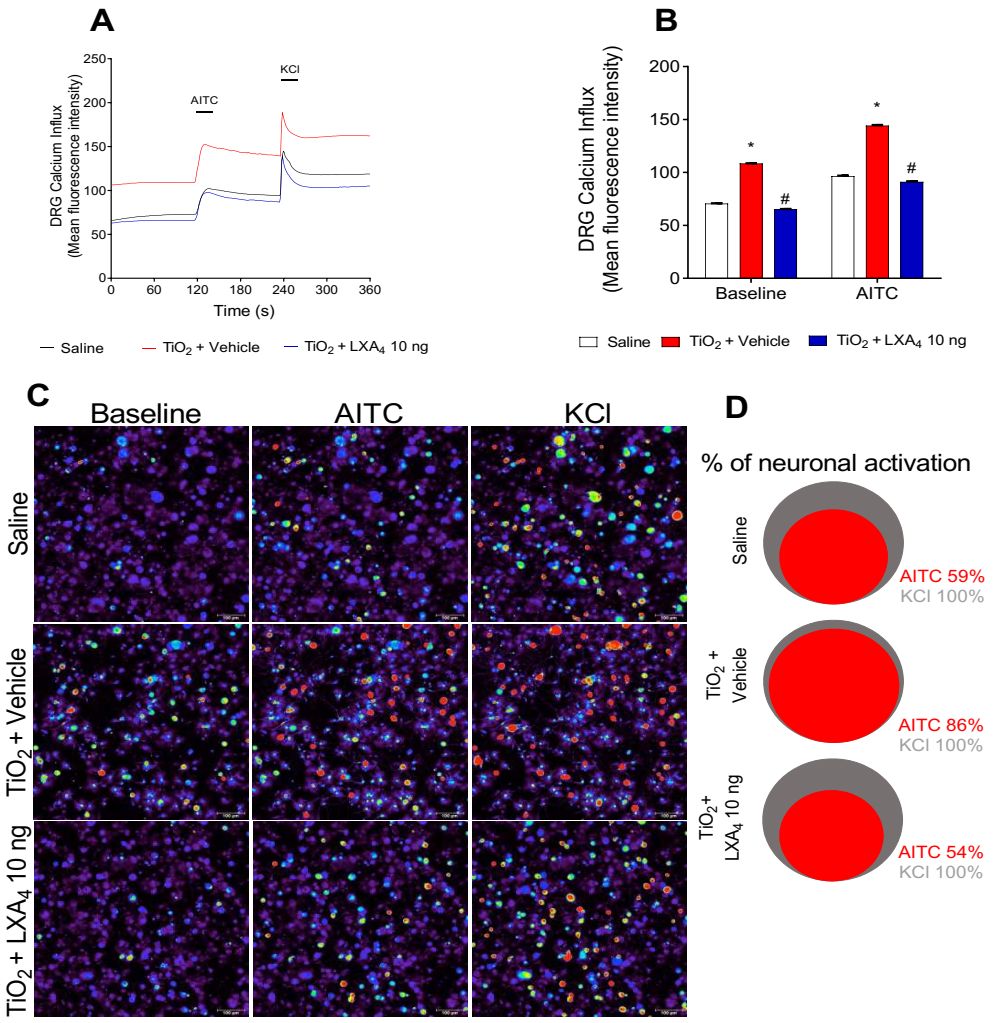

Figure S1. LXA_4 reduces TiO_2-induced TRPA1 activation on DRG neuron. Mice received a single treatment of LXA_4 (10ng/ animal) starting twenty-four hours after i.a. injection of TiO_2 (3mg/ joint), and on the 2nd day, the DRGs samples (L4-L6) were collected for calcium imaging using Fluo-4AM probe. The fluorescence intensity traces of calcium influx from the representative DRG fields, responsive for KCl (240-s mark, activates all neurons), during the 6 min of recording was shown in panel **(A)**. Panel **(B)** displays the mean fluorescence intensity of calcium influx of the baseline (0-s mark) and that following the stimulus with AITC (120-s mark, a TRPA1 agonist). Panel **(C)** shows representative fields of DRG neurons (baseline fluorescence, the fluorescence after AITC, and after KCl). Panel (**D**) shows Venn Diagram comparing the percent of neurons population with AITC activation (red) that had responded to KCl stimulation (grey). Results are expressed as mean ± SEM, n = 4 DRG seeded plates (each plate is a neuronal culture pooled from 10 mice) per group per experiment, two independent experiments

(*p<0.05 vs. saline group; #p<0.05 vs. TiO_2 group, two-way ANOVA followed by Tukey's post-test).

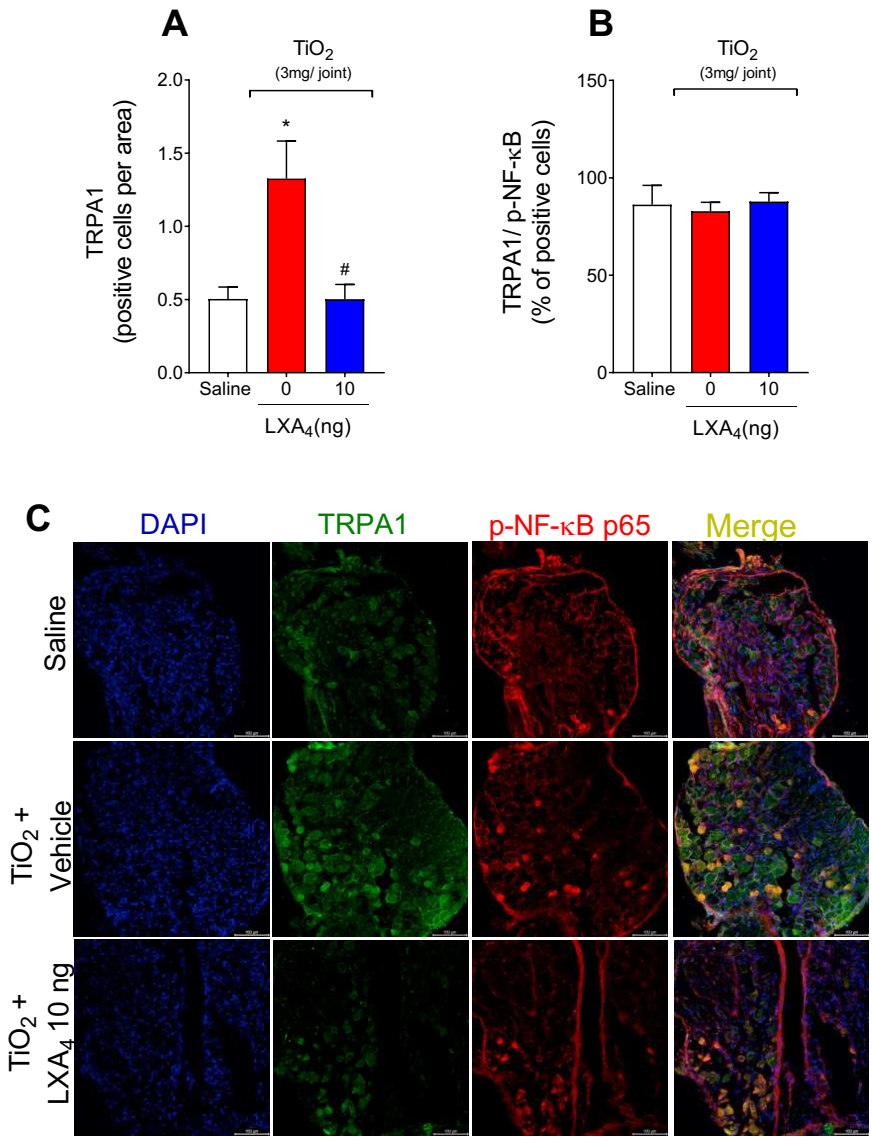

Figure S2. LXA_4 inhibits TRPA1 expression induced by TiO_2. On the 2nd day of the model, DRGs samples (L4-L6) were dissected for TRPA1 and p65 p-NF-κB staining by immunofluorescence technique. Panels **(A and B)** shows the quantitation analyses of the number of TRPA1 positive cells per area **(A)** and TRPA1 cells co-stained with p65 p-NF-κB (percent of positive cells) **(B)**. The panel **(C)** shows the representative images of $TRPA1^+$ cells (green), p65 p-NF-$κB^+$ cells (red) and merge of double labeling of TRPA1 and p-NF-κB in DRG samples (20x magnification with 1.0 zoom in). The nuclear staining was performed by DAPI. Results are expressed as mean ± SEM, n=8 mice per group per experiment (*p<0.05 vs. saline group; #p<0.05 vs. TiO_2 group, one-way ANOVA followed by Tukey's post-test).

5. ARTIGO 2

Como trabalho de qualificação de doutorado apresentado ao programa de pós graduação em Patologia experimental, é apresentado o segundo artigo realizado no Laboratório de Dor, Inflamação, Neuropatia e Câncer (LADINC) intitulado "*Curcumin ameliorates TiO_2-induced arthritis by reducing leukocyte recruitment, oxidative stress, and TRPV1 neuronal activation",* a ser submetido na revista Inflammation research (IF: 6.9) sob autoria de Telma Saraiva-Santos, Mariana M. Bertozzi, Victor Fattori, Tiago H. Zaninelli, Camila R. Ferraz, Marília F. Manchope, Soraia M. Pierotti, Anelise Franciosi, Kenji W. Ruiz-Myiazawa, Sérgio M. Borghi, Rúbia Casagrande and Waldiceu A. Verri Jr1.

Curcumin ameliorates TiO_2-induced arthritis by reducing leukocyte recruitment, oxidative stress, and TRPV1 neuronal activation

Telma Saraiva-Santos[1], Mariana M. Bertozzi[1], Victor Fattori[1], Tiago H. Zaninelli[1], Camila R. Ferraz[1], Marília F. Manchope[1], Soraia M. Pierotti[1], Anelise Franciosi[1], Kenji W. Ruiz-Myiazawa[1], Sérgio M. Borghi[1,2], Rúbia Casagrande[3] and Waldiceu A. Verri Jr[1]*.

[1]Laboratory of Pain, Inflammation, Neuropathy, and Cancer, Department of Pathology, Londrina State University, Londrina, Paraná, Brazil.

[2]Center for Research in Health Sciences, University of Northern Paraná, Londrina, Paraná, Brazil.

3Department of Pharmaceutical Sciences, Center of Health Sciences, Londrina State University, Londrina, Paraná, Brazil.

*Correspondence:

Waldiceu A. Verri, Jr

Phone number: + 55 43 3371 4979. Fax: + 55 43 3371 4387. E-mail: waverri@uel.br or waldiceujr@yahoo.com.br. Laboratory of Pain, Inflammation, Neuropathy, and Cancer, Department of Pathology, Londrina State University, Rod. Celso Garcia Cid KM480 PR445, Zip Code 86057-970, PO box 10.011, Londrina, Parana, Brazil.

Abstract

Objective and design To investigate the effects of curcumin in titanium dioxide (TiO_2)-induced chronic arthritis in mice.

Treatment Curcumin (10 or 100 mg/kg, orally, daily) or with vehicle (20% tween 80 in saline) for 30 days starting 24 h after TiO_2 injection.

Methods: Chronic arthrithis was induced upon intra-articular injection of TiO_2 (3 mg/mouse). Mechanical hyperalgesia was determined using electronic version of von Frey filaments and thermal hyperalgesia using Hargreaves apparatus, edema, histopathological alterations (using hematoxylin-eosin stain [HE]), leukocyte recruitment, and oxidative stress (TBARS and NBT assays) were evaluated on 30th day. On the 2nd day, we determined the leukocyte recruitment, IL-1β levels, oxidative stress (ROS and NO levels), neuronal activation, and response to capsaicin and AITC using calcium influx imaging; and TRPV1 and TRPA1 staining by immunofluorescence assay on DRG neurons.

Results Curcumin treatment reduced mechanical and thermal hyperalgesia, articular edema and histopathological alterations induced by TiO_2. Curcumin also reduced leukocyte recruitment, IL-1β level, and oxidative stress induced by TiO_2. Curcumin inhibited TiO_2-induced TRPV1 (by capsaicin stimulation) and TRPA1 (by AITC stimulation) activation, decreasing TRPV1 staining and co-stained with p-NFκB in DRG neurons.

Conclusion Curcumin ameliorates TiO_2-induced chronic arthritis by reducing knee joint leukocyte recruitment, oxidative stress, and reducing the activation of TRPV1-positive DRG neurons.

Keywords Curcumin, Arthroplasty, Pain, Aseptic inflammation, TRPV1, ROS.

1. Introduction

Pain is a debilitating symptom of arthritis and the leading cause of patients seeking medical care [1,2]. The activation of primary sensory neurons transmits the nociceptive information to the spinal cord resulting in nociceptive sensation [3]. In this context, transient receptor potential (TRP) channels are expressed in the peripheral nerves and neurons, contributing to intracellular calcium regulation in acute and chronic pain. These channels have been studied as target mechanisms for developing novel analgesics in cancer, neuropathic and chronic pain [4–6].

Osteoarthritis and rheumatoid arthritis are common worldwide disorders with a significant prevalence. Despite current treatments show efficacy for a fraction of patients, many other patients still report pain and functional limitations [7,8]. Upon long lasting and uncontrolled inflammation, knee replacement is an alternative to recover from joint destruction, reduce pain, and improve life quality [9–11]. Total knee arthroplasty is a recurrent joint replacement procedure that is expected to increase substantially in the coming years [12]. This procedere is projected to grow by 673% from 2005 to 2030 in the USA, making a total of pproximately 3.5 million surgeries [13]. However, despite the success of joint prostheses, the deterioration of the prosthetic components is the most associated complication. Release of metallic nanoparticles in the periprosthetic space promotes osteolysis and the requirement for arthroplasty revision [14–16].

The titanium dioxide (TiO_2) nanoparticle is widely used in pharmaceutical products and orthopedic prostheses [17]. This molecule is the crucial component involved in prosthesis wear process-induced arthritis. Resident macrophages recognize and internalize the TiO_2 debris, promoting activation and TNF-α and IL-1β release [18]. Borghi, et al. [19] demonstrated in an experimental mouse model that intra-articular administration of TiO_2 induces chronic arthritis, increasing mechanical hyperalgesia, edema, histopathological changes, and inflammatory parameters. Currently, non-steroidal anti-inflammatory drugs (NSAIDs), corticosteroids, and opioids are available for patients with prosthesis-induced arthritis. While effective for a fraction of patients, these treatments are often expensive [20] show intense adverse effects and should be use with cautious by patients with commobidities [21]. Therefore, investigating novel drugs with anti-inflammatory properties and minimum side effects is necessary to treat prosthesis-induced arthritis.

Vegetables, fruits, and drinks (e.g., wine and tea) of the human diet contain a significant amount of polyphenols. Daily doses of these compounds enhance life quality

and decrease the risk of many inflammatory diseases [22]. Curcumin is a polyphenol found in turmeric (*Curcuma longa)*, commonly used as a spice [23]. This polyphenol is extensively investigated as a therapeutic approach concerning antioxidant, antitumor, antifungal, anti-inflammatory, and immunomodulatory properties [24–26]. The analgesic effect of curcumin was demonstrated in an acute model of pain induced by superoxide anion by reducing pro-inflammatory cytokines and improving antioxidant capacity [27]. Curcumin treatment reduced cancer-induced bone pain in mice [28], osteoarthritis progression, and pain [29,30]. The analgesic effect of curcumin was demonstrated via modulation of TRPV1 channels in ulcerative colitis [31] and inhibition of TRPV1-mediated pain hypersensitivity in the orofacial pain model [32]. Curcumin is a potent antioxidant acting via the nuclear factor erythroid 2-related factor 2 (Nrf2)-Keap1 pathway, reducing oxidative stress and lipid peroxidation in several animal models [33–37]. In addition, the anti-inflammatory effects of curcumin were demonstrated by reducing the cyclooxygenase-2 (COX-2) pathway [38], nuclear factor kappa B (NF-κB) activation [39,40], interleukin-1β (IL-1β) [41,42] and tumor necrosis factor-alpha (TNF-α) levels, and leukocyte recruitment [39,43]. These findings demonstrated the potential of curcumin to act in different inflammatory diseases, such as TiO_2 articular inflammation. Therefore, in this study, we aim to investigate the anti-inflammatory, antioxidant, and analgesic effects of curcumin in prothesis-induced arthritis.

2. Materials and Methods

2.1.Animals

Male Swiss mice weighing 20 to 25g were used. The animals were housed in standard clear plastic cages with free access to water and food, controlled temperature (21°±1°C), and a light/dark cycle of 12/12h. Mice were acclimated at least 1 hour before the experiments in the testing room, and all the behavioral tests were performed between 9 a.m. and 5 p.m. Animal care and handling procedures were developed accordingly to the International Association for Study of Pain (IASP) guidelines and with the approval of the Londrina State University Ethics Committee on Animal Research and Welfare (process number 21934.2015.55). All efforts were made to minimize the number of animals used and their suffering.

2.2.Experimental procedures

We performed experiments to evaluate pain, inflammation, oxidative stress, and histopathological alterations to determine the disease phenotype upon curcumin treatment (Fig. 1; protocol 1). Mice (n=6 per group per experiment) were treated per oral (p.o.) with 100µl of 10 or 100 mg/kg of curcumin or with vehicle (20% tween 80 in saline) twenty-four hours after a single intra-articular (i.a.) injection of TiO_2 (3mg/10µl/knee joint) and after that, mice were treated daily until the 30^{th} day. A dose-response experiment was performed to determine the best curcumin dose. The mechanical threshold was evaluated twenty-four hours after the TiO_2 stimulus, after curcumin treatment (1h) on the first day and every other day (from the 2nd to the 30th day). The dose of 100mg/kg of curcumin was chosen and used in the following experiments based on mechanical hyperalgesia and edema results. The thermal hyperalgesia was evaluated using Hargreaves apparatus every three days for 30 days. The edema was evaluated before, after curcumin treatment, and every other day for 30 days. On the 30th day after the stimulus, knee joints were collected to evaluate the histopathological index (using hematoxylin-eosin stain [HE]), myeloperoxidase (MPO) and N-acetyl-beta-D-glucosaminidase (NAG) activity. The knee joint lavages were collected to determine the leukocyte recruitment, and knee joint samples were used to evaluate the oxidative stress (lipid peroxidation [TBARS] and superoxide anion [nitroblue tetrazolium reduction levels).

Based on the previous results that demonstrated an effective reduction of pain and edema after two days of TiO_2 injection, the 2nd day of the model was chosen to elucidate the effects of curcumin treatment in the early stage of TiO_2-induced pain and

inflammation (Fig. 1; protocol 2). The knee joint washes were collected to quantify the leukocyte recruitment and oxidative stress (total reactive oxygen [ROS] using the probe2',7'–dichlorofluorescein diacetate [DCF-DA] assay, and nitric oxide [NO] species using the probe 5,6-diaminofluorescein diacetate [DAF-2DA]). The knee joint tissue was used to measure the IL-1β levels as per enzyme-linked immunosorbent assay (ELISA). The ipsilateral dorsal root ganglia (DRG) (L4-L6) were collected on the 2nd day of the model, the calcium influx imaging was determined using confocal microscopy, and transient receptor potential cation channel subfamily V member 1 (TRPV1), transient receptor potential ankyrin 1 (TRPA1) and p-NFκB staining were determined by immunofluorescence assay.

2.3.Chemical compounds

Curcumin (Santa Cruz Biotechnology, Dallas, TX, USA), pure TiO_2, MW 79.90, was purchased from Synth (Diadema, SP, Brazil) (the particle size was < 1 μm with an average of 862.2 nm as determined by size distribution analysis [Malvern Instruments Ltd, UK]). Saline solution (NaCl 0.9%; Frenesius Kabi Brasil Ltda, Aquiraz, CE, Brazil); ethylenediaminetetraacetic acid disodium salt (EDTA; Synth, Diadema, SP, Brazil). DCF-DA probe was purchased from Sigma-Aldrich (#D6883; San Luis, MO, EUA). DAF-2DA probe was purchased from Sigma-Aldrich (#251505-M; San Luis, MO, EUA). Hank's balanced Salt Solution (HBSS) was from Thermo Fisher Scientific (Waltham, MA, USA). The fluorescent antibodies used were: anti-phospho NFκB p65 (#sc-136548; mouse, Santa Cruz Biotechnology, Dallas, TX, USA); anti-capsaicin receptor antibody (#ab5566; Guinea pig, Merck Millipore, Burlington, MA, USA); anti-TRPA1/TSA antibody (#ab58844; Rabbit, Abcam, Cambridge, MA, USA); anti-mouse secondary antibody (Alexa Fluor 647-Goat, #115-605-003; Jackson ImmunoResearch, West Grove, PA, USA); anti-rabbit secondary antibody (Alexa fluor 488-Goat, #A-11008; Thermo Fisher Scientific, Waltham, MA, USA); anti-Guinea pig secondary antibody (Alexa Fluor 488- Goat, #A11073, Thermo Fisher Scientific, Waltham, MA, USA). 4′,6-Diamidine-2′-phenylindole dihydrochloride (DAPI) was from Thermo Fisher Scientific (Waltham, MA, USA). The panoptic kit for differential counts of recruited leukocytes was from Laborclin (Pinhais, PR, Brazil). Neurobasal-A medium (NBM) was purchased from Life Technologies (Thermo Fisher Scientific); Dispase II was from RocheApplied Sciences (Indianapolis, IN, USA); 4-(2-hydroxyethyl)-1- piperazine ethane sulfonic acid

(HEPES)-buffered saline was from Millipore Sigma (Burlington, MA, USA); and Fluo-4AM was from Invitrogen (#F14201, Carlsbad, CA, USA).

2.4. Mechanical hyperalgesia

As previously described, the knee joint mechanical hyperalgesia was evaluated by an electronic version of von Frey's filaments [44]. In a quiet room with a controlled temperature, mice were placed in acrylic cages with wire grid floors 15-30 before the start of testing. The test involves evoking a hind paw flexion reflex with a handheld force transducer (Electronic von Frey aesthesiometer; Insight instruments, Ribeirao Preto, SP, Brazil) adapted with a 4.15 mm2 polypropylene tip (to evaluate knee joint pain to exclude the subcutaneous effect). The investigator was trained to apply the tip perpendicularly to the central area of the plantar hind paw with a gradual increase in pressure. The gradual increase in pressure was manually performed in blinded experiments. The upper limit pressure was 15 g. The end-point was characterized by removing the paw followed by precise flinching movements. After paw withdrawal, the intensity of the pressure was automatically recorded, and the final value for the response was obtained by averaging three measurements. The tests were performed before and after the curcumin treatment and every other day until the 30th. The flexion-elicited withdrawal threshold is expressed in grams (g).

2.5. Thermal hyperalgesia

The Hargreaves apparatus (Model 390G, IITC Life Science, Woodland 178 Hills, CA, USA) was used to assess the articular thermal hyperalgesia. Mice were habituated to the apparatus for two hours during three consecutive days. After that, a baseline measurement was obtained before the TiO_2 injection. We measure the pain sensitivity to a heat stimulus (heat hyperalgesia) using a radiant heat source to stimulate the paw by gradually increasing the temperature of the plantar surface. The tests were performed before and after the curcumin treatment and every three days until the 30th. The pain threshold was determined as the latency (in seconds) to evoke a response of paw withdrawal: paw flinches or licking. In this experiment, the device was set to 30% radiant heat source intensity and a cut-off time of 15s of exposure to prevent tissue damage.

2.6. Knee joint edema

The volume of the tibiofemoral joint was measured by the transverse diameters using a caliper (Digmatic Caliper, Mitutoyo Corporation, Kanagawa, Japan). The edema was determined for each mouse knee joint by the difference indicated times post-stimulus and zero time. The test was performed one hour after the curcumin treatment, on the first day, and every other day until the 30th. The results were expressed as Δ mm/joint.

2.7. Histopathological analysis

The tibiofemoral joints were collected on the 30th day to assess the histopathological alterations and fixed in 10% buffered formaldehyde. The decalcification was performed 48 hours in 20% EDTA (disodium salt solution, pH 7.4). Afterward, the samples were processed for paraffin embedding, and longitudinal sections (10 μm) were stained with HE. The blinded examination was performed and scored by a pathologist under a light microscope (Olympus CX31RTSF, 197 Tokyo, Japan). The histopathological scores were determined by summing synovial hyperplasia, inflammatory infiltrates, and vascular proliferation scores [45]. The degrees of the following parameters were: (a) synovial hyperplasia (from 0 = no pannus formation to 3 = most severe pannus formation); (b) inflammatory infiltrate (from 0 = no inflammation to 3 = most severe inflammation; and (c) angiogenesis (from 0 = no vascular proliferation to 3 = most severe proliferation). Vascular proliferation was considered the number of capillary blood vessels. The final score was determined by summating all three parameters (a–c), resulting in a score for each sample expressed as the mean of nine samples accordingly to the groups.

2.8. Myeloperoxidase (MPO) and N-acetylglucosaminidase activity (NAG) assays

MPO and NAG were indirect markers of neutrophil and macrophage recruitment, respectively. The assays were performed as previously described [46]. Briefly, knee joint samples were collected on the 30th day in 400 μL of 50 mM K2HPO4 buffer (pH 6.0) containing 0.5% HTAB and then homogenized in ice-cold Tissue-Tearor (Biospec). Afterward, homogenates were centrifuged (16100g, 2 min, 4 °C), and the supernatants were collected. For the MPO assay, aliquots of 30 μL of supernatant were placed in a 96-well plate and mixed with 200 μL of 50 mM K2HPO4 buffer (pH 6.0) containing 0.0167% ortho-dianisidine dihydrochloride and 0.05% H2O2. The absorbance was determined after 5 min at 450 nm (Multiskan GO microplate spectrophotometer,

ThermoScientific, Vantaa, Finland). The MPO activity of samples was compared to a standard curve of neutrophils and presented as MPO activity. The results were expressed as MPO activity (neutrophils/mg of tissue).

For NAG activity assay, an adapted colorimetric method was applied. Initially, 10 µL of the supernatant obtained from the MPO activity procedure was separated and added in a 96-well plate, followed by 40 µL of 50 mM phosphate buffer, pH 6.0. The reaction was started by the addition of 2.24 mM 4-nitrophenyl N-acetyl-β-D-glucosaminide. The plate was subsequently incubated at 37◦C for 10min, and the reaction was stopped by adding 100 µL of 0.2 M glycine buffer, pH 10.6. NAG enzymatic activity was determined spectrophotometrically at 400 nm (Multiskan GO Microplate, Thermo Fischer Scientific, Vantaa, Finland), and results were presented as NAG activity (macrophages/mg of tissue).

2.9.Knee joint recruitment

On the 2nd and 30th day, the knee joint cavities were washed with 50 µl of saline/ EDTA (3 washes of 3.33µl) solution, and the recovered solution was used to evaluate total and differential cell counts. The total cell counts were performed in the Neubauer chamber using Turk's solution, and the samples were cytocentrifuged and the slices stained with a panoptic kit under a light microscope (Olympus CX31RTSF, 197 Tokyo, Japan) to evaluate differential cell counts (100 cells per slide). Results were expressed as total leukocytes, polymorphonuclear, and mononuclear cells (cells × 10^3/ synovial cavity).

2.10 Nitroblue tetrazolium reduction

On the 30th day, the knee joint samples were collected to assess the superoxide anion production by reducing the redox dye nitroblue tetrazolium (NBT) [19,45]. The samples were homogenized with 500 µl of saline and centrifuged (10 min, 3,300 g, 4°C). After, 100 µL of nitroblue tetrazolium solution (1 mg/mL) (NBT, Sigma) was added to homogenate samples (37°C for 5 min). The supernatant was removed, and the formazan precipitated was solubilized with KOH and dimethylsulfoxide (DMSO). The optical density was measured using a microplate spectrophotometer reader (Multiskan GO Microplate Spectrophotometer, Thermoscientific, Vantaa, Finland) at 600 nm. Results were presented as NBT reduction (OD/mg of tissue).

2.11 Lipid peroxidation

As previously described, lipid peroxidation was measured by the levels of thiobarbituric acid reactive substances (TBARS) [47]. For this, the knee joint samples were collected on the 30th day, TCA 10% was added to the homogenate, and centrifuged (3 min, 1000g, 4 °C). The protein-free supernatant was then separated and mixed with TBA (15 min, 100°C). Malondialdehyde (MDA), an intermediate lipid peroxidation product, was determined by the difference between absorbance at 535 and 572 nm using a microplate spectrophotometer reader. The TBARS were corrected per the total protein concentration and the results presented as TBARS (ΔOD A535–A572 /mg of protein).

2.12 Cytokine production

The knee joint samples were collected on the 2nd day after the intra-articular injection of TiO_2 to measure the IL-1β production. The samples were homogenized and centrifugated (3000 rpm × 15 min × 4°C), and the IL-1β levels were determined from the supernatant by ELISA. Results were expressed as pg of cytokine per 100 mg of tissue.

2.13 Total intracellular reactive oxygen species and nitrogen oxide detection

The DCF-DA and DAF-2DA fluorescent probes were used to determine the presence of ROS and nitrogen oxide, respectively. On the 2nd day after the TiO_2 injection, the knee joint cavities were washed on FACS buffer (PBS and 0.5% BSA) containing EDTA, which was recovered to DCF-DA and DAF-2DA assay. The recovered articular fluids were seeded on Nunc™ Glass Bottom Dishes for 30 min at 37°C. Samples were then loaded with 10 μM (DCF-DA) or (DAF-2DA) for 30 min 37°C, washed with HBSS, and imaged in a Confocal Microscope (TCS SP8, Leica Microsystems) with a 63x objective. Total intracellular ROS or NO detection was analyzed from the mean fluorescence intensity measured with the LAS X software (Leica Microsystems).

2.14 Calcium imaging

On the 2nd day after the TiO_2 injection, DRG samples (L4-L6 segments) were collected to evaluate calcium imaging as previously described [48]. DRGs were dissected into NBM, dissociated in 1 mg/ml collagenase A and 2,4 U/ml de dispase II in HEPES (20 min at 37˚C). After trituration with decreasing-size glass Pasteur pipettes, DRG cells

were centrifuged over a 10% BSA gradient and plated on laminin-coated cell culture dishes. The samples were then loaded with 1.2 μM of Fluo-4 a.m. in NBM (30 min at 37°C), washed with HBSS, and imaged in a Confocal Microscope (TCS SP8, Leica Microsystems). The plates were recorded for 6 min to evaluate TRPV1 and TRPA1 activation, 2 min of initial reading (0-120s, baseline values), followed by stimulation with 100 nM capsaicin (a TRPV1 agonist, 120-240s) or 100 μM AITC (a TRPA1 agonist, 120-240s), and 40 mM of KCl (240-360s), activates all neurons. Only the KCl-responsive cells were considered in the analyses of capsaicin-responsive or AITC-responsive cells. Calcium flux was analyzed from the mean fluorescence (KCl responsive neurons) measured with the LAS X software (Leica Microsystems).

2.15 DRG immunofluorescence

The DRGs (L4-L6 segments) were collected for immunofluorescence assay on the 2nd day after TiO_2 intra-articular injection. The DRGs were dissected, fixed in PFA 4% (twenty-four hours), and processed in 30% sucrose (in PBS) and a solution with sucrose and OCT (1:1) for twenty-four hours. The samples were frozen in OCT, and the slide sections of 10 μM were used for staining. The slides were blocked with BSA 3% (in PBS with 0.3% of triton x-100) for 1 hour. The primary antibodies anti p65 p-NF-κB (1:200), anti-TRPA1/TSA (1:100) and anti-TRPV1 (1:500) were incubated overnight at 4°C. The secondary antibody Alexa 647 anti-mouse, Alexa 488 anti-guinea pig, and Alexa 488 anti-rabbit (1:500) were incubated for 2 hours at room temperature. The DAPI was used as nuclear staining. Imaging was performed using a confocal microscope (Leica TCS SP8, Leica, Wetzlar, 332 Germany) with a 20x objective with a zoom-in of 1.5. Images were processed using Leica EL6000 333 software (Leica, Wetzlar, Germany). The results are expressed as the number of positive cells per area and percent of positive cells (double stained), manually quantitated.

2.16 Statistical analysis

Data were analyzed using GraphPad Prism statistical software (GraphPad Software, Inc., USA-500.288, version 8.0). Results are presented as the mean ± SEM for parametric data and medians and interquartile ranges for non-parametric data. To this end, we used Shapiro–Wilk normality test and Brown-Forsythe homogeneity test. For in vivo experiments, an n of 6, 9 or 10 mice in each group per experiment represents two separate experiments depending on the methodology (indicated in the figure legends). The in vitro

experiments with DRG samples were performed using an n of 4 pools [DRGs (L4-L6) of 10 mice to form 1 pool] per group and represent two separate experiments. Two-way repeated-measures analysis of variance (ANOVA) followed by Tukey's post-test was used to compare all groups and doses when responses were measured at different times after the stimulus injection. The analyzed factor were treatments, time, and time versus treatment interaction. Parametric results were evaluated by one-way ANOVA followed by Tukey's post-test for data from a single time point. Kruskal–Wallis followed by Dunn post-test or two-way were used for non-parametric results. $P<0.05$ was considered significant.

3 Results

3.1 Curcumin reduces mechanical and thermal hyperalgesia and knee joint edema induced by TiO_2

We have previously demonstrated that curcumin at 10 mg/kg reduces superoxide anion-induced inflammation and pain [49]. Based on that study, we first want to determine the best analgesic dose in this model using curcumin at 10 or 100 mg/kg. The animals received an intra-articular injection of TiO_2 (3mg/10µl/animal), and twenty-four hours after, were treated with 10 or 100 mg/kg of curcumin (100µl; p.o). Intra-articular injection of TiO_2 induced mechanical and thermal hyperalgesia for 30 days as well as knee joint edema (Fig. 2A-C). We observed that curcumin reduced mechanical hyperalgesia in a dose-dependent manner. Because the dose of 10 mg/kg did not reduce the mechanical hyperalgesia, curcumin at 100 mg/kg was chosen for the following experiments (Fig. 2A). We observed that this dose reduced both thermal hyperalgesia (Fig. 2B) and knee joint edema (Fig.2C) induced by TiO_2.

3.2 Curcumin reduces TiO_2-induced histopathological alterations in the knee joint

TiO_2-induced arthritis promotes changes that can be observed as a higher histopathological score compared with the control group (saline) [19]. Therefore, we investigated the effects of curcumin treatment on histopathological changes. Curcumin reduced TiO_2-induced synovial hyperplasia, inflammatory infiltrates, and vascular proliferation observed in the histopathological index analyses (Fig. 3A).

3.3 Curcumin reduces articular neutrophil and macrophage recruitment induced by TiO_2

The next step was to investigate whether curcumin could reduce leukocyte recruitment to the knee joint. For that, knee joint was collected to determine MPO and NAG activity and knee joint wash collected to determine total number of leukocytes, mononuclear, and polymorphonuclear cells recruited to the articular cavity. We observed that TiO_2 intra-articular injection increased neutrophil (Fig. 4A) and macrophage (Fig. 4B) recruitment on the 30^{th} day, and the treatment with curcumin at 100 mg/kg reduced it (Fig. 4A and B). We also found that intra-articular injection of TiO_2 increased the number of leukocytes recruited to the knee joint 30th day after the stimulus (Fig. 4C-E), and curcumin treatment at 100 mg/kg reduced TiO_2-induced recruitment of total leukocytes (Fig. 4C), polymorphonuclear (Fig. 4E), and mononuclear (Fig. 4D) cells.

3.4 Curcumin reduces TiO_2-induced oxidative stress

Considering the crucial role of oxidative stress in TiO_2-induced arthritis [19,45], we evaluated whether the treatment with curcumin reduces the oxidative stress induced by TiO_2. For this, knee joint samples were collected on the 30th day to determine the superoxide anion production by reducing the redox dye NBT and lipid peroxidation by the levels of TBARS. Our data demonstrated that TiO_2 increased the production of superoxide anion (Fig. 5A) and lipid peroxidation (Fig. 5B), which were reduced by curcumin treatment.

3.5 Curcumin reduces leukocyte recruitment, IL-β levels, and oxidative stress in the early stage of TiO_2-induced arthritis

Based on the previous results that demonstrated an effective reduction of pain and edema after two days of TiO_2 injection (Fig. 2), we next wanted to determine the extent to which curcumin could be effective in the early stage of TiO_2-induced pain and inflammation. For that, we collected samples two days after TiO_2 injection. To elucidate the initial anti-inflammatory effects of curcumin, we evaluated the leukocyte recruitment and IL-1β production on the knee joint. TiO_2 increased the number of leukocytes recruited to the knee joint on the 2nd day after the stimulus (Fig. 6A-C), and macrophages were the most recruited cell (Fig. 6B). Curcumin treatment at 100 mg/kg reduced TiO_2-induced recruitment of total leukocytes (Fig. 6A), mononuclear (Fig. 6B), and polymorphonuclear (Fig. 6C) cells, indicating that is effective at this treatment schedule as well.

The IL-1β levels were also measured in the knee joint on the 2nd day of the model (Fig. 6D). We observe that TiO_2 injection induced IL-1β production on the 2nd day, and curcumin treatment reduced IL-1β levels (Fig. 6D).

Moreover, the knee joint washes were collected on the 2nd day, and ROS and NO production were measured in the synovial fluid leukocytes using DCF-DA, and DAF-2DA probes, respectively. This probe, when oxidized, generates a fluorescence product (DCF or DAF) proportional to overall intracellular levels of ROS and NO (Fig. 7). The treatment with curcumin (100mg/kg) inhibited the DCF fluorescence intensity (Fig. 7A and B) and reduced the DAF fluorescence intensity (Fig. 7C and D) induced by TiO_2 injection.

These data demonstrated the anti-inflammatory effects of curcumin in the early stage of prosthesis-induced arthritis, reducing leukocyte recruitment and IL-1β levels in knee

joints (Fig. 6). Besides that, curcumin treatment has an antioxidant effect reducing TiO_2-induced production of ROS and NO (Fig. 7).

3.6 Curcumin treatment inhibits TiO_2-induced TRPV1 expression and activation in DRG neurons

Our next steps were then to determine whether TiO_2 produces neuronal changes and whether curcumin could reduce that. For that, we perform calcium imaging using the Fluo4-AM fluorescent. As consistent with data from other animal models [48,50], DRG neurons from TiO_2 stimulated mice presented a higher baseline level of calcium influx than DRG from the saline group (Fig. 8A-C). Curcumin-treated mice showed reduced baseline activation of DRG neurons in TiO_2-induced inflammation (Fig. 8A-C). In addition, 82% of DRG neurons from TiO_2-stimulated mice were responsive to capsaicin stimulus while in curcumin-treated animals only 19% (Fig. 8A-D). This demonstrates that curcumin reduced 77% of the responsiveness of DRG neurons to capsaicin (Fig. 8D). Considering these results, we investigated whether curcumin modulates the TRPV1 expression or activation in this animal model. For that, we performed immunofluoresncece by double staining TRPV1 and pNF-kB. We observed that the TiO_2 injection not only increased TRPV1 staining, but also increased the percent of TRPV1-positive neurons co-stained with p-NFκB. This demonstrates that TRPV1-positive neurons are activated in this prosthesis-induced arthritis model. Importantly, treatment with curcumin at 100 mg/kg reduced these parameters (Fig. 9B and C).

3.7 Curcumin treatment inhibits TiO_2-induced TRPA1 activation without modulating the expression in DRG neurons

Since we observed activation of TRPV1-positive DRG neurons, we then investigated whether curcumin modulates TRPA1 using the same approach as above. Similarly, we observed that DRG neurons from TiO2-stimulated mice presented a higher baseline level when compared to saline group. Moreover, we found that in the TiO_2-induced group 96% of the DRG neurons were responsive to AITC stimulus while in the curcumin-treated group only 35% (Fig. 10 A-D). This demonstrates that curcumin reduced 63% of the responsiveness of DRG neurons to AITC (Fig. 10D).

Considering these results, we investigated whether curcumin modulates the TRPA1 expression or activation in this animal model. For that, we performed immunofluoresncece by double staining TRPA1 and pNF-kB. We observed that TRPA1

staining was increased in DRG neurons of TiO2-stimulated mice when compared to saline group. However, we did not observe a difference between the stimulated group (TiO_2 injection) and control (saline) in NF-κB activation of TRPA1-positive neurons (Fig. 11B and C). This indicates that while it seems that TiO_2 increased TRPA1 expression and responsiveness to AITC, that subpopulation of nociceptors did not show NF-kB activation in our model.

5. Discussion

The management of inflammatory pain in prosthesis component-induced arthritis is relevant to promote joint function re-establishment and improving life quality [51]. In this sense, new natural product approaches are widely explored as anti-inflammatory and analgesic, such as curcumin, demonstrating a promising therapeutic [24–26]. In this study, we demonstrated the beneficial effects of curcumin treatment in TiO_2-induced arthritis. Specifically, we found that curcumin reduced mechanical and thermal hyperalgesia, knee joint edema, and histopathological alterations associated with TiO_2 injection. We also found that curcumin reduced decreased proteoglycan degradation. These anti-inflammatory and analgesic effects were explained by reduction of oxidative stress as observed by reduction in superoxide anion production and lipid peroxidation levels. In addition, we found reduction ROS and NO production in synovial wash leukocytes, supporting the antioxidant effect. We also demonstrated that curcumin decreased macrophage and neutrophil recruitment and IL-1β levels in the knee joint. We additionally explored the analgesic mechanisms in nociceptor sensory neurons. We demonstrated that curcumin reduced the activation of DRG neurons observed by a lower baseline levels of calcium influx. On cultured DRG neurons, curcumin-treated animals also showed reduced TRPV1 and TRPA1 responsiveness to capsaicin or AITC, respectively. Additionally, we found that curcumin decreased NF-kB activation on TRPV1-positive neuron.

Release of metallic nanoparticles as a result of deterioration of the prosthetic components promotes osteolysis and the requirement for arthroplasty revision [14–16]. As a result, chronic pain is a common symptom in aseptic loosening [52]. We have previously demonstrated that TiO_2, one of the major components of prosthesis, induced chronic inflammatory arthritis in mice [19]. TiO_2 intraarticular injection induces articular edema, leukocyte recruitment, histopathological alterations, cartilage erosion and cytokine production [19,45]. This indicate this model might be useful for the screening of novel or repurposed drugs for such treatment. We have previously demonstrated that curcumin inhibits pain-like behavior and mechanical and thermal hyperalgesia in the superoxide anion-induced pain model [27]. In a CFA-induced pain model, intrathecal administration of curcumin inhibited glia activation, reducing pain hypersensitivity [53]. Furthermore, the antinociceptive effects of curcumin were also demonstrated in neuropathic [54–57] and cancer-induced bone pain [28] models. Several clinical trials have demonstrated the potential analgesic effect of curcumin as a safe and efficient

treatment for osteoarthritis [58–62]. Based on this, we aimed at testing the effect of curcumin in our mouse model. In corroboration with the literature, we found that curcumin reduced TiO_2-induced mechanical and thermal hyperalgesia as well as knee joint edema, indicating that it might be useful for the treatment of such condition.

TRPV1 and TRPA1 are non-selective cation channels in the peripheral and central nervous systems that receive a calcium influx that promotes pain sensitivity when activated [63,64]. These pain-related channels were widely investigated as analgesic targets in different models [6,65,66]. Therefore, we investigated the modulation of the pain-related-ion channels to elucidate the curcumin analgesic effect in this model. Curcumin blocks capsaicin-induced TRPV1 activation in the orofacial pain model [32] and downregulates the colonic expression and phosphorylation of TRPV1 on DRG neurons in dextran sulfate sodium (DSS)-induced colitis [31]. NF-κB is a transcription factor that regulates immune and inflammatory responses [67]. NF-κB activation has been demonstrated in the pathogenesis of arthritis by regulating different inflammatory genes [68–70]. In DRG neurons, NF-κB activation regulates the neuronal function and leads to chronic hyperexcitability [71]. It was demonstrated that the p65 subunit of NF-κB could upregulate the TRPV1 expression [72]. We show that curcumin inhibited TRPV1 and TRPA1 baseline neuronal activation as well as the responsiveness their agonists in cultured DRG neurons during the early stage of the prosthesis-induced arthritis model. These findings might explain part of curcumin's analgesic mechanisms being through targeting these ion channels.

Phagocyte of prosthetic wear debris by macrophages is crucial to developing the pathophysiology of prosthesis-induced arthritis. After macrophage activation, the release of inflammatory mediators, such as TNF-α and IL-1β, results in the recruitment, multiplication, differentiation, and maturation of osteoclast precursors [73]. Our data show that curcumin treatment reduced these parameters. Moreover, we observed a reduction in the recruitment of leukocytes (macrophages and neutrophils) to the knee joint wash after curcumin treatment. In vitro, curcumin contribute to M2 macrophage polarization in the titanium-induced inflammation model [74]. IL-1β is a crucial cytokine involved in pain, inflammation, and autoimmune conditions. IL-1β production is associated with the induction and maintenance of pain in chronic states, suggesting that the modulation of these cytokine levels can be a therapeutic target [75]. The effect of curcumin in reducing IL-1β levels was demonstrated in superoxide anion-induced pain

[76] and in the serum of patients with inflammatory backgrounds [77]. Our data corroborate these studies showing that curcumin reduced IL-1β levels in the knee joint.

In vivo TiO_2 stimulus increases superoxide anion production and lipid peroxidation, leading to oxidative stress in the knee joint [19]. Reactive oxygen and nitrogen species produced at the site of inflammation contribute to pain and the direct activation of nociceptive neurons [78]. Here we found that TiO_2 increased superoxide anion production and lipid peroxidation. In knee joint was recruited leukocytes, we observed an increase in ROS and NO levels. Importantly, NO is involved in the pathogenesis of inflammatory disorders of the joint [79,80]. NO, and superoxide generates peroxynitrite that contributes to destructive events in cartilage, such as apoptosis [81,82]. Macrophages and neutrophils express NOX2 that regulates superoxide anion production that, in turn, will lead to the production of the other ROS and, in the end, lipid peroxidation [83]. The superoxide anion radical also contributes to inflammatory hyperalgesia [84]. In RAW 264.7 cells culture, curcumin administration reduced oxidative stress via Nrf2/Keap1 by increasing antioxidant capacity [35]. Based on that and the fact curcumin is widely recognized as an antioxidant molecule [33,85,86], we next wanted to determine whether treatment with curcumin could reduce TiO_2-induced oxidative stress. We found that curcumin reduced oxidative stress in the knee joint tissue and specifically in recruited leukocytes. This is in corroboration with data demonstrating that curcuminn reduces gp91phox expression in inflammatory pain induced by superoxide anion [76], iNOS induction by LPS in the mammary gland [87] and primary microglia [87]. Altogether, these data elucidate the antioxidant effect of curcumin by reducing oxidative stress, lipid peroxidation, and superoxide anion production in prosthesis-induced arthritis.

6. Conclusion

Our data suggest that curcumin treatment ameliorates TiO_2-induced chronic arthritis. Curcumin treatment attenuates TiO_2-induced inflammatory pain, knee joint edema, histopathological alterations, and leukocyte recruitment by decreasing oxidative stress and IL-1β levels. We further observed that curcumin attenuates the expression and activation of TRPV1 nociceptor neuron. Thus, this study demonstrated that curcumin could be promising approach to treat complications related to implant-induced inflammation.

7. References

1. Bas DB, Su J, Wigerblad G, Svensson CI. Pain in rheumatoid arthritis: models and mechanisms. Pain Manag [Internet]. Pain Manag; 2016 [cited 2022 Dec 2];6:265–84. Available from: https://pubmed.ncbi.nlm.nih.gov/27086843/

2. Dowell D, Ragan KR, Jones CM, Baldwin GT, Chou R. CDC Clinical Practice Guideline for Prescribing Opioids for Pain - United States, 2022. MMWR Recomm Rep. NLM (Medline); 2022;71:1–95.

3. Verri WA, Cunha TM, Parada CA, Poole S, Cunha FQ, Ferreira SH. Hypernociceptive role of cytokines and chemokines: Targets for analgesic drug development? Pharmacol Ther. Pergamon; 2006;112:116–38.

4. Schumacher MA. TRP Channels in Pain and Inflammation: Therapeutic Opportunities. Pain Pract [Internet]. NIH Public Access; 2010 [cited 2022 Dec 2];10:185. Available from: /pmc/articles/PMC3112370/

5. Levine JD, Alessandri-Haber N. TRP channels: Targets for the relief of pain. Biochimica et Biophysica Acta (BBA) - Molecular Basis of Disease. Elsevier; 2007;1772:989–1003.

6. Duitama M, Vargas-López V, Casas Z, Albarracin SL, Sutachan JJ, Torres YP. TRP Channels Role in Pain Associated With Neurodegenerative Diseases. Front Neurosci. Frontiers Media S.A.; 2020;14:782.

7. Arden N, Nevitt MC. Osteoarthritis: epidemiology. Best Pract Res Clin Rheumatol [Internet]. Best Pract Res Clin Rheumatol; 2006 [cited 2022 Dec 2];20:3–25. Available from: https://pubmed.ncbi.nlm.nih.gov/16483904/

8. Lawrence RC, Felson DT, Helmick CG, Arnold LM, Choi H, Deyo RA, et al. Estimates of the prevalence of arthritis and other rheumatic conditions in the United States. Part II. Arthritis Rheum [Internet]. Arthritis Rheum; 2008 [cited 2022 Dec 2];58:26–35. Available from: https://pubmed.ncbi.nlm.nih.gov/18163497/

9. Bruyère O, Ethgen O, Neuprez A, Zègels B, Gillet P, Huskin JP, et al. Health-related quality of life after total knee or hip replacement for osteoarthritis: a 7-year prospective study. Archives of Orthopaedic and Trauma Surgery 2012 132:11 [Internet]. Springer; 2012 [cited 2022 Dec 2];132:1583–7. Available from: https://link.springer.com/article/10.1007/s00402-012-1583-7

10. Dailiana ZH, Papakostidou I, Varitimidis S, Liaropoulos L, Zintzaras E, Karachalios T, et al. Patient-reported quality of life after primary major joint arthroplasty: A prospective comparison of hip and knee arthroplasty. BMC Musculoskelet Disord

[Internet]. BioMed Central; 2015 [cited 2022 Dec 2];16:1–8. Available from: https://bmcmusculoskeletdisord.biomedcentral.com/articles/10.1186/s12891-015-0814-9

11. Jones CA, Voaklander DC, Johnston WC, Suarez-Almazor ME. The effect of age on pain, function, and quality of life after total hip and knee arthroplasty. Arch Intern Med [Internet]. Arch Intern Med; 2001 [cited 2022 Dec 2];161:454–60. Available from: https://pubmed.ncbi.nlm.nih.gov/11176772/

12. Canovas F, Dagneaux L. Quality of life after total knee arthroplasty. Orthop Traumatol Surg Res [Internet]. Orthop Traumatol Surg Res; 2018 [cited 2022 Dec 2];104:S41–6. Available from: https://pubmed.ncbi.nlm.nih.gov/29183821/

13. Kurtz S, Ong K, Lau E, Mowat F, Halpern M. Projections of primary and revision hip and knee arthroplasty in the United States from 2005 to 2030. J Bone Joint Surg Am [Internet]. J Bone Joint Surg Am; 2007 [cited 2022 Dec 2];89:780–5. Available from: https://pubmed.ncbi.nlm.nih.gov/17403800/

14. Sansone V, Pagani D, Melato M. The effects on bone cells of metal ions released from orthopaedic implants. A review. Clin Cases Miner Bone Metab [Internet]. Clin Cases Miner Bone Metab; 2013 [cited 2022 Dec 2];10:34–40. Available from: https://pubmed.ncbi.nlm.nih.gov/23858309/

15. Kurtz SM, Ong KL, Schmier J, Mowat F, Saleh K, Dybvik E, et al. Future clinical and economic impact of revision total hip and knee arthroplasty. J Bone Joint Surg Am [Internet]. J Bone Joint Surg Am; 2007 [cited 2022 Dec 2];89 Suppl 3:144–51. Available from: https://pubmed.ncbi.nlm.nih.gov/17908880/

16. Hellman EJ, Capello WN, Feinberg JR. Omnifit cementless total hip arthroplasty. A 10-year average followup. Clin Orthop Relat Res [Internet]. Clin Orthop Relat Res; 1999 [cited 2022 Dec 2];364:164–74. Available from: https://pubmed.ncbi.nlm.nih.gov/10416406/

17. Grande F, Tucci P. Titanium Dioxide Nanoparticles: a Risk for Human Health? Mini Rev Med Chem [Internet]. Mini Rev Med Chem; 2016 [cited 2022 Dec 2];16:762–9. Available from: https://pubmed.ncbi.nlm.nih.gov/26996620/

18. Dörner T, Haas J, Loddenkemper C, von Baehr V, Salama A. Implant-related inflammatory arthritis. Nat Clin Pract Rheumatol [Internet]. Nat Clin Pract Rheumatol; 2006 [cited 2022 Dec 2];2:53–6. Available from: https://pubmed.ncbi.nlm.nih.gov/16932652/

19. Borghi SM, Mizokami SS, Pinho-Ribeiro FA, Fattori V, Crespigio J, Clemente-Napimoga JT, et al. The flavonoid quercetin inhibits titanium dioxide (TiO2)-induced chronic arthritis in mice. J Nutr Biochem [Internet]. J Nutr Biochem; 2018 [cited 2022 Dec 2];53:81–95. Available from: https://pubmed.ncbi.nlm.nih.gov/29197723/
20. Hawkey CJ. Nonsteroidal anti-inflammatory drug gastropathy. Gastroenterology [Internet]. W.B. Saunders; 2000 [cited 2022 Dec 2];119:521–35. Available from: https://pubmed.ncbi.nlm.nih.gov/10930388/
21. Zobdeh F, Eremenko II, Akan MA, Tarasov V v., Chubarev VN, Schiöth HB, et al. Pharmacogenetics and Pain Treatment with a Focus on Non-Steroidal Anti-Inflammatory Drugs (NSAIDs) and Antidepressants: A Systematic Review. Pharmaceutics 2022, Vol 14, Page 1190 [Internet]. Multidisciplinary Digital Publishing Institute; 2022 [cited 2022 Dec 2];14:1190. Available from: https://www.mdpi.com/1999-4923/14/6/1190/htm
22. Sharifi-Rad J, Rayess Y el, Rizk AA, Sadaka C, Zgheib R, Zam W, et al. Turmeric and Its Major Compound Curcumin on Health: Bioactive Effects and Safety Profiles for Food, Pharmaceutical, Biotechnological and Medicinal Applications. Front Pharmacol [Internet]. Frontiers Media SA; 2020 [cited 2022 Dec 2];11:1021. Available from: /pmc/articles/PMC7522354/
23. Kocaadam B, Şanlier N. Curcumin, an active component of turmeric (Curcuma longa), and its effects on health. Crit Rev Food Sci Nutr [Internet]. Crit Rev Food Sci Nutr; 2017 [cited 2022 Dec 2];57:2889–95. Available from: https://pubmed.ncbi.nlm.nih.gov/26528921/
24. Oliviero F, Scanu A, Zamudio-Cuevas Y, Punzi L, Spinella P. Anti-inflammatory effects of polyphenols in arthritis. J Sci Food Agric [Internet]. John Wiley & Sons, Ltd; 2018 [cited 2022 Dec 2];98:1653–9. Available from: https://onlinelibrary.wiley.com/doi/full/10.1002/jsfa.8664
25. Jyotirmayee B, Mahalik G. A review on selected pharmacological activities of Curcuma longa L. https://doi.org/101080/1094291220222082464 [Internet]. Taylor & Francis; 2022 [cited 2022 Dec 2];25:1377–98. Available from: https://www.tandfonline.com/doi/abs/10.1080/10942912.2022.2082464
26. Gupta SC, Patchva S, Koh W, Aggarwal BB. Discovery of Curcumin, a Component of the Golden Spice, and Its Miraculous Biological Activities. Clin Exp Pharmacol Physiol [Internet]. NIH Public Access; 2012 [cited 2022 Dec 2];39:283. Available from: /pmc/articles/PMC3288651/

27. Fattori V, Pinho-Ribeiro FA, Borghi SM, Alves-Filho JC, Cunha TM, Cunha FQ, et al. Curcumin inhibits superoxide anion-induced pain-like behavior and leukocyte recruitment by increasing Nrf2 expression and reducing NF-κB activation. Inflamm Res [Internet]. Inflamm Res; 2015 [cited 2022 Dec 2];64:993–1003. Available from: https://pubmed.ncbi.nlm.nih.gov/26456836/
28. Zhao G, Shi Y, Gong C, Liu T, Nan W, Ma L, et al. Curcumin Exerts Antinociceptive Effects in Cancer-Induced Bone Pain via an Endogenous Opioid Mechanism. Front Neurosci. Frontiers Media S.A.; 2021;15:967.
29. Zhang Z, Leong DJ, Xu L, He Z, Wang A, Navati M, et al. Curcumin slows osteoarthritis progression and relieves osteoarthritis-associated pain symptoms in a post-traumatic osteoarthritis mouse model. Arthritis Res Ther [Internet]. BioMed Central Ltd.; 2016 [cited 2022 Dec 2];18:1–12. Available from: https://arthritis-research.biomedcentral.com/articles/10.1186/s13075-016-1025-y
30. Feng K, Ge Y, Chen Z, Li X, Liu Z, Li X, et al. Curcumin Inhibits the PERK-eIF2 α-CHOP Pathway through Promoting SIRT1 Expression in Oxidative Stress-induced Rat Chondrocytes and Ameliorates Osteoarthritis Progression in a Rat Model. Oxid Med Cell Longev [Internet]. Oxid Med Cell Longev; 2019 [cited 2022 Dec 2];2019. Available from: https://pubmed.ncbi.nlm.nih.gov/31223428/
31. Yang M, Wang J, Yang C, Han H, Rong W, Zhang G. Oral administration of curcumin attenuates visceral hyperalgesia through inhibiting phosphorylation of TRPV1 in rat model of ulcerative colitis. Mol Pain [Internet]. Mol Pain; 2017 [cited 2022 Dec 2];13. Available from: https://pubmed.ncbi.nlm.nih.gov/28812431/
32. Yeon KY, Kim SA, Kim YH, Lee MK, Ahn DK, Kim HJ, et al. Curcumin Produces an Antihyperalgesic Effect via Antagonism of TRPV1. http://dx.doi.org/101177/0022034509356169 [Internet]. SAGE Publications; 2009 [cited 2022 Dec 2];89:170–4. Available from: https://journals.sagepub.com/doi/10.1177/0022034509356169
33. Ashrafizadeh M, Ahmadi Z, Mohammadinejad R, Farkhondeh T, Samarghandian S. Curcumin Activates the Nrf2 Pathway and Induces Cellular Protection Against Oxidative Injury. Curr Mol Med [Internet]. Curr Mol Med; 2020 [cited 2022 Dec 2];20:116–33. Available from: https://pubmed.ncbi.nlm.nih.gov/31622191/
34. Samarghandian S, Azimi-Nezhad M, Farkhondeh T, Samini F. Anti-oxidative effects of curcumin on immobilization-induced oxidative stress in rat brain, liver and kidney.

Biomed Pharmacother [Internet]. Biomed Pharmacother; 2017 [cited 2022 Dec 2];87:223–9. Available from: https://pubmed.ncbi.nlm.nih.gov/28061405/
35. Lin X, Bai D, Wei Z, Zhang Y, Huang Y, Deng H, et al. Curcumin attenuates oxidative stress in RAW264.7 cells by increasing the activity of antioxidant enzymes and activating the Nrf2-Keap1 pathway. PLoS One [Internet]. PLoS One; 2019 [cited 2022 Dec 2];14. Available from: https://pubmed.ncbi.nlm.nih.gov/31112588/
36. Jin W, Botchway BOA, Liu X. Curcumin Can Activate the Nrf2/HO-1 Signaling Pathway and Scavenge Free Radicals in Spinal Cord Injury Treatment. Neurorehabil Neural Repair [Internet]. Neurorehabil Neural Repair; 2021 [cited 2022 Dec 2];35:576–84. Available from: https://pubmed.ncbi.nlm.nih.gov/33980059/
37. di Tu Q, Jin J, Hu X, Ren Y, Zhao L, He Q. Curcumin Improves the Renal Autophagy in Rat Experimental Membranous Nephropathy via Regulating the PI3K/AKT/mTOR and Nrf2/HO-1 Signaling Pathways. Biomed Res Int. Hindawi Limited; 2020;2020.
38. Wang Q, Ye C, Sun S, Li R, Shi X, Wang S, et al. Curcumin attenuates collagen-induced rat arthritis via anti-inflammatory and apoptotic effects. Int Immunopharmacol [Internet]. Int Immunopharmacol; 2019 [cited 2022 Dec 2];72:292–300. Available from: https://pubmed.ncbi.nlm.nih.gov/31005039/
39. Gupta B, Ghosh B. Curcuma longa inhibits TNF-alpha induced expression of adhesion molecules on human umbilical vein endothelial cells. Int J Immunopharmacol [Internet]. Int J Immunopharmacol; 1999 [cited 2022 Dec 2];21:745–57. Available from: https://pubmed.ncbi.nlm.nih.gov/10576620/
40. Wang Y, Tang Q, Duan P, Yang L. Curcumin as a therapeutic agent for blocking NF-κB activation in ulcerative colitis. https://doi.org/101080/0892397320181469145 [Internet]. Taylor & Francis; 2018 [cited 2022 Dec 2];40:476–82. Available from: https://www.tandfonline.com/doi/abs/10.1080/08923973.2018.1469145
41. Rinkunaite I, Simoliunas E, Alksne M, Dapkute D, Bukelskiene V. Anti-inflammatory effect of different curcumin preparations on adjuvant-induced arthritis in rats. BMC Complement Med Ther [Internet]. BMC Complement Med Ther; 2021 [cited 2022 Dec 2];21. Available from: https://pubmed.ncbi.nlm.nih.gov/33478498/
42. Liu Y, Chen L, Shen Y, Tan T, Xie N, Luo M, et al. Curcumin Ameliorates Ischemia-Induced Limb Injury Through Immunomodulation. Medical Science Monitor. International Scientific Information, Inc.; 2016;22:2035–42.
43. Kumar A, Dhawan S, Hardegen NJ, Aggarwal BB. Curcumin (Diferuloylmethane) Inhibition of Tumor Necrosis Factor (TNF)-Mediated Adhesion of Monocytes to

Endothelial Cells by Suppression of Cell Surface Expression of Adhesion Molecules and of Nuclear Factor-κB Activation. Biochem Pharmacol. Elsevier; 1998;55:775–83.
44. Guerrero ATG, Verri WA, Cunha TM, Silva TA, Schivo IRS, Dal-Secco D, et al. Involvement of LTB4 in zymosan-induced joint nociception in mice: participation of neutrophils and PGE2. J Leukoc Biol [Internet]. J Leukoc Biol; 2008 [cited 2022 Dec 2];83:122–30. Available from: https://pubmed.ncbi.nlm.nih.gov/17913976/
45. Manchope MF, Artero NA, Fattori V, Mizokami SS, Pitol DL, Issa JPM, et al. Naringenin mitigates titanium dioxide (TiO2)-induced chronic arthritis in mice: role of oxidative stress, cytokines, and NFκB. Inflammation Research 2018 67:11 [Internet]. Springer; 2018 [cited 2022 Dec 2];67:997–1012. Available from: https://link.springer.com/article/10.1007/s00011-018-1195-y
46. Ferraz CR, Manchope MF, Andrade KC, Saraiva-Santos T, Franciosi A, Zaninelli TH, et al. Peripheral mechanisms involved in Tityus bahiensis venom-induced pain. Toxicon. Pergamon; 2021;200:3–12.
47. Guedes RP, Dal Bosco L, Teixeira CM, Araújo ASR, Llesuy S, Belló-Klein A, et al. Neuropathic pain modifies antioxidant activity in rat spinal cord. Neurochem Res [Internet]. 2006 [cited 2022 Dec 2];31:603–9. Available from: https://europepmc.org/article/med/16770731
48. Fattori V, Pinho-Ribeiro FA, Staurengo-Ferrari L, Borghi SM, Rossaneis AC, Casagrande R, et al. The specialised pro-resolving lipid mediator maresin 1 reduces inflammatory pain with a long-lasting analgesic effect. Br J Pharmacol. 2019;176:1728–44.
49. Fattori V, Pinho-Ribeiro FA, Borghi SM, Alves-Filho JC, Cunha TM, Cunha FQ, et al. Curcumin inhibits superoxide anion-induced pain-like behavior and leukocyte recruitment by increasing Nrf2 expression and reducing NF-κB activation. Inflammation Research 2015 64:12 [Internet]. Springer; 2015 [cited 2022 Dec 13];64:993–1003. Available from: https://link.springer.com/article/10.1007/s00011-015-0885-y
50. Bertozzi MM, Saraiva-Santos T, Zaninelli TH, Pinho-Ribeiro FA, Fattori V, Staurengo-Ferrari L, et al. Ehrlich Tumor Induces TRPV1-Dependent Evoked and Non-Evoked Pain-like Behavior in Mice. Brain Sci. 2022;12:1247.
51. Piscitelli P, Iolascon G, Innocenti M, Civinini R, Rubinacci A, Muratore M, et al. Painful prosthesis: approaching the patient with persistent pain following total hip and knee arthroplasty. Clinical Cases in Mineral and Bone Metabolism [Internet]. CIC

Edizioni Internazionali; 2013 [cited 2022 Dec 3];10:97. Available from: /pmc/articles/PMC3797010/

52. Gallo J, Goodman SB, Konttinen YT, Raska M. Particle disease: Biologic mechanisms of periprosthetic osteolysis in total hip arthroplasty. Innate Immun [Internet]. SAGE PublicationsSage UK: London, England; 2013 [cited 2022 Dec 3];19:213–24. Available from: https://journals.sagepub.com/doi/10.1177/1753425912451779

53. Chen JJ, Dai L, Zhao LX, Zhu X, Cao S, Gao YJ. Intrathecal curcumin attenuates pain hypersensitivity and decreases spinal neuroinflammation in rat model of monoarthritis. Sci Rep [Internet]. Sci Rep; 2015 [cited 2022 Dec 3];5. Available from: https://pubmed.ncbi.nlm.nih.gov/25988362/

54. Liu S, Li Q, Zhang MT, Mao-Ying QL, Hu LY, Wu GC, et al. Curcumin ameliorates neuropathic pain by down-regulating spinal IL-1β via suppressing astroglial NALP1 inflammasome and JAK2-STAT3 signalling. Sci Rep [Internet]. Sci Rep; 2016 [cited 2022 Dec 3];6. Available from: https://pubmed.ncbi.nlm.nih.gov/27381056/

55. Di YX, Hong C, Jun L, Renshan G, Qinquan L. Curcumin attenuates mechanical and thermal hyperalgesia in chronic constrictive injury model of neuropathic pain. Pain Ther [Internet]. Pain Ther; 2014 [cited 2022 Dec 3];3:59–69. Available from: https://pubmed.ncbi.nlm.nih.gov/25135388/

56. Ceyhan D, Kocman AE, Yildirim E, Ozatik O, Aydin S, Kose A. Comparison of the Effects of Curcumin, Tramadol and Surgical Treatments on Neuropathic Pain Induced by Chronic Constriction Injury in Rats. Turk Neurosurg [Internet]. Turk Neurosurg; 2018 [cited 2022 Dec 3];28:288–95. Available from: https://pubmed.ncbi.nlm.nih.gov/28481389/

57. Zhang X, Guan Z, Wang X, Sun D, Wang D, Li Y, et al. Curcumin Alleviates Oxaliplatin-Induced Peripheral Neuropathic Pain through Inhibiting Oxidative Stress-Mediated Activation of NF-κB and Mitigating Inflammation. Biol Pharm Bull [Internet]. Biol Pharm Bull; 2020 [cited 2022 Dec 3];43:348–55. Available from: https://pubmed.ncbi.nlm.nih.gov/31776306/

58. Wang Z, Singh A, Jones G, Winzenberg T, Ding C, Chopra A, et al. Efficacy and Safety of Turmeric Extracts for the Treatment of Knee Osteoarthritis: a Systematic Review and Meta-analysis of Randomised Controlled Trials. Curr Rheumatol Rep [Internet]. Curr Rheumatol Rep; 2021 [cited 2022 Dec 3];23. Available from: https://pubmed.ncbi.nlm.nih.gov/33511486/

59. Zeng L, Yang T, Yang K, Yu G, Li J, Xiang W, et al. Efficacy and Safety of Curcumin and Curcuma longa Extract in the Treatment of Arthritis: A Systematic Review and Meta-Analysis of Randomized Controlled Trial. Front Immunol. Frontiers Media S.A.; 2022;13:2347.
60. Shep D, Khanwelkar C, Gade P, Karad S. Safety and efficacy of curcumin versus diclofenac in knee osteoarthritis: A randomized open-label parallel-arm study. Trials [Internet]. BioMed Central Ltd.; 2019 [cited 2022 Dec 3];20:1–11. Available from: https://trialsjournal.biomedcentral.com/articles/10.1186/s13063-019-3327-2
61. Zeng L, Yu G, Hao W, Yang K, Chen H. The efficacy and safety of Curcuma longa extract and curcumin supplements on osteoarthritis: a systematic review and meta-analysis. Biosci Rep [Internet]. Biosci Rep; 2021 [cited 2022 Dec 3];41. Available from: https://pubmed.ncbi.nlm.nih.gov/34017975/
62. Paultre K, Cade W, Hernandez D, Reynolds J, Greif D, Best TM. Therapeutic effects of turmeric or curcumin extract on pain and function for individuals with knee osteoarthritis: a systematic review. BMJ Open Sport Exerc Med [Internet]. BMJ Open Sport Exerc Med; 2021 [cited 2022 Dec 3];7. Available from: https://pubmed.ncbi.nlm.nih.gov/33500785/
63. Hu F, Song X, Long D. Transient receptor potential ankyrin 1 and calcium: Interactions and association with disease (Review). Exp Ther Med [Internet]. Exp Ther Med; 2021 [cited 2022 Dec 3];22. Available from: https://pubmed.ncbi.nlm.nih.gov/34737802/
64. Gouin O, L'Herondelle K, Lebonvallet N, le Gall-Ianotto C, Sakka M, Buhé V, et al. TRPV1 and TRPA1 in cutaneous neurogenic and chronic inflammation: pro-inflammatory response induced by their activation and their sensitization. Protein & Cell 2017 8:9 [Internet]. Springer; 2017 [cited 2022 Dec 3];8:644–61. Available from: https://link.springer.com/article/10.1007/s13238-017-0395-5
65. Marrone MC, Morabito A, Giustizieri M, Chiurchiù V, Leuti A, Mattioli M, et al. TRPV1 channels are critical brain inflammation detectors and neuropathic pain biomarkers in mice. Nature Communications 2017 8:1 [Internet]. Nature Publishing Group; 2017 [cited 2022 Dec 3];8:1–18. Available from: https://www.nature.com/articles/ncomms15292
66. Fernandes ES, Awal S, Karadaghi R, Brain SD. TRP Receptors in Arthritis, Gaining Knowledge for Translation from Experimental Models. Open Pain J [Internet]. Bentham Science Publishers Ltd.; 2013 [cited 2022 Dec 3];6:50–61. Available from:

https://www.researchgate.net/publication/236158976_TRP_Receptors_in_Arthritis_Gaining_Knowledge_for_Translation_from_Experimental_Models
67. Liu T, Zhang L, Joo D, Sun SC. NF-κB signaling in inflammation. Signal Transduction and Targeted Therapy 2017 2:1 [Internet]. Nature Publishing Group; 2017 [cited 2022 Dec 3];2:1–9. Available from: https://www.nature.com/articles/sigtrans201723
68. Gilston V, Jones HW, Soo CC, Coumbe A, Blades S, Kaltschmidt C, et al. NF-kappa B activation in human knee-joint synovial tissue during the early stage of joint inflammation. Biochem Soc Trans [Internet]. Biochem Soc Trans; 1997 [cited 2022 Dec 3];25. Available from: https://pubmed.ncbi.nlm.nih.gov/9388734/
69. Marok R, Winyard PG, Coumbe A, Kus ML, Gaffney K, Blades S, et al. Activation of the transcription factor nuclear factor-kappaB in human inflamed synovial tissue. Arthritis Rheum [Internet]. Arthritis Rheum; 1996 [cited 2022 Dec 3];39:583–91. Available from: https://pubmed.ncbi.nlm.nih.gov/8630106/
70. Tak PP, Gerlag DM, Aupperle KR, van de Geest DA, Overbeek M, Bennett BL, et al. Inhibitor of Nuclear Factor B Kinase Is a Key Regulator of Synovial Inflammation. Arthritis Rheum [Internet]. 2001 [cited 2022 Dec 3];44:1897–907. Available from: https://onlinelibrary.wiley.com/terms-and-conditions
71. Xie MX, Zhang XL, Xu J, Zeng WA, Li D, Xu T, et al. Nuclear Factor-kappaB Gates Nav1.7 Channels in DRG Neurons via Protein-Protein Interaction. iScience. Elsevier; 2019;19:623–33.
72. Zhang BY, Zhang YL, Sun Q, Zhang PA, Wang XX, Xu GY, et al. Alpha-lipoic acid downregulates TRPV1 receptor via NF-κB and attenuates neuropathic pain in rats with diabetes. CNS Neurosci Ther [Internet]. John Wiley & Sons, Ltd; 2020 [cited 2022 Dec 3];26:762–72. Available from: https://onlinelibrary.wiley.com/doi/full/10.1111/cns.13303
73. Nich C, Takakubo Y, Pajarinen J, Ainola M, Salem A, Sillat T, et al. Macrophages – Key Cells in the Response to Wear Debris from Joint Replacements. J Biomed Mater Res A [Internet]. NIH Public Access; 2013 [cited 2022 Dec 3];101:3033. Available from: /pmc/articles/PMC3775910/
74. Li B, Hu Y, Zhao Y, Cheng M, Qin H, Cheng T, et al. Curcumin attenuates titanium particle-induced inflammation by regulating macrophage polarization in vitro and in vivo. Front Immunol. Frontiers Media S.A.; 2017;8:55.

75. Ren K, Torres R. Role of interleukin-1β during pain and inflammation. Brain Res Rev [Internet]. NIH Public Access; 2009 [cited 2022 Dec 3];60:57. Available from: /pmc/articles/PMC3076185/

76. Fattori V, Pinho-Ribeiro FA, Borghi SM, Alves-Filho JC, Cunha TM, Cunha FQ, et al. Curcumin inhibits superoxide anion-induced pain-like behavior and leukocyte recruitment by increasing Nrf2 expression and reducing NF-κB activation. Inflammation Research 2015 64:12 [Internet]. Springer; 2015 [cited 2022 Dec 3];64:993–1003. Available from: https://link.springer.com/article/10.1007/s00011-015-0885-y

77. Gorabi AM, Razi B, Aslani S, Abbasifard M, Imani D, Sathyapalan T, et al. Effect of curcumin on proinflammatory cytokines: A meta-analysis of randomized controlled trials. Cytokine [Internet]. Cytokine; 2021 [cited 2022 Dec 3];143. Available from: https://pubmed.ncbi.nlm.nih.gov/33934954/

78. Salvemini D, Little JW, Doyle T, Neumann WL. Roles of reactive oxygen and nitrogen species in pain. Free Radic Biol Med [Internet]. Free Radic Biol Med; 2011 [cited 2022 Dec 4];51:951–66. Available from: https://pubmed.ncbi.nlm.nih.gov/21277369/

79. Sharma JN, Al-Omran A, Parvathy SS. Role of nitric oxide in inflammatory diseases. Inflammopharmacology 2007 15:6 [Internet]. Springer; 2008 [cited 2022 Dec 4];15:252–9. Available from: https://link.springer.com/article/10.1007/s10787-007-0013-x

80. Dey P, Panga V, Raghunathan S. A Cytokine Signalling Network for the Regulation of Inducible Nitric Oxide Synthase Expression in Rheumatoid Arthritis. PLoS One [Internet]. Public Library of Science; 2016 [cited 2022 Dec 4];11:e0161306. Available from: https://journals.plos.org/plosone/article?id=10.1371/journal.pone.0161306

81. del Carlo M, Loeser RF. Nitric oxide–mediated chondrocyte cell death requires the generation of additional reactive oxygen species. Arthritis Rheum [Internet]. John Wiley & Sons, Ltd; 2002 [cited 2022 Dec 4];46:394–403. Available from: https://onlinelibrary.wiley.com/doi/full/10.1002/art.10056

82. Pacher P, Beckman JS, Liaudet L. Nitric oxide and peroxynitrite in health and disease. Physiol Rev [Internet]. Physiol Rev; 2007 [cited 2022 Dec 4];87:315–424. Available from: https://pubmed.ncbi.nlm.nih.gov/17237348/

83. Lambeth JD. NOX enzymes and the biology of reactive oxygen. Nature Reviews Immunology 2004 4:3 [Internet]. Nature Publishing Group; 2004 [cited 2022 Dec 4];4:181–9. Available from: https://www.nature.com/articles/nri1312

84. Cuzzocrea S, Pisano B, Dugo L, Ianaro A, Ndengele M, Salvemini D. Superoxide-related signaling cascade mediates nuclear factor-kappaB activation in acute inflammation. Antioxid Redox Signal [Internet]. Antioxid Redox Signal; 2004 [cited 2022 Dec 4];6:699–704. Available from: https://pubmed.ncbi.nlm.nih.gov/15242550/

85. Jakubczyk K, Drużga A, Katarzyna J, Skonieczna-żydecka K. Antioxidant Potential of Curcumin—A Meta-Analysis of Randomized Clinical Trials. Antioxidants [Internet]. Multidisciplinary Digital Publishing Institute (MDPI); 2020 [cited 2022 Dec 4];9:1–13. Available from: /pmc/articles/PMC7694612/

86. Gupta SC, Patchva S, Koh W, Aggarwal BB. Discovery of curcumin, a component of golden spice, and its miraculous biological activities. Clin Exp Pharmacol Physiol [Internet]. Clin Exp Pharmacol Physiol; 2012 [cited 2022 Dec 13];39:283–99. Available from: https://pubmed.ncbi.nlm.nih.gov/22118895/

87. Jung KK, Lee HS, Cho JY, Shin WC, Rhee MH, Kim TG, et al. Inhibitory effect of curcumin on nitric oxide production from lipopolysaccharide-activated primary microglia. Life Sci [Internet]. Life Sci; 2006 [cited 2022 Dec 4];79:2022–31. Available from: https://pubmed.ncbi.nlm.nih.gov/16934299/

Figures and legends

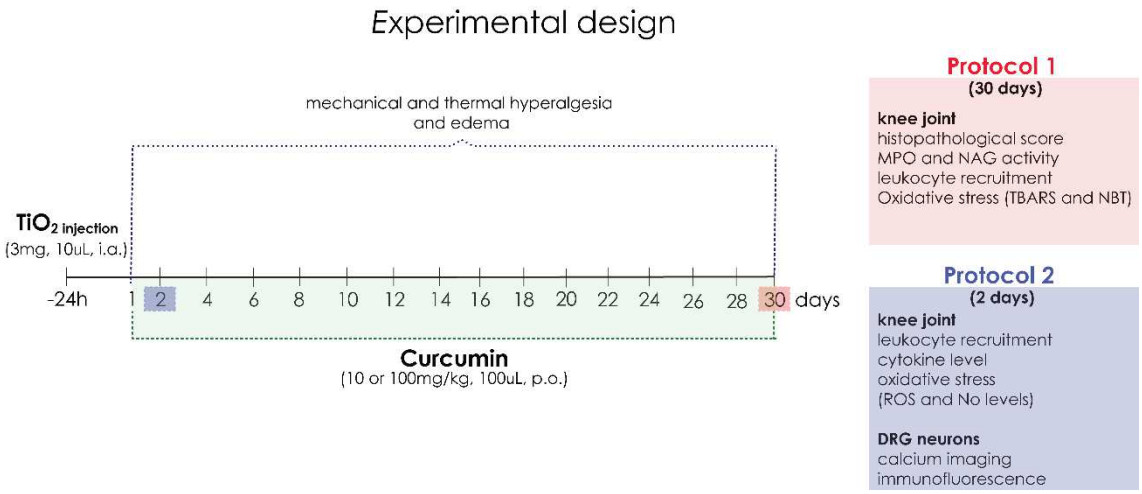

Fig. 1 Experimental design. **Protocol 1** represents 30 days of experimental design; mice were treated per oral (p.o.) with curcumin at 10 or 100 mg/kg, or vehicle (20% tween 80 in saline) daily starting twenty-four hours after a single intra-articular (i.a.) injection of TiO_2 (3mg/10µl/knee. Mechanical hyperalgesia and knee joint edema were evaluated twenty-four hours after the TiO_2 stimulus, after curcumin treatment (1h) on the first day, and every other day (from the 2nd to the 30th). The thermal hyperalgesia was evaluated every three days for 30 days. On the 30th day after the stimulus, knee joints were collected to evaluate the histopathological alterations, MPO, and NAG activity. The synovial wash was collected to determine the leukocyte recruitment, and knee joint samples were used to evaluate the oxidative stress (TBARS and NBT levels). **Protocol 2** represents 2 days of experimental design; knee joint washes were collected to quantify the leukocyte recruitment and oxidative stress (ROS and NO). The knee joint tissue was used to measure the IL-1β levels by ELISA. The DRG neurons (L4-L6) were used to determine the calcium influx imaging using confocal microscopy; TRPV1, TRPA1, and p-NFκB staining were determined by immunofluorescence assay.

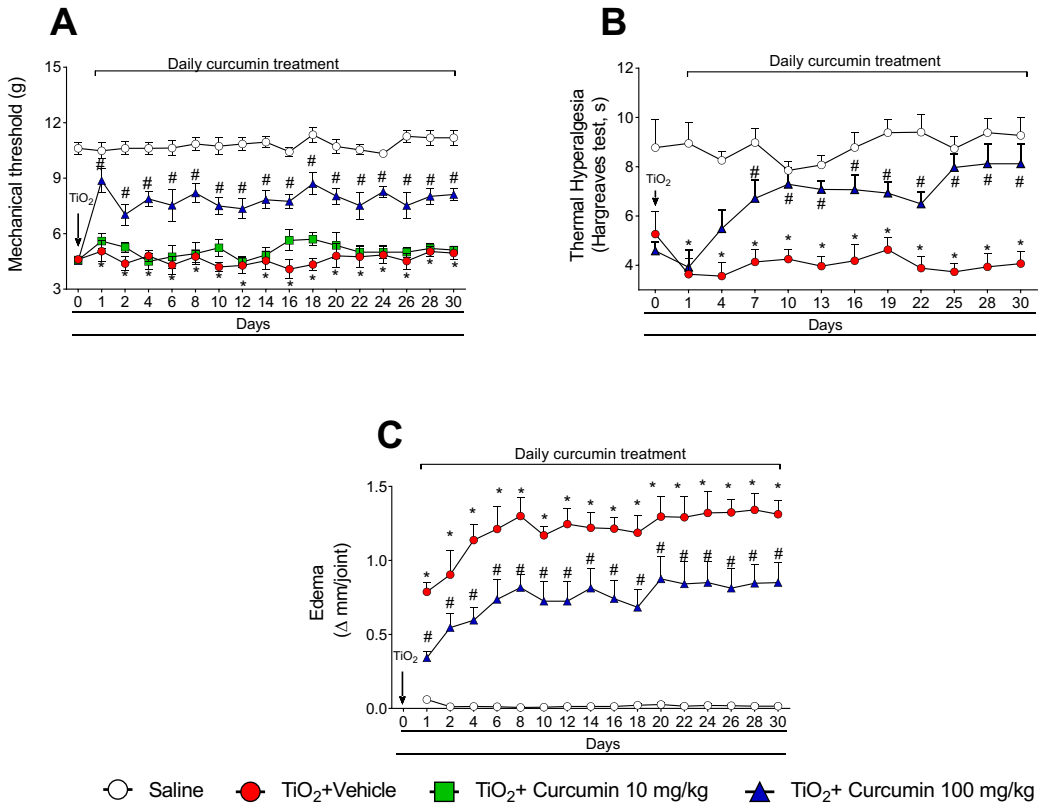

Fig. 2 Curcumin reduces TiO_2-induced mechanical and thermal hyperalgesia and articular edema. Mice were treated daily for 30 days with curcumin (10 or 100 mg/kg; p.o.) or vehicle (20% tween 80 in saline) starting twenty-four hours after TiO_2 intra-articular injection (3mg/joint). The articular mechanical hyperalgesia **A** and edema **C** were evaluated before and after curcumin treatment and subsequently every other day for 30 days. Knee joint thermal hyperalgesia were measured on day one and every three days until the 30th **B**. Results are expressed as mean ± SEM of six mice per group per experiment and are representative of two separate experiments (*$p < 0.05$ vs. saline group; #$p<0.05$ vs. TiO_2 and curcumin (10mg/kg) groups, repeated measures two-way ANOVA followed by Tukey's post-test.

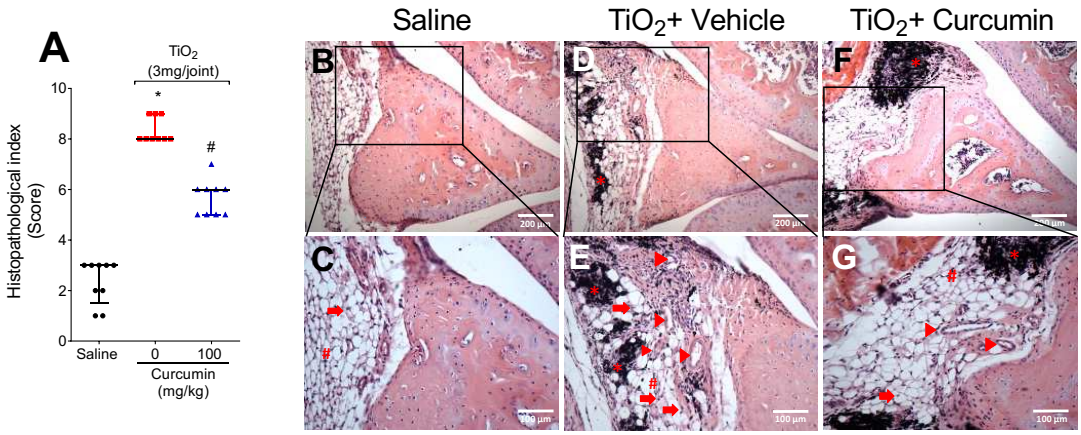

Fig. 3 Curcumin reduces articular histopathological changes induced by TiO_2. Mice were treated with 100 mg/kg of curcumin (p.o.) or vehicle (20% tween 80 in saline) daily twenty-four hours after TiO_2 intra-articular injection (3mg/joint) for 30 days. On the 30th day, the knee joint was collected and stained with HE and toluidine blue— histopathological index **A** and analysis **B-G**. The panel shows saline **B and C**, TiO_2 treated with vehicle **D and E**, and TiO_2 treated with curcumin **F and G**. The representative images demonstrated the invasive pannus (arrowhead), leukocyte infiltration (arrow), and angiogenesis (asterisk). Original magnification 10x **B, D and E** and 20x **C, E and G**. Results are expressed as medians and interquartile ranges of nine mice per group per experiment, two independent experiments (*$p<0.05$ vs. saline group; #$p<0.05$ vs. TiO_2 group, Kruskal-Wallis followed by Dunn's post-test).

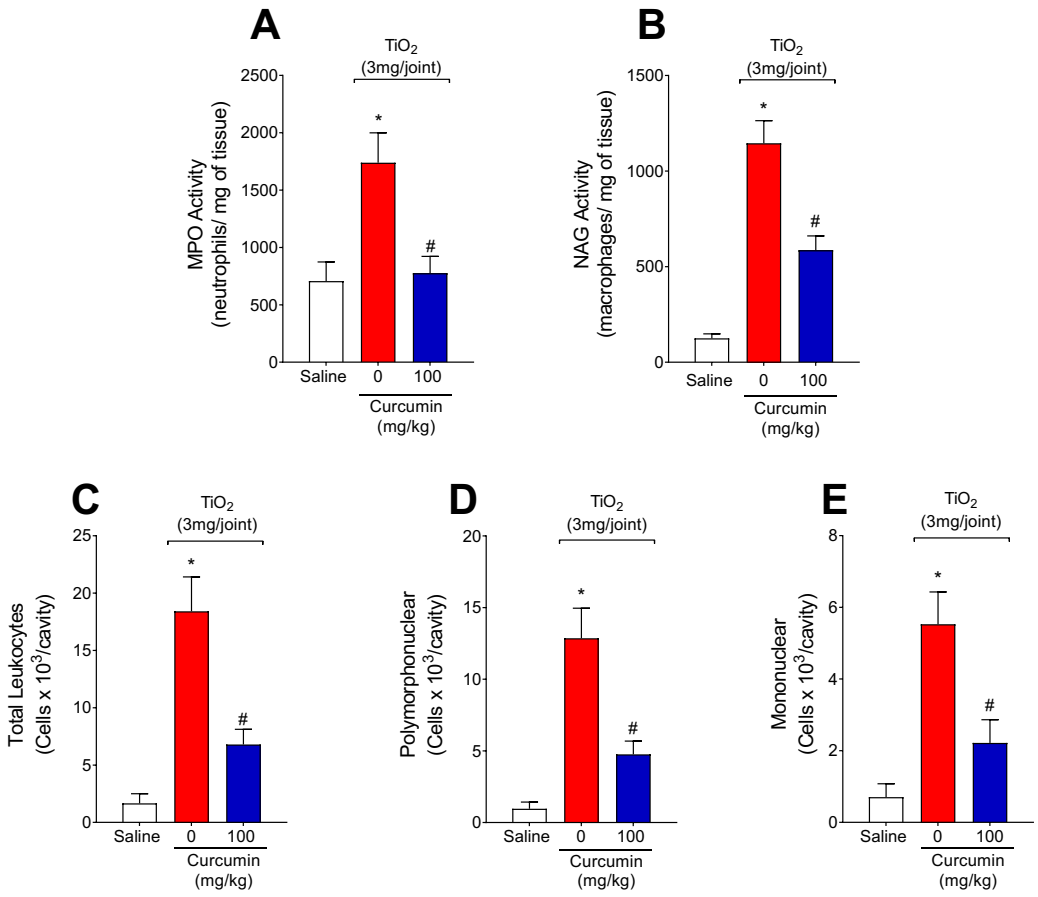

Fig. 4 Curcumin reduces macrophage and neutrophil recruitment to the knee joint induced by TiO_2. Twenty-four hours after the TiO_2 injection, mice received daily treatment with 100 mg/kg of curcumin or vehicle (20% tween 80 in saline) for 30 days. The knee joint samples and to assess the MPO **A** and NAG **B** activity. Knee joint washes were collected to count total leukocytes **C**, polymorphonuclear **D**, and mononuclear **E** cells. Results are expressed as mean ± SEM of six mice per group per experiment, two independent experiments (*$p<0.05$ vs. saline group; #$p<0.05$ vs. TiO_2 group, one-way ANOVA followed by Tukey's post-test).

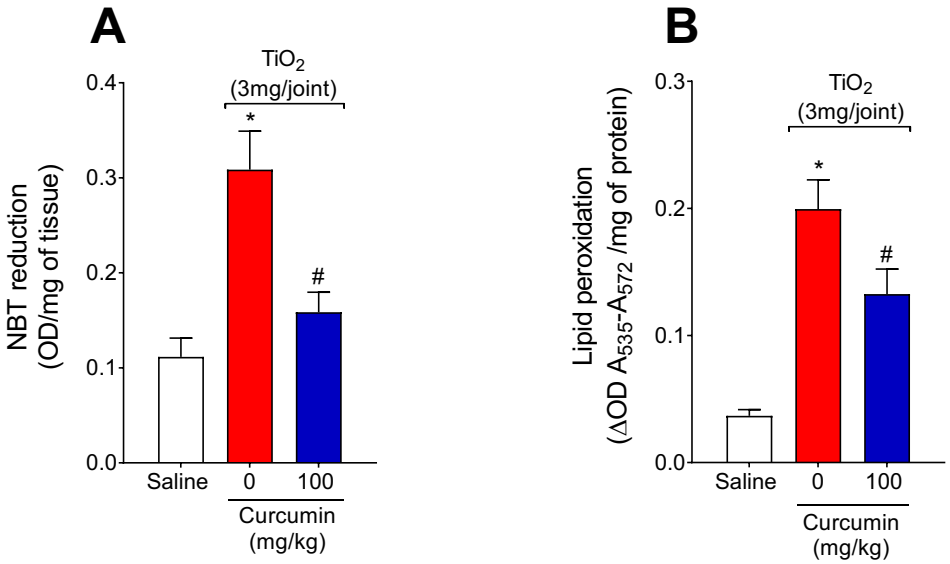

Fig. 5 Treatment with curcumin reduces TiO_2-induced oxidative stress. Mice received curcumin (100 mg/kg, p.o.) or vehicle (20% tween 80 in saline) treatment daily for 30 days after TiO_2 intra-articular injection, and the superoxide anion production **A** and lipid peroxidation levels **B** were determined on the 30th day. Results are expressed as mean ± SEM of six mice per group per experiment, two independent experiments (*p<0.05 vs. saline group; #p<0.05 vs. TiO_2 group, one-way ANOVA followed by Tukey's post-test).

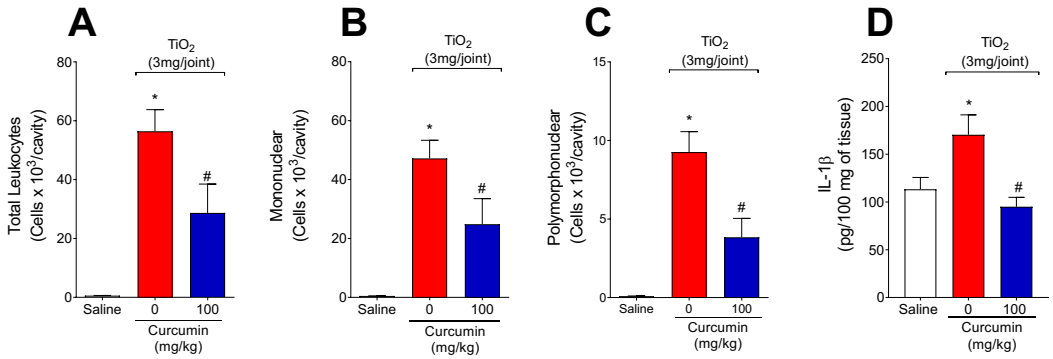

Fig. 6 Curcumin reduces TiO_2-induced leukocyte recruitment and IL-β levels in the knee joint. Mice were treated with curcumin (100 mg/kg, p.o.) or vehicle (20% tween 80 in saline) twenty-four hours after TiO_2 intra-articular injection, and on the 2nd day, knee joint washes were collected to count total leukocytes **A**, mononuclear **B**, and polymorphonuclear cells **C**. Knee joints were collected, and ELISA measured IL-1β levels **D**. Results are expressed as mean ± SEM of six mice per group per experiment,

two independent experiments (*p<0.05 vs. saline group; #p<0.05 vs. TiO_2 group, one-way ANOVA followed by Tukey's post-test).

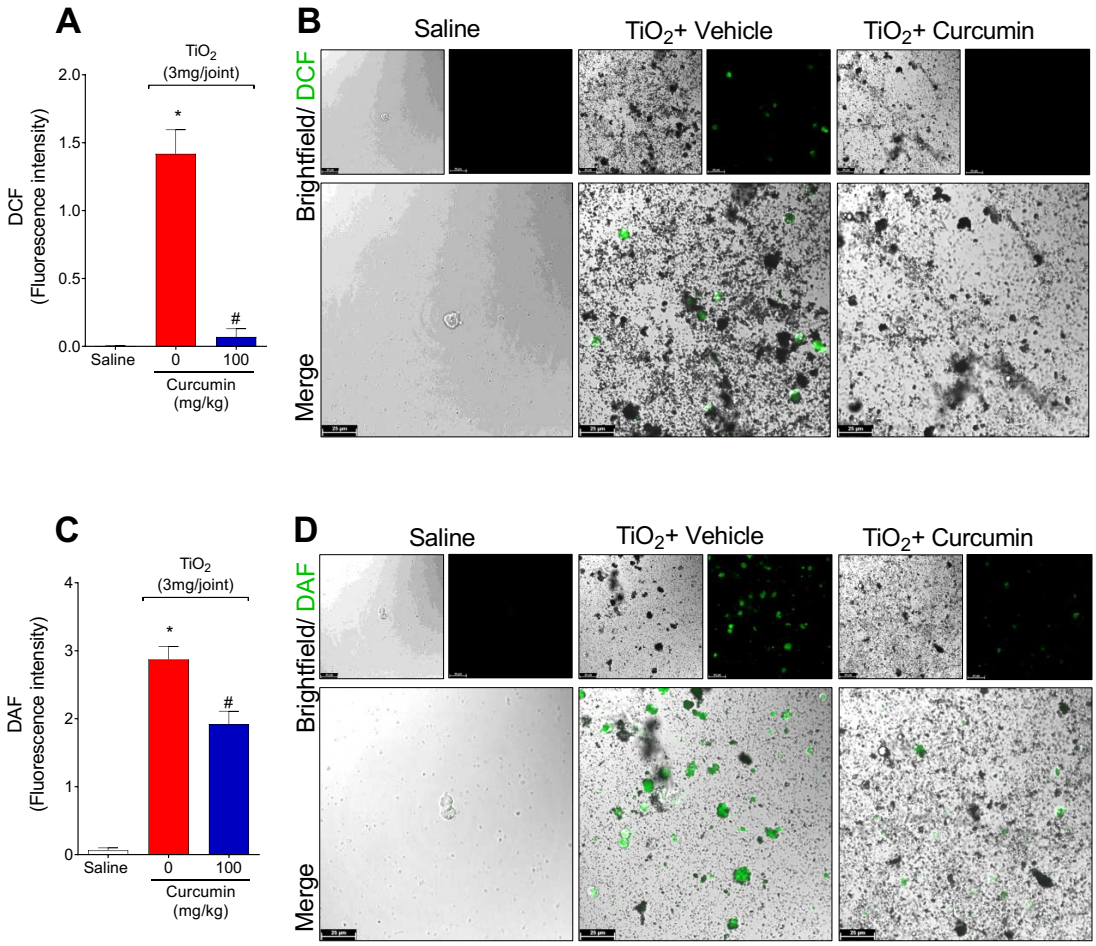

Fig. 7 Curcumin reduces TiO_2-induced oxidative stress induced by TiO_2. Mice were treated with curcumin (100 mg/kg, p.o.) or vehicle (20% tween 80 in saline) twenty-four hours after TiO_2 intra-articular injection, and on the 2nd day, knee joint washes were collected, and DCF-DA or DAF-2DA was added to knee joint wash cells for 30 min. Intracellular ROS and NO levels from intact cells were analyzed using the brightfield and green channels in a confocal microscope at 63x magnification. DCF fluorescence intensity **A** indicates ROS production, and DAF fluorescence intensity **C** indicates NO production, which was quantitated. **B** representative DCF fluorescence images for the negative control, TiO_2, and curcumin groups. **D** representative DAF fluorescence images for the negative control, TiO_2, and curcumin groups. Results are expressed as mean ± SEM of six mice per group per experiment, two independent experiments (*p<0.05 vs. saline group; #p<0.05 vs. TiO_2 group, one-way ANOVA followed by Tukey's post-test).

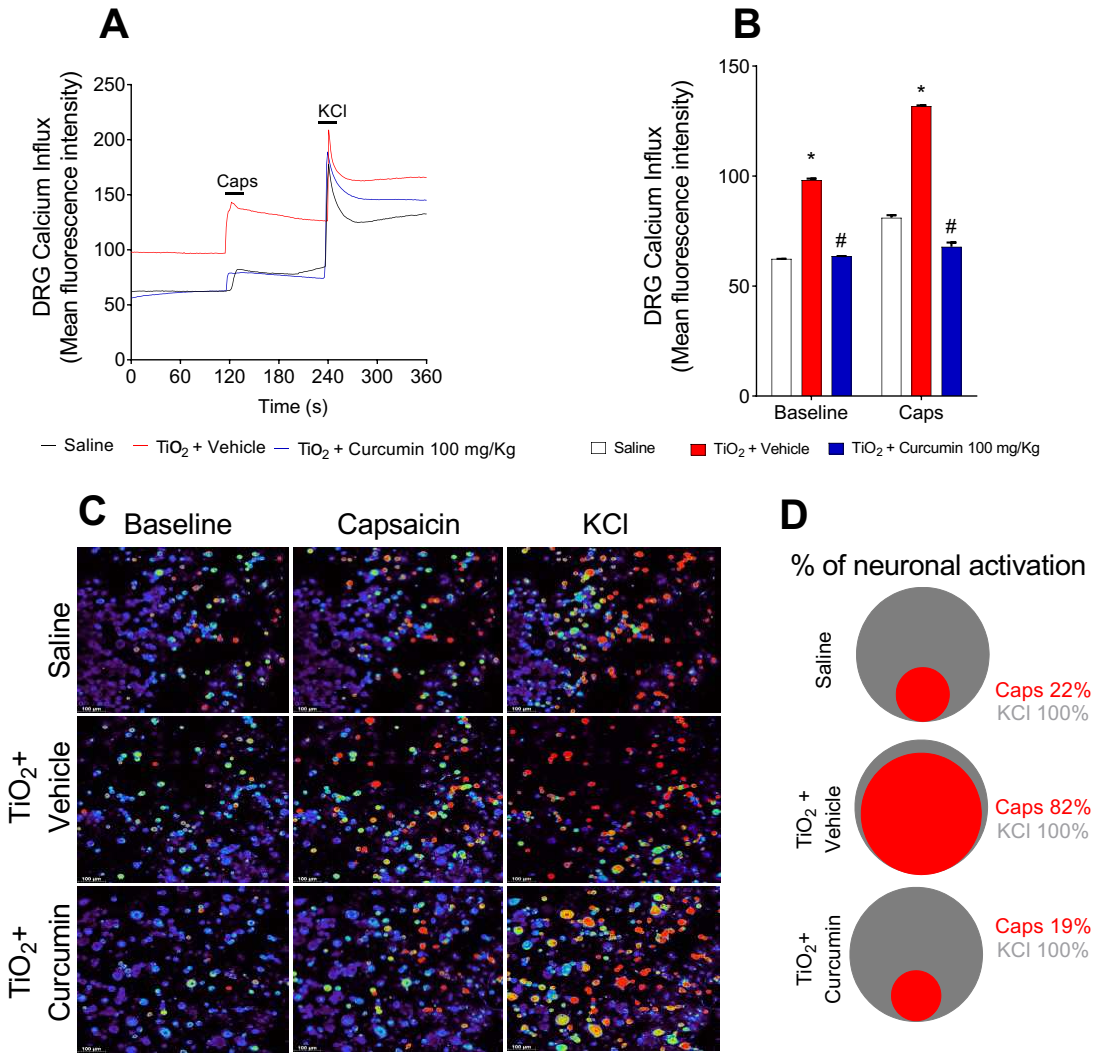

Fig. 8 Curcumin inhibits TiO_2-induced TRPV1 activation on DRG neurons. Mice were treated with curcumin (100 mg/kg, p.o.) or vehicle (20% tween 80 in saline) twenty-four hours after TiO_2 intra-articular injection, and on the 2nd day of the model, the DRG samples (L4-L6) were collected for calcium imaging using Fluo-4 AM probe. The fluorescence intensity traces of calcium influx from the representative DRG fields, responsive for KCl (240-s mark, activates all neurons), during the 6 min of recording was shown in panel **A**. **B** displays the mean fluorescence intensity of calcium influx of the baseline (0-s mark) and that following the stimulus with capsaicin (120-s mark, a TRPV1 agonist). **C** representative fields of DRG neurons (baseline fluorescence, the fluorescence after capsaicin, and after KCl). **D** Venn Diagram comparing the percent of neurons population with increased capsaicin activation (red) that had responded to KCl stimulation (grey). Results are expressed as mean ± SEM, n = 4 DRG seeded plates (each plate is a neuronal culture pooled from 10 mice) per group per experiment, two

independent experiments (*p<0.05 vs. saline group; #p<0.05 vs. TiO_2 group, two-way ANOVA followed by Tukey's post-test).

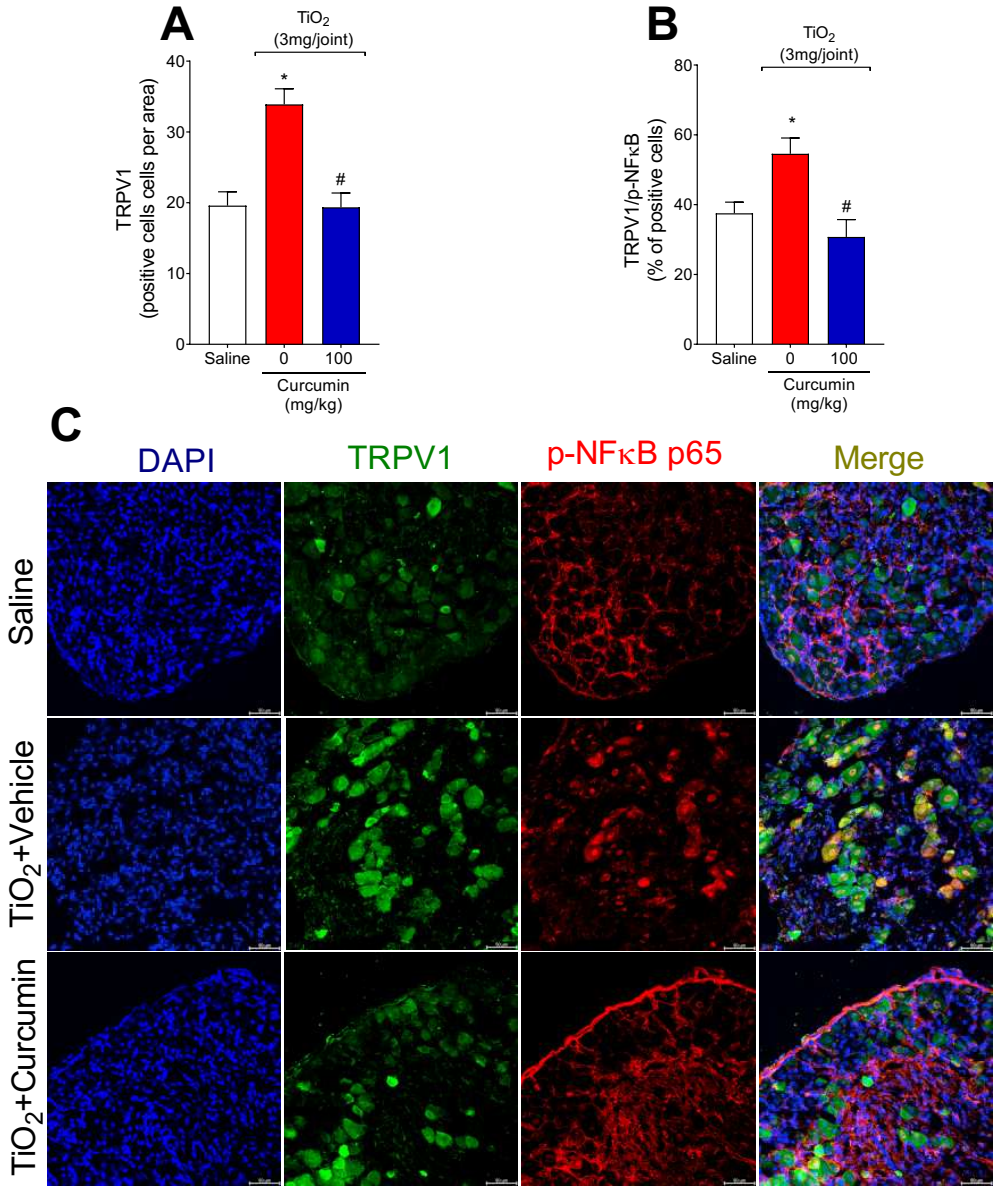

Fig. 9 Curcumin treatment inhibits NF-κB activation in TRPV1-positive neurons induced by TiO_2. Mice were treated with curcumin (100 mg/kg, p.o.) or vehicle (20% tween 80 in saline) twenty-four hours after TiO_2 intra-articular injection. DRGs samples (L4-L6) were collected on the 2nd day of the model to evaluate TRPV1 and p-NFκB p65 staining by immunofluorescence. **A** quantitation analysis by the number of positive cells per area TRPV1 on DRGs. **B** percent of positive cells co-stained with p-NFκB p65. **C** representative images of TRPV1-positive cells (green), p-NFκB p65 positive cells (red), with nuclear staining by DAPI (blue), and the merge of double labeling of TRPV1 and NF-κB in DRG samples (20x magnification with 1.5 zoom in). Results are expressed as

mean ± SEM, n=10 mice per group per experiment, two independent experiments (*p<0.05 vs. saline group; #p<0.05 vs. TiO_2 group, one-way ANOVA followed by Tukey's post-test).

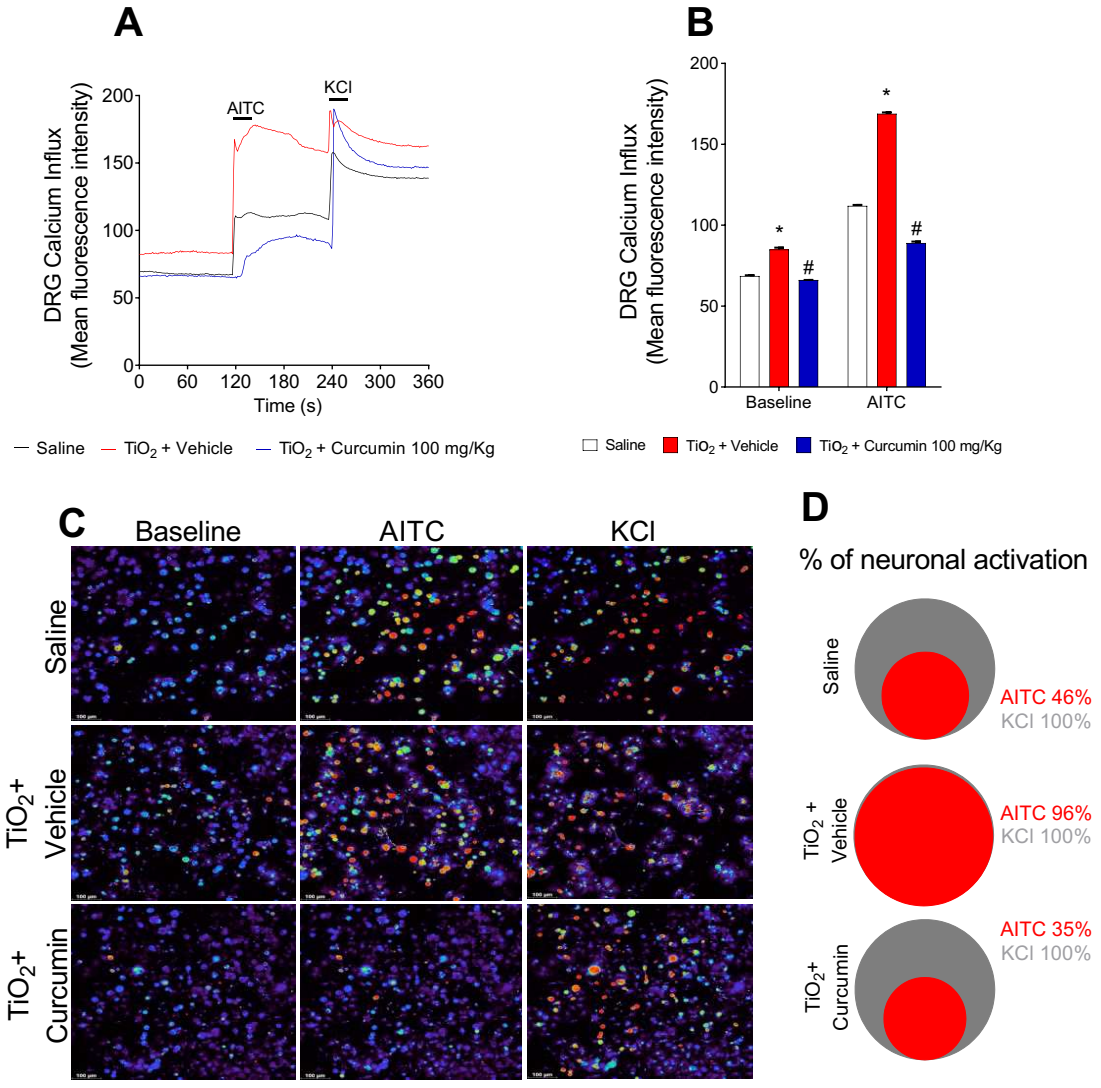

Fig. 10 Curcumin inhibits TiO_2-induced TRPA1 activation on DRG neurons. Mice were treated with curcumin (100 mg/kg, p.o.) or vehicle (20% tween 80 in saline) twenty-four hours after TiO_2 intra-articular injection, and on the 2nd day of the model, the DRGs samples (L4-L6) were collected for calcium imaging using Fluo-4 AM probe. The fluorescence intensity traces of calcium influx from the representative DRG fields, responsive for KCl (240-s mark, activates all neurons), during the 6 min of recording was shown in panel **A**. **B** displays the mean fluorescence intensity of calcium influx of the baseline (0-s mark) and that following the stimulus with AITC (120-s mark, a TRPA1 agonist). **C** shows representative fields of DRG neurons (baseline fluorescence, the

fluorescence after AITC, and after KCl). **D** Venn Diagram comparing the percent of neurons population with increased AITC activation (red) that had responded to KCl stimulation (grey). Results are expressed as mean ± SEM, n = 4 DRG seeded plates (each plate is a neuronal culture pooled from 10 mice) per group per experiment, two independent experiments (*p<0.05 vs. saline group; #p<0.05 vs. TiO_2 group, two-way ANOVA followed by Tukey's post-test).

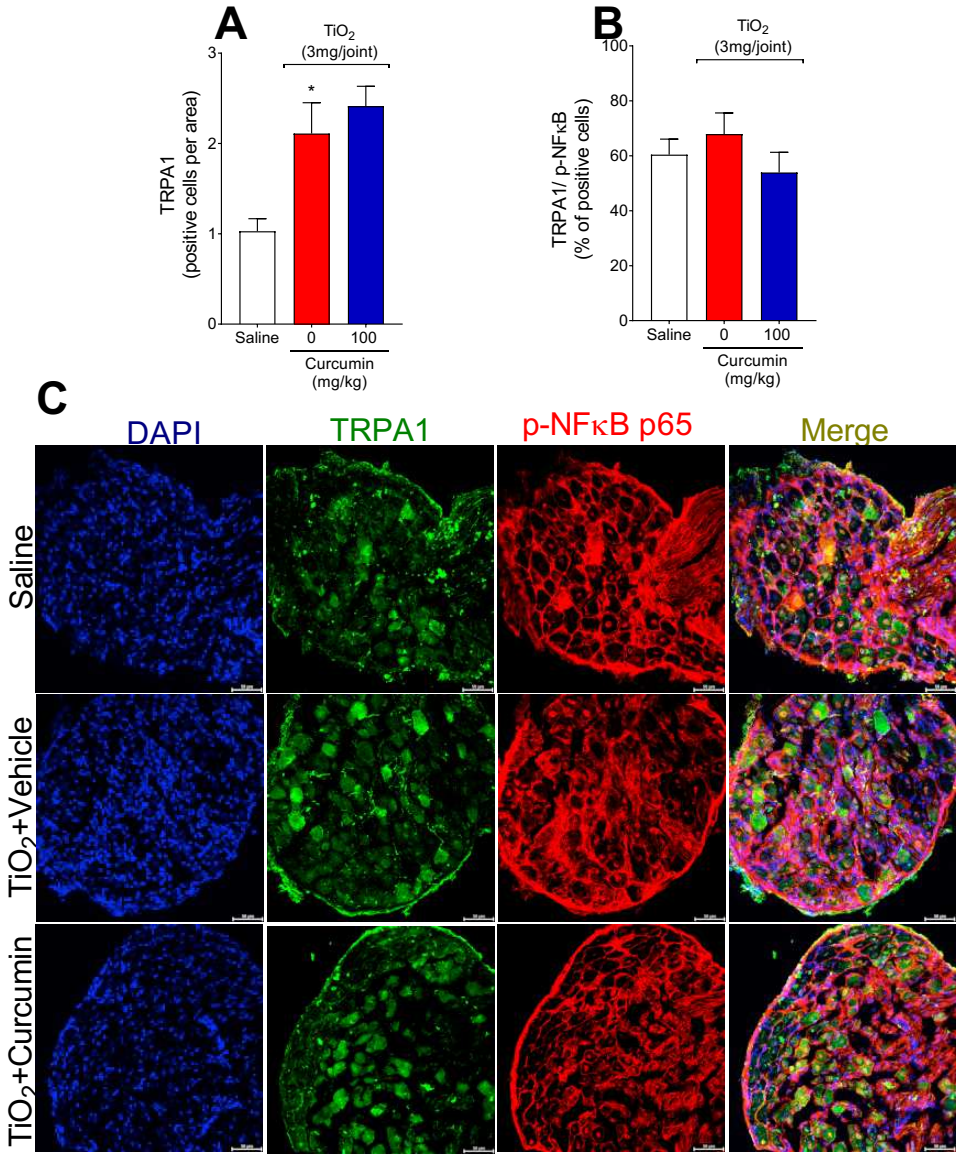

Fig. 11 Curcumin treatment does not reduce TRPA1 staining induced by TiO_2. Mice were treated with curcumin (100 mg/kg, p.o.) or vehicle (20% tween 80 in saline) twenty-four hours after TiO_2 intra-articular injection, and DRGs samples (L4-L6) were collected on the 2nd day of the model to evaluate TRPA1 and p-NFκB p65 staining by immunofluorescence. **A** quantitation analysis by the number of positive cells per area

TRPA1 on DRGs. **B** percent of positive cells co-stained with p-NFκB p65. **C** representative images of TRPA1-positive cells (green), p-NFκB p65 positive cells (red), with nuclear staining by DAPI (blue), and the merge of double labeling of TRPA1 and NF-κB in DRG samples (20x magnification with 1.5 zoom in). Results are expressed as mean ± SEM, n=10 mice per group per experiment, two independent experiments (*$p<0.05$ vs. saline group; #$p<0.05$ vs. TiO_2 group, one-way ANOVA followed by Tukey's post-test).

6. CONCLUSÃO

O presente estudo elucidou os efeitos analgésicos, anti-inflamatório e efeitos antioxidantes do mediador lipídico pró-resolução LXA_4 e do polifenol curcumina em modelo animal de artrite induzida por TiO_2, um modelo de dor e inflamação induzida pelo uso de prótese. Nós demonstramos que o tratamento com LXA_4 reduz a dor inflamatória, edema articular, recrutamento de leucócitos induzido por TiO_2, pela inibição do estresse oxidativo, redução da produção de citocinas pró-inflamatórias. Esses efeitos se dão pela redução da ativação de NF-κB em macrófagos recrutados, diminuição da expressão de Nrf2, bem como pela diminuição da ativação neuronal no gânglio da raiz dorsal, atuando na redução da expressão de TRPV1 nesses neurônios, possivelmente via seu receptor ALX/FPR2. Além disso, também demonstramos os potenciais efeitos da curcumina também na redução da dor, edema, reduzindo recrutamento de leucócitos, estresse oxidativo e atuando via diminuição da ativação e expressão de TRPV1 em neurônios nociceptivos. Desta forma, é possível que um MLPR e um polifenol que são amplamente explorados como ferramentas terapêuticas, como a LXA_4 e curcumina, respectivamente, sejam uma promissora abordagem para atenuar as complicações relacionadas à inflamação induzida por implantes atuando como importantes anti-inflamatórios, antioxidantes e analgésicos.

ANEXO- Lista de artigos de colaboração no período de doutoramento.

1.1. Artigos

Zucoloto AZ, Manchope MF, Borghi SM, **Dos Santos TS**, Fattori V, Badaro-Garcia S, Camilios-Neto D, Casagrande R, Verri WA Jr. Probucol Ameliorates Complete Freund's Adjuvant-Induced Hyperalgesia by Targeting Peripheral and Spinal Cord Inflammation. Inflammation. 2019 Aug;42(4):1474-1490. doi: 10.1007/s10753-019-01011-3. PMID: 31011926.

Bussmann AJC, Borghi SM, Zaninelli TH, **Dos Santos TS**, Guazelli CFS, Fattori V, Domiciano TP, Pinho-Ribeiro FA, Ruiz-Miyazawa KW, Casella AMB, Vignoli JA, Camilios-Neto D, Casagrande R, Verri WA Jr. The citrus flavanone naringenin attenuates zymosan-induced mouse joint inflammation: induction of Nrf2 expression in recruited CD45+ hematopoietic cells. Inflammopharmacology. 2019 Dec;27(6):1229-1242. doi: 10.1007/s10787-018-00561-6. Epub 2019 Jan 5. PMID: 30612217.

Rasquel-Oliveira FS, Manchope MF, Staurengo-Ferrari L, Ferraz CR, **Saraiva-Santos T,** Zaninelli TH, Fattori V, Artero NA, Badaro-Garcia S, de Freitas A, Casagrande R, Verri WA Jr. Hesperidin methyl chalcone interacts with NFκB Ser276 and inhibits zymosan-induced joint pain and inflammation, and RAW 264.7 macrophage activation. Inflammopharmacology. 2020 Aug;28(4):979-992. doi: 10.1007/s10787-020-00686-7. Epub 2020 Feb 11. PMID: 32048121.

Ferraz CR, Carvalho TT, Fattori V, **Saraiva-Santos T**, Pinho-Ribeiro FA, Borghi SM, Manchope MF, Zaninelli TH, Cunha TM, Casagrande R, Clissa PB, Verri WA Jr. Jararhagin, a snake venom metalloproteinase, induces mechanical hyperalgesia in mice with the neuroinflammatory contribution of spinal cord microglia and astrocytes. Int J Biol Macromol. 2021 May 15;179:610-619. doi: 10.1016/j.ijbiomac.2021.02.178. Epub 2021 Mar 1. PMID: 33662422.

Ferraz CR, Manchope MF, Andrade KC, **Saraiva-Santos T**, Franciosi A, Zaninelli TH, Bagatim-Souza J, Borghi SM, Cândido DM, Knysak I, Casagrande R, Kwasniewski FH, Verri WA. Peripheral mechanisms involved in Tityus bahiensis venom-induced pain. Toxicon. 2021 Sep;200:3-12. doi: 10.1016/j.toxicon.2021.06.013. Epub 2021 Jun 18. PMID: 34153310.

Bussmann AJC, Zaninelli TH, **Saraiva-Santos T**, Fattori V, Guazelli CFS, Bertozzi MM, Andrade KC, Ferraz CR, Camilios-Neto D, Casella AMB, Casagrande R, Borghi SM, Verri WA Jr. The Flavonoid Hesperidin Methyl Chalcone Targets Cytokines and Oxidative Stress to Reduce Diclofenac-Induced Acute Renal Injury: Contribution of the Nrf2 Redox-Sensitive Pathway. Antioxidants (Basel). 2022 Jun 27;11(7):1261. doi: 10.3390/antiox11071261. PMID: 35883752; PMCID: PMC9312103.

Bussmann AJC, Ferraz CR, Lima AVA, Castro JGS, Ritter PD, Zaninelli TH, **Saraiva-Santos T**, Verri WA Jr, Borghi SM. Association between IL-10 systemic low level and highest pain score in patients during symptomatic SARS-CoV-2

infection. Pain Pract. 2022 Apr;22(4):453-462. doi: 10.1111/papr.13101. Epub 2022 Feb 4. PMID: 35080097.

Preisler, A. C., Carvalho, L. B., **Saraiva-Santos, T.**, Verri Jr, W. A., Mayer, J. L. S., Fraceto, L. F., ... & Oliveira, H. C. (2022). Interaction of Nanoatrazine and Target Organism: Evaluation of Fate and Photosystem II Inhibition in Hydroponically Grown Mustard (Brassica juncea) Plants. Journal of Agricultural and Food Chemistry. DOI: 10.1021/acs.jafc.2c01601

Zaninelli TH, Fattori V, **Saraiva-Santos T**, Badaro-Garcia S, Staurengo-Ferrari L, Andrade KC, Artero NA, Ferraz CR, Bertozzi MM, Rasquel-Oliveira F, Manchope MF, Amaral FA, Teixeira MM, Borghi SM, Rogers MS, Casagrande R, Verri WA Jr. RvD1 disrupts nociceptor neuron and macrophage activation and neuroimmune communication, reducing pain and inflammation in gouty arthritis in mice. Br J Pharmacol. 2022 Sep;179(18):4500-4515. doi: 10.1111/bph.15897. Epub 2022 Jul 7. PMID: 35716378.

Bertozzi MM, **Saraiva-Santos T**, Zaninelli TH, Pinho-Ribeiro FA, Fattori V, Staurengo-Ferrari L, Ferraz CR, Domiciano TP, Calixto-Campos C, Borghi SM, Zarpelon AC, Cunha TM, Casagrande R, Verri WA. Ehrlich Tumor Induces TRPV1-Dependent Evoked and Non-Evoked Pain-like Behavior in Mice. Brain Sci. 2022 Sep 15;12(9):1247. doi: 10.3390/brainsci12091247. PMID: 36138983; PMCID: PMC9496717.

1.2. Capítulo de livro

Ferraz, C. R., Rasquel-Oliveira, F. S., Borghi, S. M., Franciosi, A., Carvalho, T. T., **Saraiva-Santos, T**., ... & Verri Jr, W. A. (2022). Interlinking interleukin-33 (IL-33), neuroinflammation and neuropathic pain. In The Neurobiology, Physiology, and Psychology of Pain (pp. 171-181). Academic Press. DOI: 10.1016/B978-0-12-820589-1.00016-6